


*Appendix 1*

**Smeringaiova I**, Reinstein Merjava S, Stranak, Z, Studeny P, Bednar J, Jirsova K (2018). Endothelial wound repair of the organ-cultured porcine corneas. *Curr Eye Research*, 43(7), 856-865.



## Endothelial Wound Repair of the Organ-Cultured Porcine Corneas

Ingrida Smeringaiova <sup>a,b</sup>, Stanislava Reinstein Merjava<sup>a</sup>, Zbynek Stranak<sup>c</sup>, Pavel Studeny<sup>c</sup>, Jan Bednar<sup>b</sup>, and Katerina Jirsova<sup>b</sup>

<sup>a</sup>Laboratory of the Biology and Pathology of the Eye, Clinic of Pediatrics and Adolescent Medicine, First Faculty of Medicine, Charles University and General University Hospital in Prague, Prague, Czech Republic; <sup>b</sup>Laboratory of the Biology and Pathology of the Eye, Institute of Biology and Medical Genetics, First Faculty of Medicine, Charles University and General University Hospital in Prague, Prague, Czech Republic; <sup>c</sup>Department of Ophthalmology, Third Faculty of Medicine, Charles University and University Hospital Kralovske Vinohrady, Prague, Czech Republic

### ABSTRACT

**Purpose:** To assess whether injured porcine endothelium of small and large corneoscleral disc differ in its reparative/regenerative capacity under various conditions of organ culture storage.

**Material and methods:** 166 paired porcine corneas were trephined to obtain tissues with diameter 12.0 mm and 17.5 mm (with area neighboring endothelial periphery). In tested discs, central endothelium was mechanically wounded. Density of live endothelial cells (LECD), percentage of dead cells (%DC), coefficient of variation and cell hexagonality were assessed in central and paracentral endothelium following 5- or 9-day incubation in medium with 2% or 10% fetal bovine serum. The parameters were assessed also in fresh and intact cultured discs. Dead endothelial cells (EC) were visualized by trypan blue, cell borders by Alizarin Red S dye. Endothelial imprints were immunoassayed for the proliferation marker Ki-67 and the nucleolar marker fibrillarlin.

**Results:** In fresh corneas, the LECD/mm<sup>2</sup> (mean  $\pm$  standard deviation) were 3998.0  $\pm$  215.4 (central area) and 3888.2  $\pm$  363.1 (paracentral area). Only the length of storage had significant effect on wound repair. Lesion was repaired partially after 5-day and fully after 9-day cultivation. After 9-day storage in medium with 10% serum, the mean LECD detected in small discs were 2409.4  $\pm$  881.8 (central area) and 3949.5  $\pm$  275.5 (paracentral area) and in large discs the mean LECD were 2555.0  $\pm$  347.0 (central area) and 4007.5  $\pm$  261.2 (paracentral area). Ki-67 showed cell proliferation associated with healing of EC of both large and small corneas.

**Conclusions:** The lesions were completely repaired within 9 days of storage. Presence of the area, where stem cells appear to be located, contributes to stimulation of endothelial reparation less than serum concentration and time of culture. Both cell migration and proliferation contribute to the wound repair.

### ARTICLE HISTORY

Received 6 February 2018

Revised 19 March 2018

Accepted 24 March 2018

### KEYWORDS

Porcine corneal endothelium; endothelial cell density; endothelial wound repair; organ culture; endothelial cell proliferation

## Introduction

A monolayer of corneal endothelial cells (EC) plays an essential role in the maintenance of corneal transparency by controlling stromal hydration. Under physiological conditions, human ECs are arrested in the G1-phase of the cell cycle, but they retain their proliferative potential.<sup>1-3</sup> The endothelial cell density (ECD) gradually decreases after the birth.<sup>4</sup> In most European eye tissue banks, corneas with ECD less than 2000 and 2500 cells per mm<sup>2</sup> are usually not used for penetrating or endothelial lamellar keratoplasty, respectively.<sup>5-7</sup>

In case of endothelium wound, the dead cells (DC) detach from the underlying Descemet's membrane (DM) and remaining ECs enlarge and migrate toward the lesion to cover the denuded area.<sup>8,9</sup> Besides this reparative capacity,<sup>3,10</sup> some evidences show that putative stem cells for human ECs may reside in specific stem cell niches in locations close to corneal periphery or in the Schwalbe's line, forming a discontinuous cord in the transition zone (TZ) between the corneal endothelium and the trabecular meshwork.<sup>10-12</sup> It is supposed that throughout the life these cells slowly divide and continuously migrate toward the

center of cornea and support its self-renewal.<sup>13</sup> Besides endothelium repair, the tissue regeneration plays a secondary role, and is probably stimulated by disruption of cell-cell contacts and by growth-factors stimulation.<sup>3,14</sup>

Porcine tissue was suggested as a close equivalent of human tissue<sup>15-17</sup> and pigs as a reliable model to study mechanisms of human diseases due to anatomical and biochemical similarities.<sup>15,18,19</sup> Porcine cornea has oval shape with an average diameter 14.2 mm horizontally  $\times$  12.0 mm vertically and lacks Bowman's layer.<sup>20,21</sup> In average, it is almost twice as thick as the human cornea (473-597  $\mu$ m),<sup>22</sup> but its thickness can reach up to 832.6  $\pm$  40.18  $\mu$ m.<sup>23</sup> Compared to human, porcine cornea is less stiff, probably due to collagen fibril arrangement, which is circular, in contrast to the orthogonal orientation of fibrils in human corneal stroma.<sup>20,21,24,25</sup> A typical lifespan of domestic pigs is 10-20 years.<sup>26</sup> Pig of age of 5-6 months corresponds to human age of 7.7-9.3 years, based on relative lifespan and development of puberty/sexual activity.<sup>17</sup> The porcine endothelium does not proliferate *in vivo*, but retains its proliferative capacity and thus can be stimulated to divide by

external factors.<sup>27,28</sup> In the pig eye, the ECD decreases and cell size increases with advancing age or as a response to the injury.<sup>17</sup>

The first goal of this study was to determine whether after a mechanical damage of central endothelium the pig corneas with the presence of TZ will repair more quickly than corneas without TZ. The second goal was to compare the reparative capacity of endothelium when stored under various organ culture (OC) conditions (serum concentration, storage period).

## Materials and methods

### Sample preparation and grouping

The study followed the standards of the Ethics Committee of the General University Hospital in Prague and Charles University, Prague. All animal care procedures were in accordance with the Principles of Czech Agriculture and Food Inspection Authority of the Czech Republic. Whole eyes ( $n = 166$ ) were obtained from commercially slaughtered 5–6 months old domestic pigs and processed within 3 h after enucleation. Eyes with transparent corneas and with no visible pathological signs were properly rinsed in distilled water, decontaminated in 5% polyvinylpyrrolidone iodine solution (EGIS Pharmaceuticals, Hungary) for 5 min, and washed with phosphate-buffered saline (PBS) afterwards (10× stock solution from Gibco, Life Technologies, Paisley, UK).

From paired eyes, two corneoscleral discs (discs) of the same diameter, either 12.0 mm or 17.5 mm, were trephined. The larger discs contained a corneal button with a 2–3 mm rim of sclera and thus contained the cells located in the TZ (Figure 1). The discs

were divided into two groups (G): A group 1 (G1), the native discs with intact ECs that were not cultured ( $n = 42$ ) and used as controls of condition of ECs directly after preparation, and a group 2 (G2), the discs that were organ cultured ( $n = 124$ ). Cultured corneas of G2 were divided in 16 subgroups (C1–C16, six corneas per each group at least), as summarized in Figure 2 and Table 1, based on three factors: (a) on vitality of the central endothelium that remained intact (–) or was centrally injured (+); (b) on duration of OC, which was either 5 or 9 days in total (5d, 9d); and (c) on the concentration of foetal bovine serum (FBS) included in OC medium that was either 2% or 10% (see following text for details).

### Organ culture conditions

All obtained G2 discs were stored with endothelium side upward in 100 ml sealable glass bottle with 50 ml of OC medium composed of Earle's salts Minimum Essential Medium containing L-glutamine; 25 mM HEPES (Sigma-Aldrich, St. Louis, MO, USA); 2.24 g/l NaHCO<sub>3</sub>; 1× antibiotic–antimycotic solution (Gibco, Life Technologies, Thermo Fisher Scientific, Waltham, MA, USA), and 2% (v/v) or 10% FBS (Invitrogen, Gibco, Glasgow, UK). The discs were cultured for 5 or 9 days at 31°C in normal atmosphere. The OC period included 24–36 h deswelling period of discs placed in OC medium enriched by 5% (v/v) dextran 500 (Sigma-Aldrich, Buchs, Switzerland) at room temperature (RT).

### Mechanical damage of endothelium

G2 group was used to study the pace of wound closure (repair) and accompanying morphological changes of ECs.

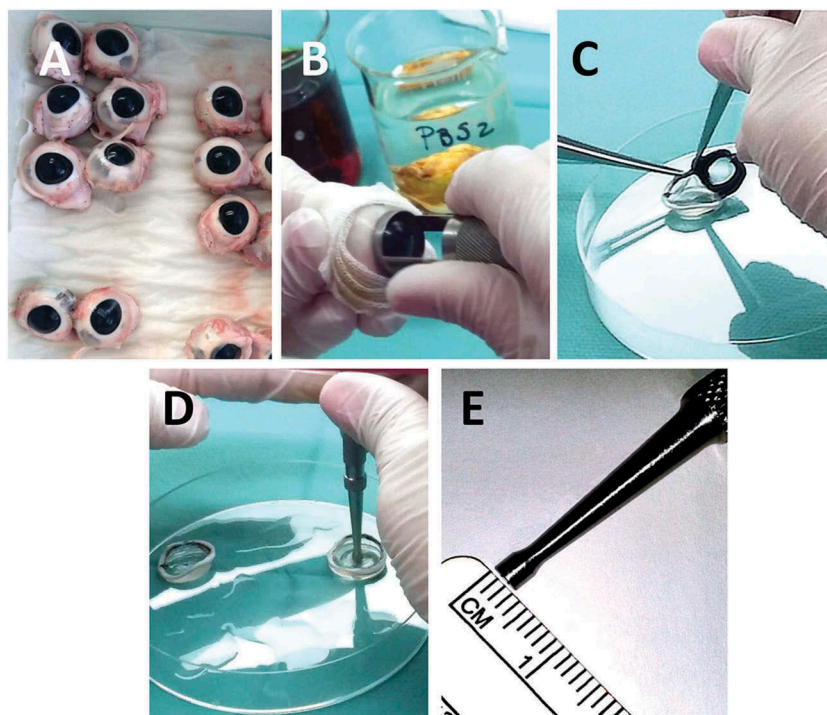


**Figure 1. Preparation of the corneoscleral discs from porcine eyes.** (A) Paired porcine eyes were washed with distilled water and stored in a closed wet-chamber. (B) Eyes were decontaminated in 5% polyvinylpyrrolidone iodine solution and rinsed with phosphate-buffered saline (PBS). Two corneoscleral discs with diameter either 12 mm or 17.5 mm were trephined from a pair of eyes; (C) the discs were then placed into Petri dish and the vitreous, lens, and iris were then gently removed; (D) the endothelium, overlaid by PBS, was centrally injured using a custom-made 3-mm metal rod with flat tip and rounded edge (E).

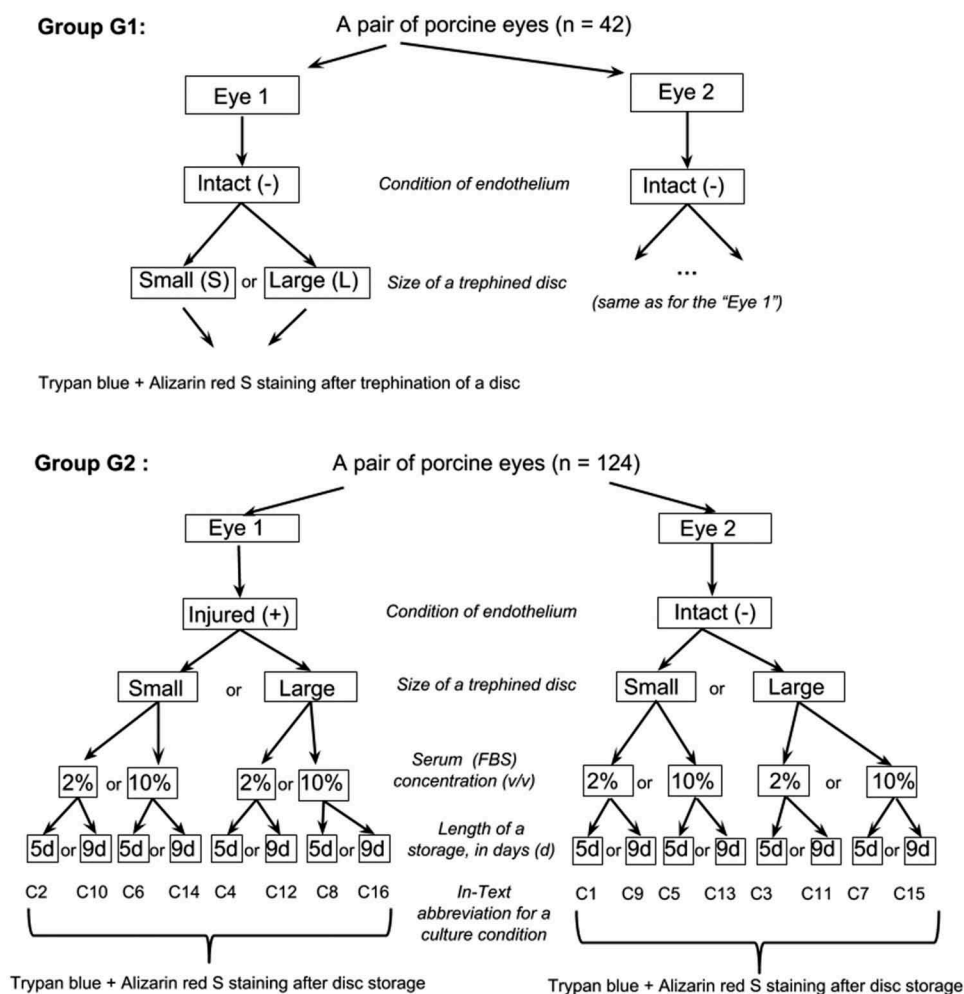


**Figure 2. A schema illustrating experimental groups of corneoscleral discs used in the study.** The discs were divided into two groups (G): group G1 ( $n = 42$ ) of non-cultured intact discs with endothelium in native state, and group G2 ( $n = 124$ ) of cultured discs, either intact (-) or injured (+). Cultured corneas were then divided in 16 subgroups (C1–C16), on the basis of one of the three factors: on condition of endothelium (injured or intact); on OC duration (5 or 9 days, 'd'); or on concentration of serum (FBS) in culture medium (2% or 10%, v/v).

**Table 1.** The corneal endothelial parameters, endothelial cell density of live cells (LECD), and the percentage of dead cells (%DC) in the central (C) and paracentral (PC) endothelium of corneoscleral discs (intact or injured), cultured under different conditions.

Cond. (days, FBS)	Small (S), large (L), injured (+), intact (-)	Group	N	LECD (C) (cells/mm <sup>2</sup> ± SD)	LECD (PC) (cells/mm <sup>2</sup> ± SD)	DC (C) (%)	DC (PC) (%)
5d, 2%	S(-)	C1	7	4203.5 ± 248.0	4110.8 ± 245.7	0.4 ± 0.9	0.4 ± 0.6
	S(+)	C2	7	229.7 ± 201.8	2957.3 ± 807.5	78.2 ± 16.2	2.7 ± 4.9
	L(-)	C3	9	4193.0 ± 341.1	4117.2 ± 322.1	0.4 ± 0.6	0.6 ± 0.6
	L(+)	C4	8	351.0 ± 390.1	3425.7 ± 266.1	63.7 ± 31.8	2.2 ± 4.7
5d, 10%	S(-)	C5	7	4024.3 ± 447.8	3970.9 ± 185.5	-	0.1 ± 0.1
	S(+)	C6	9	404.1 ± 275.2	3156.6 ± 477.8	48.0 ± 29.9	1.1 ± 1.8
	L(-)	C7	8	4004.9 ± 547.6	4165.0 ± 368.2	0.3 ± 0.9	0.1 ± 0.1
	L(+)	C8	8	742.0 ± 502.0	3236.4 ± 833.7	29.7 ± 16.9	0.5 ± 0.8
9d, 2%	S(-)	C9	7	3778.7 ± 395.8	3729.7 ± 275.0	0.3 ± 0.4	0.6 ± 0.9
	S(+)	C10	8	1657.3 ± 597.8	3431.8 ± 400.7	13.9 ± 25.9	1.0 ± 1.7
	L(-)	C11	7	4065.4 ± 621.3	3977.7 ± 229.6	0.5 ± 0.2	0.4 ± 0.3
	L(+)	C12	6	1902.1 ± 700.0	3867.8 ± 316.0	13.4 ± 21.7	0.6 ± 0.6
9d, 10%	S(-)	C13	6	3996.2 ± 604.1	4096.0 ± 379.1	0.4 ± 0.6	0.1 ± 0.1
	S(+)	C14	8	2409.4 ± 881.8	3949.5 ± 275.5	6.8 ± 17.9	0.6 ± 0.9
	L(-)	C15	8	4375.3 ± 297.9	4033.3 ± 313.8	0.1 ± 0.2	0.4 ± 0.8
	L(+)	C16	8	2555.0 ± 347.0	4007.5 ± 261.2	1.7 ± 2.8	0.1 ± 0.1

Cond., storage condition; d = days of organ culture, incl. 24-36-h deswelling in cultivation medium with dextran; FBS, concentration (v/v) of fetal bovine serum in storage medium; S, small corneoscleral discs with a diameter 12 mm; L, large corneoscleral discs with a diameter 17.5 mm; C, central endothelium; PC, paracentral endothelium (adjacent to former lesion); SD, standard deviation; (+) injured disc (sample); (-) intact disc (control); LECD, endothelial cell density of live cells; DC, percentage of dead cells.

From paired eyes, the EC monolayer of one disc was centrally injured ( $n = 62$ ) and the endothelium of contralateral eye was left intact ( $n = 62$ ) and served as control to

assess side effects of the culture conditions on intact EC monolayer. A circular lesion was introduced to the endothelial monolayer by a custom-made steel rod with a



flat tip and a rounded edge (Figure 1), having 3.0 mm diameter and the area of 6.8 mm<sup>2</sup>. The diameter of the damage corresponded to 5% of an area of average porcine EC monolayer, which is about 136 mm<sup>2</sup>.<sup>21</sup> The tip of the rod was pressed gently onto the center of disc for 5 s. A care was taken to not tear the underlying DM. The size and shape of the lesion, the integrity of DM, and the viability of ECs outside the lesion were inspected with inverted light microscope Olympus CKX41 (Olympus, Hamburg, Germany) after staining with 0.2% trypan blue (TB) (Sigma-Aldrich, St. Louis, MO, USA) in PBS. If the damage of ECs exceeded about 5% outside the lesion or if the clear circular wound area was not seen, the disc was excluded from the experiment.

### Visualization of endothelial cells

For assessment of morphometric parameters of ECs after preparation (G1) and after OC (G2), including residual wounds, the EC borders were visualized by staining with 0.2% TB for 3 min, followed by staining with 0.2% Alizarin Red S (pH 4.2) (Sigma-Aldrich, Saint Louis, MO, USA) and fixation in 96% ethanol for 3 min as described previously.<sup>29–31</sup> Central part (8.0 mm in diameter) of each disc was punched out with the Barron Donor Cornea Punch (Altomed Limited, Boldon, UK) and the circle was flattened between a slide and coverslip, immersed in a drop of physiological saline for consequent microscopic assessment.

### Assessment of endothelial parameters

The ECD, live endothelial density (LECD), both expressed in number of cells per mm<sup>2</sup>, %DC, the coefficient of variation of the cell area (CV), and the percentage of hexagonal cells (6A) were assessed as described previously.<sup>6</sup> The EC parameters of native discs (G1) were assessed within a few minutes after preparation. The ones of cultured discs (G2) were assessed directly after the end of incubation in deswelling medium. The EC parameters were assessed in two areas of interest: (a) in the central area (C), corresponding to area of lesion (6.8 mm<sup>2</sup>) and (b) in the paracentral area (PC), corresponding to area in close proximity of lesion, i.e., 2 mm wide ring, surrounding the central lesion (Figure 3). Light microscope Olympus BX51 and Vosskühler VDS CCD-1300 camera (VDS Vosskühler GmbH, Osnabrueck, Germany) were used to record one C and four non-overlapping PC images of the EC monolayer at magnification of 200× (covered area of 0.3 mm<sup>2</sup>). Additional four non-overlapping PC images of the EC monolayer were taken at magnification of 100× in order to cover larger area of EC monolayer, needed for assessment of %DC. The EC parameters were then calculated from collected images by a semi-automated Lucia computer analysis system (Laboratory Imaging, Prague, Czech Republic). The ECD was calculated from 200 ECs in the C of discs and in each of the four PC areas. The areas of nude DM were evaluated as areas of dead EC, thus included into final %DC parameter.

### Immunolocalization of Ki-67 and fibrillarlin

For assessment of ECs in proliferative state, at least three G1 discs and three representative G2 discs from each condition were examined. The discs were washed with PBS, their EC monolayer was imprinted onto the polycarbonate membrane (PCM) (Merck Millipore, Tullagreen, Ireland), and the samples were frozen immediately at –80°C, as described previously.<sup>32</sup> Immunostaining for Ki-67 and fibrillarlin followed protocol for flat-mounted whole corneas,<sup>33</sup> with minor modifications. Briefly, the EC imprints on PCM were thawed and fixed in 0.5% (v/v) paraformaldehyde in PBS solution at RT for 30 min. The ECs on PCM were washed in PBS and permeabilized by 1% Triton-X 100 in PBS for 5 min. The ECs were then exposed to 0.33% Triton-X 100 in 2.5% bovine serum albumin (BSA) in PBS (blocking solution). Primary and secondary antibodies were used as follows: mouse monoclonal anti-Ki-67, clone MIB-1 (dilution 1/100; M7240, Dako, Glostrup, Denmark), and antibody against human nucleolar fibrillarlin (dilution 1/1000), kindly donated by Dr. U. Scheer (Biocenter of the University of Wurzburg); secondary antibody goat anti-mouse IgG conjugated with Alexa Fluor 594 (dilution 1/300, #A11032; Invitrogen, Molecular Probes, Eugene, OR, USA), and anti-human secondary antibody conjugated with Alexa Fluor 488 (dilution 1/50; Invitrogen, #H10120). All antibodies were diluted in blocking buffer (0.33% Triton-X 100 in 0.1% BSA) and samples incubated at RT for 1.5 h in a dark wet-chamber. Imprints were then transferred to the microscope slide and the nuclei counterstained with Vectashield – DAPI mounting medium (Vector Laboratories, Inc., Burlingame, USA). A non-confluent culture of HeLa cells (kindly donated by Dr. Dusan Cmarko) served as positive control for Ki-67. Before microscopic assessment, PCM were moistened by a drop of PBS to increase their transparency and then placed between microscope slide and coverslip. Images of EC were recorded with fluorescent microscope Olympus BX51 at 200× magnification and the Ki-67 positive cells (if present) were counted in each of the collected images.

### Statistical analysis

The final values of EC parameters were expressed as mean ± standard deviation (SD). Two means ± SD were counted from collected data (EC parameters) for each of the 16 culture conditions (C1–C16), one in central and one in paracentral endothelium. To evaluate statistically significant differences in EC parameters (LECD, %DC, CV, 6A), we compared groups of samples varying in disc size (12.0-mm vs. 17.5-mm diameter), groups of samples incubated in a medium with 2% vs. 10% FBS, and the groups of discs cultured for a different time (5 days vs. 9 days). Data analysis was carried out using MS Excel software (Microsoft Corp., Redmond, WA, USA), and *F*-test and two-sample two-tailed Student's *t*-test were performed. The differences were considered statistically significant if the *P*-value was 0.05 or less.

## Results

### Wound repair of endothelium under OC

All used porcine corneas in native state were thick and flexible with wide transparent portion of cornea, and became slightly

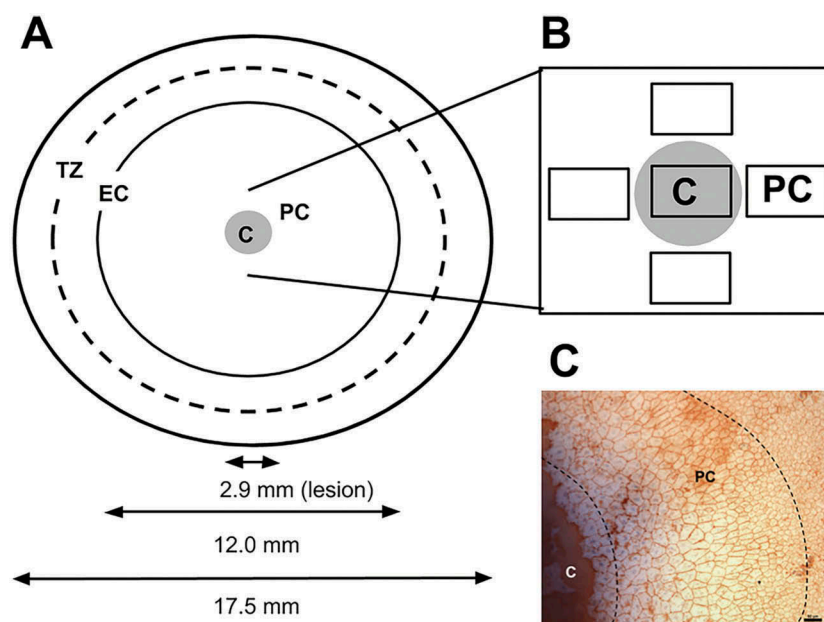


**Figure 3. A schema illustrating endothelial damage and assessed areas in porcine corneoscleral discs. (A)** Two corneoscleral discs with diameter either 12 mm or 17.5 mm were trephined from a pair of eyes. The grey circle indicates the endothelial lesion with diameter of 2.9 mm. TZ between corneal endothelium (EC) and sclera is marked with dashed line. **(B)** One central (C) and four non-overlapping bright-field photographs from paracentral (PC) area were taken at a magnification 100× and 200× for the assessment of DCs and endothelial cell density, respectively. **(C)** Bright-field photograph (scale bar = 50 μm) of the endothelium, indicating the central lesion and paracentral area. In paracentral area, a five to ten cell wide zone is visible, in which a gradual change in cell shape was observed. Borders of endothelial cells are visualized with Alizarin Red S dye.

**Table 2.** The corneal endothelial parameters, the percentage of hexagonal cells (6A) and the coefficient of variation (CV), in the central (C) and paracentral (PC) endothelium of corneoscleral discs (intact or injured), cultured under different conditions.

Cond. (days, FBS)	Small (S), large (L), injured (+), intact (-)		6A (C) (%)	6A (PC) (%)	CV (C)	CV (PC)
5d, 2%	S(-)	C1	51.0 ± 4.6	51.0 ± 4.0	14.1 ± 1.9	15.8 ± 2.2
	S(+)	C2	35.1 ± 16.6	47.5 ± 5.6	22.8 ± 10.8	34.5 ± 23.1
	L(-)	C3	48.7 ± 2.2	49.2 ± 2.0	14.4 ± 1.2	17.6 ± 3.8
	L(+)	C4	37.1 ± 14.2	51.3 ± 3.4	31.4 ± 17.5	25.7 ± 9.2
5d, 10%	S(-)	C5	50.6 ± 4.2	51.3 ± 3.5	15.4 ± 3.5	17.3 ± 2.1
	S(+)	C6	42.4 ± 4.6	49.2 ± 3.1	31.7 ± 8.6	35.2 ± 19.6
	L(-)	C7	54.0 ± 5.1	52.2 ± 3.3	19.8 ± 11.7	17.1 ± 4.0
	L(+)	C8	42.0 ± 5.8	48.8 ± 3.2	33.2 ± 13.9	26.7 ± 17.3
9d, 2%	S(-)	C9	51.3 ± 4.0	48.7 ± 4.1	16.4 ± 3.5	17.9 ± 1.9
	S(+)	C10	44.2 ± 4.5	47.4 ± 3.2	28.4 ± 6.6	21.4 ± 5.5
	L(-)	C11	49.6 ± 5.3	47.8 ± 5.3	18.0 ± 8.9	18.2 ± 4.8
	L(+)	C12	44.1 ± 3.4	47.7 ± 3.3	33.2 ± 10.1	20.0 ± 4.3
9d, 10%	S(-)	C13	48.1 ± 4.0	50.1 ± 3.9	19.8 ± 6.6	17.8 ± 4.8
	S(+)	C14	40.2 ± 4.2	46.8 ± 3.4	28.8 ± 5.2	20.1 ± 3.7
	L(-)	C15	50.4 ± 4.5	48.3 ± 3.4	14.4 ± 1.6	17.0 ± 1.4
	L(+)	C16	37.2 ± 3.9	45.8 ± 3.3	29.2 ± 6.0	17.6 ± 2.5

Abbreviations are same as Table 1.

swollen when cultured in OC medium without dextran. Placing the corneas to OC medium with dextran resulted in thinning of stroma to about a half of its thickness observed after OC. Immediately after induction of the central injury (after TB staining), the corneal endothelium showed a circular wound with few ECs, cell debris and denuded DM. The wound borders were sharp and non-injured cells adjacent to the area of damage exhibited usual hexagonal EC morphology.

In native discs, the mean LECD ( $\pm$ SD) was  $3998.0 \pm 215.4$  (C) and  $3888.2 \pm 363.1$  (PC). The mean %DC ( $\pm$ SD) was  $0.5 \pm 0.9$  (C) and  $3.5 \pm 7.8$  (PC). The mean 6A ( $\pm$ SD) was  $50.7 \pm 4.3$  (C) and  $51.1 \pm 3.1$  (PC); and the mean CV ( $\pm$ SD) was  $13.3 \pm 1.7$  (C) and  $13.7 \pm 1.4$  (PC).

The mean values of LECD ( $\pm$ SD), %DC, 6A and CV in the C and PC endothelium of OC corneas (G2) are summarized in Table 1 and Table 2. Cultured (intact) controls had stable LECD in C and PC; %DC reached 0.6% at maximum, the 6A ranged between 47.8% and 54.0%, and CV varied from 14.1 to 19.8. In contrast, most of the EC parameters worsened in injured cultured discs – lower values of LECD and 6A and higher %DC and CV. After OC of injured discs, 6A was slightly lower in C (35.1–44.2%) than in PC (45.8–51.3%) and mean CV values varied in C (22.8–33.2) and in PC (17.6–35.2).

No significant difference of EC parameters was found between small and large control discs of G2 group. The mean values of LECD of large injured discs were numerically higher

than in small discs, but the difference was not statistically significant. Compared to small discs, the mean values of %DC were numerically lower in large discs in all conditions, gradually decreasing in direction from C2 to C16 (Table 1), i.e., with prolonged culture and increased FBS concentration. The only significant difference in %DC ( $P = 0.036$ ) was found between

**Table 3.** Statistical significance of difference in assessed corneal endothelial parameters – the density of live endothelial cells (LECD) and the percentage of dead cells (%DC) – between injured corneoscleral discs and between their respective controls (intact discs) at different conditions (C1–C16). We compared the parameters between the groups of discs differing in one of the following parameters: the size (small vs. large); the length of their organ culture (5 vs. 9 days), and the effect of different concentrations of fetal bovine serum in storage medium (2% vs. 10%). Statistical significance ( $P$ -value): \* $P \leq 0.05$ ; \*\* $P \leq 0.010$ ; \*\*\* $P \leq .005$ .

	Inj.		LECD (C)	LECD (PC)	%DC (C)	%DC (PC)
S:L	–	C1:C3	0.947	0.966	0.964	0.557
	+	C2:C4	0.443	0.154	0.265	0.863
	–	C5:C7	0.942	0.184	–	0.770
	+	C6:C8	0.101	0.809	0.148	0.377
	–	C9:C11	0.224	0.198	0.628	0.530
	+	C10:C12	0.678	0.621	0.722	<b>0.036*</b>
	–	C13:C15	0.146	0.740	0.313	0.315
	+	C14:C16	0.674	0.672	0.455	0.112
	2:10%	–	C1:C5	0.373	0.252	–
+		C2:C6	0.161	0.539	<b>0.023*</b>	0.428
–		C3:C7	0.400	0.764	0.719	<b>0.027*</b>
+		C4:C8	0.091	0.555	<b>0.017*</b>	0.308
–		C9:C13	0.443	0.079	0.931	0.135
+		C10:C14	0.066	<b>0.009**</b>	0.533	0.578
–		C11:C15	0.140	0.759	0.203	0.894
+		C12:C16	<b>0.040*</b>	0.382	0.244	0.076
5:9 d		–	C1:C9	<b>0.027*</b>	<b>0.024*</b>	0.859
	+	C2:C10	<b>1.550E–04***</b>	0.159	<b>3.500E–05***</b>	0.398
	–	C3:C11	0.533	0.436	0.836	0.424
	+	C4:C12	<b>9.532E–05***</b>	<b>0.012*</b>	<b>0.005***</b>	0.333
	–	C5:C13	0.925	0.454	–	0.861
	+	C6:C14	<b>2.408E–04***</b>	<b>0.001***</b>	<b>0.004***</b>	0.504
	–	C7:C15	0.113	0.420	0.520	0.352
	+	C8:C16	<b>7.693E–07***</b>	<b>0.036*</b>	<b>0.002***</b>	0.163

inj- injury of endothelium: intact (-) or injured (+)

paracentral %DC of small and large disc cultured for 9 days in medium with 2% FBS (C10:C12 in Table 3). For 6A and CV parameters, no statistically significant difference was observed between small and large discs.

When we compared the EC parameters in G2 group with respect to the serum concentration (2% vs. 10% FBS) we found higher LECD in 75% of discs cultured in medium with 10% FBS with two statistically significant differences (C10:C14 and C12:C16, Table 3). The %DC was lower in all C areas, except for one (C9:C13) and in all PC, after culture in medium with 10% FBS, with statistically significant difference in three cases (Table 3). The statistically significant difference in 6A was observed also in three cases: in C ( $P = 0.036$ ) and PC ( $P = 0.025$ ) of large control discs, cultured for 5 days (C3:C7) and in C ( $P = 0.005$ ) of large injured disc, cultured for 9 days (C12:C16), data not presented. No statistically significant difference was observed for CV.

In general, the prolonged storage (9d) considerably improved EC parameters of injured discs, when compared to shorter storage (5d). After 5-day culture, the lesions were partially repaired in 95% of discs, while after 9 days, complete reparation were observed in 99% of discs (Figure 4). The mean LECD in the C was significantly higher ( $P < 0.05$ ) in all injured discs after 9d cultivation, compared to central LECD of injured discs cultured for 5 days. After 9d, the mean LECD in the PC was higher in all injured discs, but the increase was statistically significant in three out of four cases. The LECD of intact cultured controls did not change significantly ( $P > 0.05$ ) after 9d culture except one case (C1:C9) when LECD of 9d cultured discs decreased significantly in both C ( $P = 0.027$ ) and PC ( $P = 0.024$ ) (Table 3). The %DC after 9d culture of injured discs was lower in C and also in PC areas with the difference significant only in C areas. The difference in 6A between 5d and 9d cultured discs was significant only in one case, in case of a slight decrease in paracentral 6A after 9d culture of large intact control

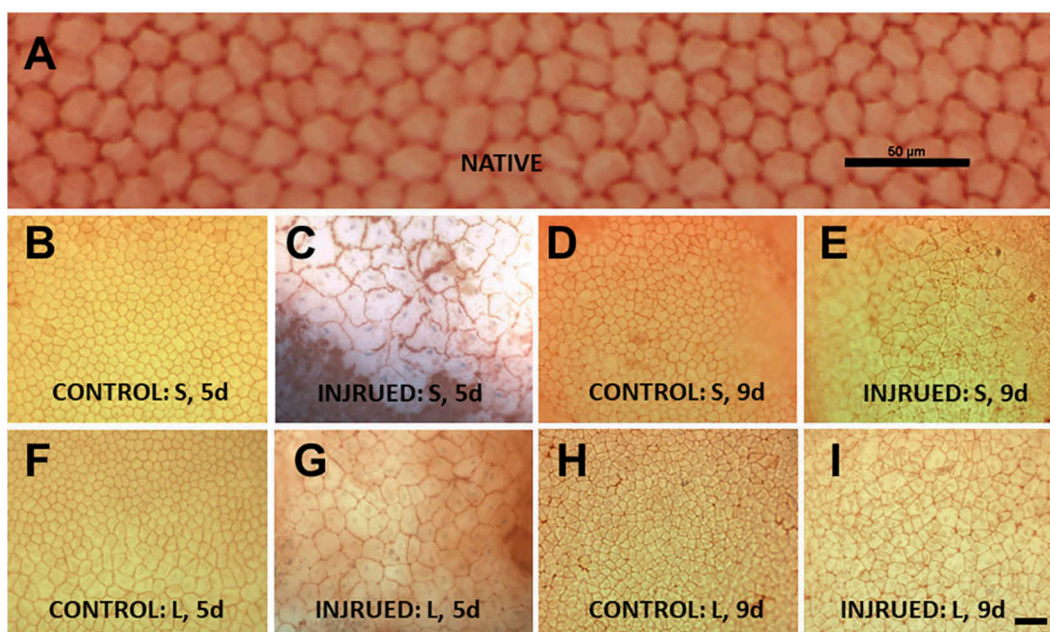


**Figure 4.** Light micrographs of the central porcine corneal endothelium of corneoscleral discs stored under different organ culture (OC) conditions. (A) Before lesion (native); (B–E) small discs (S); and (F–I) large discs (L), cultured in OC medium with 10% fetal bovine serum (FBS) for 5 (5d) or 9 days (9d). Scale bar = 50 µm.



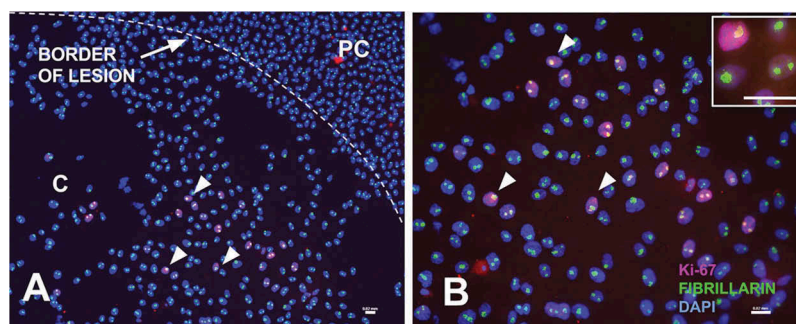


**Figure 5. Fluorescent micrographs of endothelium stained for Ki67 and fibrillarlin.** Polycarbonate membrane has a diameter of 12 mm, corresponding to central to peripheral endothelial area. Ki-67- and fibrillarlin-positive cells are visible in area of the former lesion, in disc cultured for 9 days (**A**, **B**). The Ki-67 signal appeared in dotted-like pattern in nucleus of proliferating cells (arrowheads). Fibrillarlin signal was detected in the nucleoli of all endothelial cells. Most of the Ki-67 positive cells had one or two large, round nucleoli (**insert in B**). Magnification: 100× (A), 200× (B), 1000× (insert). Scale bar: 20 μm.

disc, cultured with 10% FBS medium (C7:C15,  $P = 0.025$ ), data not shown. The CV decreased in most cases both in C and PC of discs cultured for 9 days, but in no case the difference was statistically significant (data not shown).

### Proliferation of endothelial cells in OC corneas

Strong nucleolar signal for fibrillarlin was detected in all ECs, Ki-67 was detected in cells with proliferative activity. No significant difference was observed in a number of Ki-67 cells when different sizes of disc and different concentrations of FBS were compared. More Ki-67 positive cells were detected in the discs stored for 9 days compared to those stored for 5 days. After 9-day culture, numerous Ki-67 positive cells, repopulating central part of cornea, were observed (Figure 5). After 5-day culture, Ki-67 signal was detected in few individual cells scattered throughout the area of EC imprints. Fibrillarlin staining showed mostly two to five unregularly shaped nucleoli per nucleus. Round, relatively large nucleoli, reflecting cells with high metabolic activity, were present particularly in central parts of the cornea with no differences related to the employed conditions.

### Discussion

The results of the presented study indicate that the porcine corneal endothelium of the large corneoscleral discs, which contained the TZ between the corneal endothelium and the trabecular meshwork, did not repair/regenerate significantly better compared to the discs lacking this area. The factors that influenced the improvement of the EC parameters (and wound closure) of injured disc in a most significant manner were a prolonged time of cultivation, followed by a higher serum concentration in the medium.

The existence of stem cells located in the TZ, the zone between the peripheral endothelium and the anterior extension of the trabecular meshwork, and their participation in endothelial repair has been proposed, but not definitely proved yet.<sup>11,34–36</sup> Based on this suggestion we presumed that reparative/regenerative capacity of large discs will be more efficient compared to small ones, lacking the area with the presence of putative endothelial stem cells.

When the ECs were left intact and discs were cultured (G2 control discs), no difference was observed between small and large discs neither in the central nor in the PCs. After cultivation of injured corneas (G2 sample discs), the LECDs were numerically higher in all large discs, both in the C and in the PC areas. The differences were not statistically significant. In large discs, the larger endothelial area surrounding the lesion before incubation, including the TZ, was present thus more ECs could be activated during OC and could migrate centripetally to cover the denuded DM in the center, compared to smaller discs.

The contribution of putative stem cells in TZ to increased LECDs of large discs could not be excluded, as well as confirmed by this study as we did not assess the EC parameters in the distant peripheral endothelium of porcine cornea with average area of 136 mm<sup>2</sup>.<sup>21</sup> The diameter of the endothelial area assessed by immunocytochemical staining was maximally 78.5 mm<sup>2</sup>, which is an effective membrane area of polycarbonate cell culture insert from Merck Millipore, used for transfer of EC (imprinting).

The softness of porcine corneas is a factor that could negatively influence the corneal endothelial parameters assessed during the experiment. In contrast to human cornea, a porcine cornea is not stable after trephination; when the human corneoscleral disc is placed the epithelial side down, it preserves its shape even if it is large, e.g., 17.5 mm in diameter. The situation is different with porcine corneas of both large (17.5 mm) and small diameter. The trephined corneoscleral discs tend to flatten and to copy the shape of the underlying surface. Although all corneas with more than 5% of DC around induced lesion were excluded from experiments, the consequent manipulation (transfer of cornea between media, preparation for staining) may led to more DM folds (with damaged ECs) in large discs than in small ones despite all the care and precautions taken during the tissue manipulation. We consider the softness of porcine cornea as the major difference between human and porcine corneas and in our case as the major factor, which could affect the results of this study.

It has been shown that prolonged cultivation and increased serum concentration in medium positively influence endothelial wound repair both in human<sup>30,37</sup> and pig.<sup>38</sup> In our study, the injured discs cultured in medium with 10% FBS had mostly higher values of LECD than those cultured in 2% FBS but statistically significant difference was found only in two cases. The positive effect of serum and its components on

endothelial repair/regeneration, particularly on migration and proliferation of ECs, has been reported repeatedly.<sup>2,28,39–41</sup> In this study, in contrast to serum concentration, the positive effect of prolonged storage of all injured discs on improvement (increase) of their LECD values was shown to be statistically significant.

The speed and quality of wound repair depend not only on initial quality of corneal tissue and culture conditions, but also on type and size of the wound.<sup>8,16,42,43</sup> In humans, mechanically damaged corneal endothelium can be repaired after approximately a week of OC,<sup>5,30,44</sup> e.g., a lesion covering 4.4–11% of endothelial surface of human corneas can be completely closed after 5–7 days.<sup>9,44</sup> In our porcine model, the 3-mm endothelial wound representing 5% of the endothelial surface was closed in most corneas after 9 days of OC. Likewise humans, porcine corneal ECs migrate and proliferate quite slowly and thus need prolonged time for re-establishment of the endothelial monolayer. Nevertheless, the damage of the size of 5% (6.8 mm<sup>2</sup>) may be too small for a successful activation of putative porcine corneal endothelial stem cells.

In our experimental condition, the final LECD values in the central endothelium of injured corneas after 9-day incubation did not reach those assessed in C of native corneas (about 4000 cells/mm<sup>2</sup>). It indicates that more than 9-day incubation period is needed for the full re-establishment of endothelial hexagonal mosaic, or that the EC proliferation/migration was slowed down by intercellular contact inhibition. Storage induced endothelial folds as well as natural EC loss during corneal storage *ex vivo* may counteract the positive effects of culture conditions on regeneration of endothelium. It is possible that other not yet identified mechanisms might also be present and prevent the full restoration of the endothelium with original ECD.

The proliferation capacity of porcine ECs has been confirmed by the presence of Ki67-positive ECs in the central and paracentral endothelium of all injured discs after five but particularly after 9-day OC. No expression was detected in control discs. This is in accordance with previous studies where no cells expressing Ki-67 were present in healthy human endothelium<sup>46</sup> but Ki-67 positive cells were detected at the border of healing lesions.<sup>43,46</sup>

The percentage of hexagonal ECs (6A) in native discs was higher than 50% in central and paracentral areas and the mean coefficient of variation of the EC area (CV), was about 13%, which is consistent with previously reported results (13.1% in C).<sup>47</sup> It was documented that, unlike in humans, the EC of pigs create naturally heterogeneous mosaic of polygonal cells specific for each individual animal. The average 6A of porcine corneas is not age dependent and is in range from 47 to 54%.<sup>17</sup> When central and paracentral areas were compared between respective small and large discs, the differences between 6A values and between CV values were not statistically significant in any group of cultured samples with either intact or injured endothelium. Some statistically significant changes of 6A related to serum concentration (both decrease and increase) were found in injured discs, but they cannot be considered important due to their opposite trends.

Our initial attempt to measure EC parameters of intact samples (before processing) by phase-contrast microscopy were not successful due to the thickness of porcine cornea, which prevented clear focusing on endothelial mosaic.

Therefore, we considered two other methods for EC parameters assessment: (i) the LIVE/DEAD<sup>®</sup> Cell Viability assay (Molecular Probes) and (ii) the use of TB/Alizarin Red S assay. The latter became the method of choice, mainly because it is easy and fast technique for visualization of cell nuclei and cell borders, which is beneficial when evaluation of relatively high number of samples in short time is needed, as was the case in our study. The TB/Alizarin Red S method was reported as a reliable and efficient technique in recent studies.<sup>48,49</sup>

In summary, our results indicate that the reparative capacity of porcine corneas, expressed by the EC parameters, is maintained during OC. Endothelia of large corneoscleral discs (with preserved endothelial periphery) have a tendency to repair more rapidly compared to endothelia of smaller-sized discs. Not only migration and cell surface enlargement but also proliferation of ECs contributes to the wound closure under experimental conditions used in this study. Our findings support the recent trend in tissue banks to store large corneoscleral discs for ocular transplantations, particularly for a lamellae preparation. As indicated by our results, the storage of partially damaged corneas with the presence of dead ECs or corneal lesions can still be profitable for eventual clinical use as the endothelium can be repaired in conditions compatible with medical requirements. As the human corneas are very precious material, their substitution by porcine ones for experimental studies as an *ex vivo* model seems to be very profitable for studying corneal endothelial wound closure and other endothelial processes.

## Acknowledgments

We would like to thank Dr. Dusan Cmarko and Dr. Evgeny Smirnov (Institute of Biology and Medical Genetics, Charles University, Prague) for supply of fibrillarin antibody (kindly donated by Dr. U. Scheer, Biocenter of the University of Würzburg, Würzburg, Germany) and HeLa cells.

## Declaration of interest

The authors report no conflict of interest. The authors alone are responsible for the content and writing of the paper.

## Funding

This work was supported by The Research Council of Norway, and Ministry of Education, Youth and Sports of the Czech Republic [Norwegian Financial Mechanism 28477/2014, project 7F14156]; by European Regional Development Fund [project BBMRI-CZ III: EF16\_013/0001674]; and by Charles University [SVV, project 260367/2017, project PROGRES-Q25 and Q26/LF1].

## ORCID

Ingrida Smeringaiova  <http://orcid.org/0000-0002-9254-5571>

## References

- Engelmann K, Bohnke M, Friedl P. Isolation and long-term cultivation of human corneal endothelial cells. *Invest Ophthalmol Vis Sci.* 1988;29:1656–62.
- Joyce NC, Joyce SJ, Powell SM, Meklikr B. EGF and PGE2: effects on corneal endothelial cell migration and monolayer spreading



- during wound repair in vitro. *Curr Eye Res.* 1995; 14(7):601–09. doi:10.3109/02713689508998408.
3. Joyce NC. Proliferative capacity of corneal endothelial cells. *Exp Eye Res.* 2012;95(1):16–23. doi:10.1016/j.exer.2011.08.014.
  4. Laule A, Cable MK, Hoffman CE, Hanna C. Endothelial cell population changes of human cornea during life. *Arch Ophthalmol.* 1978;96:2031–35. doi:10.1001/archophth.1978.03910060419003.
  5. Pels E, Beekhuis H, Völker-Dieben HJ. Long term tissue storage for keratoplasty. In: Brightbill FS ed. *Corneal surgery, theory, technique & tissue.* 3rd ed. Mosby, St. Louis, MO. p. 897–906. 1999.
  6. Krabcova I, Studeny P, Jirsova K. Endothelial cell density before and after the preparation of corneal lamellae for Descemet membrane endothelial keratoplasty with a stromal rim. *Cornea.* 2011;30(12):1436–41. doi:10.1097/ICO.0b013e318212497e.
  7. Claerhout I, Maas H, Pels E. European Eye Bank Association Directory Report. 18th ed. 2010. [www.europeaneyebanks.org](http://www.europeaneyebanks.org)
  8. Go W, Wm B, Hf E, Kr K. The corneal endothelium. Normal and pathologic structure and function. *Ophthalmology.* 1982;89(6):531–90.
  9. Hoppenreijns VP, Pels E, Vrensen GF, Oosting J, Treffers WF. Effects of human epidermal growth factor on endothelial wound healing of human corneas. *Invest Ophthalmol Vis Sci.* 1992;33(6):1946–57.
  10. Liu Y, Sun H, Guo P, Hu M, Zhang Y, Tighe S, et al. Characterization and prospective of human corneal endothelial progenitors. *Int J Med Sci.* 2017;14(8):705–10. doi:10.7150/ijms.19018.
  11. Parekh M, Ferrari S, Sheridan C, Kaye S, Ahmed S. Concise Review: an update on the culture of human corneal endothelial cells for transplantation. *Stem Cells Transl Med.* 2016;5(2):258–64. doi:10.5966/sctm.2015-0181.
  12. Katikireddy KR, Schmedt T, Price MO, Price FW, Jurkunas UV. Existence of neural crest-derived progenitor cells in normal and fuchs endothelial dystrophy corneal endothelium. *Am J Pathol.* 2016;186(10):2736–50. doi:10.1016/j.ajpath.2016.06.011.
  13. He Z, Campolmi N, Gain P, Ha Thi BM, Dumollard JM, Duband S, et al. Revisited microanatomy of the corneal endothelial periphery: new evidence for continuous centripetal migration of endothelial cells in humans. *Stem Cells.* 2012;30(11):2523–34. doi:10.1002/stem.1212.
  14. McGowan SL, Edelhauser HF, Pfister RR, Whitehart DR. Stem cell markers in the human posterior limbus and corneal endothelium of unwounded and wounded corneas. *Mol Vis.* 2007;13:1984–2000.
  15. Hara H, Cooper DK. Xenotransplantation: the future of corneal transplantation? *Cornea.* 2011;30:317–78. doi:10.1097/ICO.0b013e3181f237ef.
  16. Choi HJ, Lee JJ, Kim DH, Kim MK, Lee HJ, Ko AY, et al. Blockade of CD40-CD154 costimulatory pathway promotes long-term survival of full-thickness porcine corneal grafts in non-human primates: clinically applicable xenocorneal transplantation. *Am J Transplant.* 2015;15(3):628–41. doi:10.1111/ajt.13057.
  17. Lee SE, Mehra R, Fujita M, Roh DS, Long C, Lee W, et al. Characterization of porcine corneal endothelium for xenotransplantation. *Semin Ophthalmol.* 2014;29(3):127–35. doi:10.3109/08820538.2013.787104.
  18. Sullivan TP, Eaglstein WH, Davis SC, Mertz P. The pig as a model for human wound healing. *Wound Repair Regen.* 2001; 9(2):66–76. doi:10.1046/j.1524-475x.2001.00066.x.
  19. Gutierrez K, Dicks N, Glanzner WG, Agellon LB, Bordignon V. Efficacy of the porcine species in biomedical research. *Front Genet.* 2015;6:293. doi:10.3389/fgene.2015.00293.
  20. Elsheikh A, Alhasso D, Rama P. Biomechanical properties of human and porcine corneas. *Exp Eye Res.* 2008;86(5):783–90. doi:10.1016/j.exer.2008.02.006.
  21. Sanchez I, Martin R, Ussa F, Fernandez-Bueno I. The parameters of the porcine eyeball. *Graefes Arch Clin Exp Ophthalmol.* 2011;249(4):475–82. doi:10.1007/s00417-011-1617-9.
  22. Doughty MJ, Zaman ML. Human corneal thickness and its impact on intraocular pressure measures: a review and meta-analysis approach. *Surv Ophthalmol.* 2000;44(5):367–408. doi:10.1016/S0039-6257(00)00110-7.
  23. Heichel J, Wilhelm F, Kunert KS, Hammer T. Topographic findings of the porcine cornea. *Med Hypothesis Discov Innov Ophthalmol.* 2016;5(4):125–31.
  24. Hayes S, Boote C, Lewis J, Sheppard J, Abahussin M, Quantock AJ, et al. Comparative study of fibrillar collagen arrangement in the corneas of primates and other mammals. *Anat Rec (Hoboken).* 2007;290(12):1542–50. doi:10.1002/ar.20613.
  25. Jay L, Brocas A, Singh K, Kieffer JC, Brunette I, Ozaki T. Determination of porcine corneal layers with high spatial resolution by simultaneous second and third harmonic generation microscopy. *Opt Express.* 2008;16(21):16284–93. doi:10.1364/OE.16.016284.
  26. Meurens F, Summerfield A, Nauwynck H, Saif L, Gerdtts V. The pig: a model for human infectious diseases. *Trends Microbiol.* 2012;20(1):50–57. doi:10.1016/j.tim.2011.11.002.
  27. Nicholls S, Bailey M, Mitchard L, Dick AD. Can the corneal endothelium of the pig proliferate in vivo? *Acta Ophthalmol.* 2009;87:0–0. doi:10.1111/j.1755-3768.2009.2271.x.
  28. Fujita M, Mehra R, Lee SE, Roh DS, Long C, Funderburgh JL, et al. Comparison of proliferative capacity of genetically-engineered pig and human corneal endothelial cells. *Ophthalmic Res.* 2013;49(3):127–38. doi:10.1159/000342978.
  29. Taylor MJ, Hunt CJ. Dual staining of corneal endothelium with trypan blue and alizarin red S: importance of pH for the dye-lake reaction. *Br J Ophthalmol.* 1981;65:815–19. doi:10.1136/bjo.65.12.815.
  30. Nejezpinska J, Juklova K, Jirsova K. Organ culture, but not hypothermic storage, facilitates the repair of the corneal endothelium following mechanical damage. *Acta Ophthalmol.* 2009;88(4):413–19. doi:10.1111/j.1755-3768.2008.01490.x.
  31. Krabcova I, Studeny P, Jirsova K. Endothelial quality of pre-cut posterior corneal lamellae for Descemet membrane endothelial keratoplasty with a stromal rim (DMEK-S): two-year outcome of manual preparation in an ocular tissue bank. *Cell Tissue Bank.* 2013;14:325–31. doi:10.1007/s10561-012-9327-z.
  32. Merjava S, Neuwirth A, Mandys V, Cytokeratins JK. 8 and 18 in adult human corneal endothelium. *Exp Eye Res.* 2009;89(3):426–31. doi:10.1016/j.exer.2009.04.009.
  33. Forest F, Thuret G, Gain P, Dumollard Jm, Peoc'h M, Perrache C, et al. Optimization of immunostaining on flat-mounted human corneas. *Mol Vis.* 2015;21:1345–56.
  34. Bednarz J, Rodokanaki-von Schrenck A, Engelmann K. Different characteristics of endothelial cells from central and peripheral human cornea in primary culture and after subculture. *In Vitro Cell Dev Biol Anim.* 1998;34(2):149–53. doi:10.1007/s11626-998-0097-7.
  35. Whitehart DR, Parikh CH, Vaughn AV, Mishler K, Edelhauser HF. Evidence suggesting the existence of stem cells for the human corneal endothelium. *Mol Vis.* 2005;11:816–24.
  36. Yamagami S, Yokoo S, Mimura T, Takato T, Araie M, Amano S. Distribution of precursors in human corneal stromal cells and endothelial cells. *Ophthalmology.* 2007;114(3):433–39. doi:10.1016/j.ophtha.2006.07.042.
  37. Schultz G, Cipolla L, Whitehouse A, Eiferman R, Woost P, Jumblatt M. Growth factors and corneal endothelial cells: III. Stimulation of adult human corneal endothelial cell mitosis in vitro by defined mitogenic agents. *Cornea.* 1992;11(1):20–27. doi:10.1097/00003226-199201000-00003.
  38. Ayoubi MG, Armitage WJ, Easty DL. Corneal organ culture: effects of serum and a stabilised form of L-glutamine. *Br J Ophthalmol.* 1996 Aug;80(8):740–44. doi:10.1136/bjo.80.8.740.
  39. Lindl T. *Zell- und Gewebekultur.* 5th ed. Heidelberg: Spektrum Akademischer Verlag; 2002. p. 352.
  40. Joyce NC. Proliferative capacity of the corneal endothelium. *Prog Retin Eye Res.* 2003;22(3):359–89. doi:10.1016/S1350-9462(02)00065-4.

41. Meekins LC, Rosado-Adames N, Maddala R, Zhao JJ, Rao PV, Afshari NA. Corneal endothelial cell migration and proliferation enhanced by rho kinase (ROCK) inhibitors in in vitro and in vivo models. *Invest Ophthalmol Vis Sci.* 2016;57(15):6731. doi:10.1167/iov.16-20414.
42. Farjo A, McDermott M, Soong HK. Corneal anatomy, physiology, and wound healing. In: Yanoff M, Duker JS eds. *Ophthalmology.* 3rd ed. Mosby, St. Louis, MO. 203–208. 2009. p. 1552
43. Bhogal M, Matter K, Balda MS, Allan BD. Organ culture storage of pre-prepared corneal donor material for Descemet's membrane endothelial keratoplasty. *Br J Ophthalmol.* 2016;100(11):1576–83. doi:10.1136/bjophthalmol-2016-308855.
44. Doughman DJ, Van Horn D, Rodman WP, Byrnes P, Lindstrom RL. Human corneal endothelial layer repair during organ culture. *Arch Ophthalmol.* 1976;94(10):1791–96. doi:10.1001/archophth.1976.03910040565016.
45. Senoo T, Joyce NC. Cell cycle kinetics in corneal endothelium from old and young donors. *Invest Ophthalmol Vis Sci.* 2000;41(3):660–67.
46. Mimura T, Joyce NC. Replication competence and senescence in central and peripheral human corneal endothelium. *Invest Ophthalmol Vis Sci.* 2006;47:1387–96. doi:10.1167/iov.05-1199.
47. Tamayo-Arango LJ, Baraldi-Artoni SM, Laus JL, Mendes-Vicenti FA, Pigatto JA, Abib FC. Ultrastructural morphology and morphometry of the normal corneal endothelium of adult crossbred pig. *Ciencia Rural.* 2009;39(1):117–22. doi:10.1590/S0103-84782009000100018.
48. Schroeter J, Meltendorf C, Ohrloff C, Rieck P. Influence of temporary hypothermia on corneal endothelial cell density during organ culture preservation. *Graefes Arch Clin Exp Ophthalmol.* 2008;246(3):369–72. doi:10.1007/s00417-007-0711-5.
49. Schroeter J, Ruggeri A, Thieme H, Meltendorf C. Impact of temporary hyperthermia on corneal endothelial cell survival during organ culture preservation. *Graefes Arch Clin Exp Ophthalmol.* 2015;253(5):753–58. doi:10.1007/s00417-014-2903-0.

## *Appendix 2*

**Smeringaiova I**, Trosan P, Mrstinova MB, Matecha J, Burkert J, Bednar J, Jirsova, K (2017). Comparison of impact of two decontamination solutions on the viability of the cells in human amnion. *Cell Tissue Bank*, 18(3), 413-423.

# Comparison of impact of two decontamination solutions on the viability of the cells in human amnion

Ingrida Smeringaiova  · Peter Trosan · Miluse Berka Mrstinova · Jan Matecha · Jan Burkert · Jan Bednar · Katerina Jirsova

Received: 4 January 2017 / Accepted: 6 June 2017 / Published online: 4 July 2017  
© Springer Science+Business Media B.V. 2017

**Abstract** Human amniotic membrane (HAM) is used as an allograft in regenerative medicine or as a source of pluripotent cells for stem cell research. Various decontamination protocols and solutions are used to sterilize HAM before its application, but little is known about the toxicity of disinfectants on HAM cells. In this study, we tested two decontamination solutions, commercial (BASE-128) and laboratory decontamination solution (LDS), with an analogous content of antimycotic/antibiotics for their cytotoxic effect on HAM epithelial (EC) and mesenchymal stromal cells (MSC). HAM was processed in a standard way, placed on nitrocellulose scaffold, and decontaminated, following three protocols: (1) 6 h, 37 °C; (2) 24 h, room temperature; (3) 24 h, 4 °C. The viability of EC was assessed via trypan blue staining.

The apoptotic cells were detected using terminal deoxynucleotidyl transferase dUTP nick end labelling (TUNEL). The mean % ( $\pm$ SD) of dead EC (%DEC) from six fresh placentas was  $12.9 \pm 18.1$ . Decontamination increased %DEC compared to culture medium. Decontamination with BASE-128 for 6 h, 37 °C led to the highest EC viability (81.7%). Treatment with LDS at 24 h, 4 °C resulted in the lowest EC viability (55.9%) in the set. MSC were more affected by apoptosis than EC. Although the BASE-128 expresses lower toxicity compared to LDS, we present LDS as an alternative decontamination solution with a satisfactory preservation of cell viability. The basic formula of LDS will be optimised by enrichment with nutrient components, such as glucose or vitamins, to improve cell viability.

---

I. Smeringaiova · P. Trosan · J. Bednar · K. Jirsova (✉)  
Laboratory of the Biology and Pathology of the Eye,  
Institute of Inherited Metabolic Disorders, First Faculty of  
Medicine, Charles University and General University  
Hospital in Prague, Ke Karlovu 2, 128 08 Prague,  
Czech Republic  
e-mail: katerina.jirsova@lf1.cuni.cz

M. B. Mrstinova · J. Matecha  
Department of Obstetrics and Gynaecology, Second  
Faculty of Medicine, Charles University, Prague,  
Czech Republic

J. Burkert · K. Jirsova  
Department of Transplantation and Tissue Bank, Motol  
University Hospital, Prague, Czech Republic

**Keywords** Amniotic membrane · Decontamination solution · Viability · Apoptosis · Epithelial and mesenchymal cells

## Introduction

The human placenta at term has two distinguishable fetal membranes that develop separately: the amniotic membrane (HAM) on the fetal surface of placenta and the chorionic membrane underneath the HAM. The two membranes remain separable due to the existence of a spongy layer in between. HAM

consists of a monolayer of epithelial cells (EC), which resides on a resistant basement membrane, and of a mesenchymal layer at the bottom. The latter can be subdivided into the acellular compact layer, the fibroblast layer with sparsely distributed mesenchymal stromal cells (MSC), and the acellular spongy layer, contiguous with the chorionic membrane (Bourne 1960, 1962; Dua et al. 2004; Lindenmair et al. 2012).

Different mechanisms of action, such as wound-healing, anti-scarring, anti-angiogenic, anti-inflammatory, antimicrobial effects and low antigenicity, have been attributed to the soluble bioactive compounds—cytokines, growth factors, vasoactive peptides etc., produced by HAM resident cells (Gruss and Jirsch 1978; Akle et al. 1981; Dua et al. 2004).

The HAM is most often used as a temporary biologic dressing in ophthalmology, but also in plastic surgery, dermatology and gynaecology (King et al. 2007; Mamede et al. 2012; Malhotra and Jain 2014). The HAM is elastic and translucent and is devoid of nerves, smooth muscle cells, lymph and blood vessels. Beside its clinical use, HAM is used in tissue engineering as a cheap and flexible biological 3D-cell carrier for cell migration, differentiation and delivery of *in vitro* cultured cells into ocular wound (Ishino et al. 2004; Gholipourmalekabadi et al. 2016).

The HAM is available without an ethical conflict, typically procured after caesarean section delivery and decontaminated with solutions containing antibiotics and antimycotics (AA). HAM is manually dissected under sterile conditions, thoroughly washed from blood clots and debris. During HAM preparation AA solutions may be used for repeated rinsing of tissue prior to storage. Alternatively, gamma irradiation is used for HAM sterilization (Singh et al. 2007; von Versen-Hoeynck et al. 2008; Riau et al. 2010).

Despite its putative advantages over preserved HAM, such as preservation of viable cells, the transplantation of fresh HAM (tissue not subjected to preservation, used within 14 days) has not been yet established. Some attempts have been made in this matter (Ganatra and Durrani 1996; Mejía et al. 2000; Adds et al. 2001), however, there is a lack of proper evidence for its safe clinical use, without risk of transmission of infection to a patient (Khokhar et al. 2001). In most western countries, fresh HAM is not permitted for use. Donor must be tested for signs of

viral or bacterial infection at the time of delivery and 6 months later to cover window period of infection. Thus HAM must be preserved during this period. Cryopreservation is the most common method of storage, using the standard protocol proposed by Kim and Tseng (1995). Lyophilisation and storage in a dry form are other basic preservation methods (Dua et al. 2006; von Versen-Hoeynck et al. 2008; Thomassen et al. 2009).

The decontamination is highly important when HAM is intended to be stored cryopreserved in glycerol, mixture of glycerol with a culture medium or dimethyl sulfoxide solution (Maral et al. 1999; Tan et al. 2014; Duan-Arnold et al. 2015; Zidan et al. 2015; Paolin et al. 2016). During standard preservation, the morphology of HAM matrix does not seem to be altered dramatically, but the majority of resident cells seem to be devitalized (von Versen-Hoeynck et al. 2004; Hennerbichler et al. 2006; Aykut et al. 2014; Mrázová et al. 2015; Perepelkin et al. 2016).

To our best knowledge, the only commercially available decontamination solution with certification based on Directive 93/42/EEC (medical devices) is the BASE-128 from Alchimia (Italy), which contains AA (amphotericin B, cefotaxime, gentamicin, vancomycin) (Gatto et al. 2013). In most cases, laboratories prepare their own tissue sterilization solutions, composed of physiological saline or buffers and added AA and use various decontamination protocols (Lee and Tseng 1997; Ashraf et al. 2015; Duan-Arnold et al. 2015; Laurent et al. 2014). The impact of different AA present in decontamination solutions on HAM tissue is insufficiently examined (Aykut et al. 2014; Perepelkin et al. 2016).

The purpose of this study was to compare the overall effect of the commercial solution BASE-128 and laboratory decontamination solution (LDS), with analogous composition of AA, on HAM structure, focused on viability of EC. The BASE-128 is reported (by producer's *in vitro* time-kill studies) to effectively decontaminate the tissue, if one of the three protocols is followed: (1) 6 h, 37 °C, (2) 24 h, at room temperature (RT) or (3) 24 h, 4 °C. The HAM was incubated under these conditions in both BASE-128 and LDS and the viability of EC cells after decontamination was tested via trypan blue staining. Additionally, the fresh and cryopreserved samples of HAM (before/after decontamination) were tested for the presence of apoptotic (EC, MSC) cells.



## Materials and methods

### Tissue

The study followed the standards of the Ethics Committee of the General Teaching Hospital and First Medical Faculty of Charles University, and adhered to the tenets set out in the Declaration of Helsinki. Six term human placentas (P1–P6) from normal pregnancies were obtained with informed consent after delivery by elective caesarean section in the Motol University Hospital, Prague. Only healthy donors, screened for hepatitis B and C, syphilis, HIV and C-reactive protein (<10 mg/L), were involved. The placentas with evident pathologies or visible injuries, such as hematomas, were excluded. Immediately after delivery, each placenta was placed in a sterile container and overlaid with Hank's Balanced Salt Solution (HBSS, Sigma-Aldrich, Prague, Czech Republic). Special attention was paid to the gentle handling of each placenta during transport and subsequent manipulation.

### Processing

The tissue was processed in aseptic conditions within 3 h after the delivery. Briefly, the placenta was cleansed of blood clots with sterile HBSS under a biosafety cabinet and two HAM sheets were peeled off by blunt dissection starting underneath the umbilical cord insertion and proceeding towards the placental disk edge (Fig. 1a). They were gently rinsed again with HBSS to obtain thin smooth HAM and then flattened onto two sheets (9.5 × 9.5 cm each) of sterile nitrocellulose membrane (NCM) carrier (Bio-Rad, Prague, Czech Republic), the epithelium surface facing up (Fig. 1b). Prior the use, 24 rectangles were marked on NCM sheets, 3 circular apertures (3 mm in diameter) punched in each rectangle and the sheets were autoclaved. Each of the two NCM sheets with HAM was cut into 2 × 24 rectangles (samples) (Fig. 1c), representing 48 subareas of placental amnion. Samples of HAM were either evaluated for the percentage of dead epithelial cells (%DEC) immediately after processing of the tissue (fresh HAM) or forwarded to decontamination procedures (incubated in respective solutions) and evaluated for %DEC afterwards (Fig. 1d).

### Sample preparation, decontamination and cryopreservation

The HAM samples were placed into the BASE-128 solution (Alchimia, Ponte San Nicolò, Italy) or LDS with analogous AA composition. Dulbecco's Modified Eagle Medium (DMEM) with no AA (Gibco, Thermo Fisher Scientific, Prague, Czech Republic) was used as a control solution (Co). The BASE-128 is composed of a balanced saline solution, vitamins, minerals, glucose and AA: Amphotericin B sodium deoxycholate 13,500–16,500 IU/l (14.3–17.5 mg/L; potency: 944 IU/mg) (Rautmann et al. 2010), cefotaxime, gentamicin, vancomycin 115.2–140.8 mg/L (same for the three), according to the product specification sheet. The LDS was prepared by mixing the physiological saline (Fresenius Kabi, Bad Homburg, Germany) with the AA analogous to BASE-128. The AA concentrations in LDS were selected as mean values from AA concentration range published for BASE-128 by producer: Amphotericin B sodium deoxycholate 16 mg/L (Bristol-Myers Squibb, Farmar L'Aigle Usine, France), cefotaxime 130 mg/L, gentamicin 140 mg/L (Lek Pharmaceuticals, Ljubljana, Slovenia), vancomycin 130 mg/L (Mylan, S.A.S., France).

The two NCM sheets with HAM were cut into 48 rectangles (samples) (Fig. 1a–c). 12 samples per placenta, labelled as fresh HAM, were kept in DMEM for ≤1 h at RT, until assessment of %DEC. 24 samples per placenta were decontaminated with BASE-128 or LDS (12 samples each) and remaining 12 samples were stored in Co. Decontamination procedure followed three protocols: (1) 6 h at 37 °C in 5% CO<sub>2</sub> atmosphere (condition 1, C1); (2) 24 h at RT (condition 2, C2) and (3) 24 h at 4 °C (condition 3, C3). After incubation in individual conditions, the %DEC was assessed by trypan blue (TB) staining. Edge areas (3 × 10 mm) of all 48 specimens were cut (before/after decontamination) and either cryopreserved (–80 °C) embedded in Cryomount embedding medium (Histolab AB, Västra Frölunda, Sweden), or kept in Co (≤1 h at RT) for detection of apoptotic cells (EC, MSC). Cryomount medium contains water-soluble glycols and resins that help protect cell integrity during freezing.

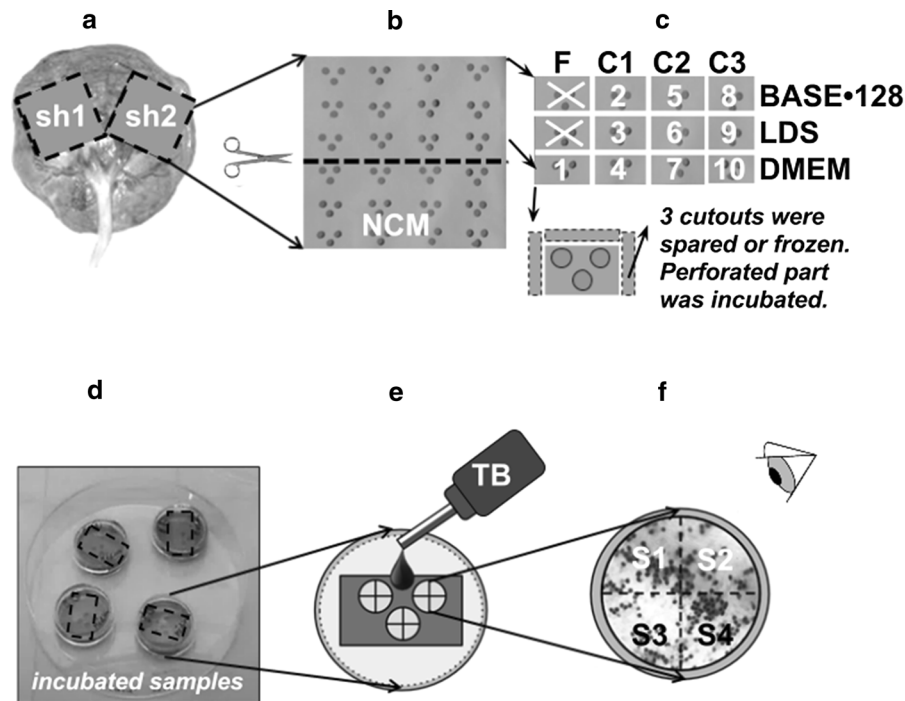


**Fig. 1** Tissue sampling procedure—scheme. Two sheets (sh) of human amniotic membrane (HAM) were dissected from placenta (a), flattened onto nitrocellulose membrane (NCM), then divided into two halves (b), each of the 4 resulting parts cut into 12 rectangular pieces (c) and incubated under three conditions: 6 h, 37 °C, 5% CO<sub>2</sub> (C1), 24 h, room temperature (RT) (C2), 24 h, 4 °C (C3) and two decontamination solutions: commercial BASE•128 and laboratory decontamination solution (LDS). Alongside the decontaminated samples of HAM, control pieces of HAM were stored in a Dulbecco's modified Eagle's

medium (DMEM) under same conditions (C1–C3). Four pieces of fresh HAM (F) were stored in DMEM at RT for the assessment of dead epithelial cells before decontamination. We obtained 10 groups of samples; some pieces were used as spare ones (X). Three cutouts from each sample were cryopreserved or stored in DMEM, at RT, for assessment of apoptotic cells (c, d). Each piece of HAM on NCM with 3 circular perforations was stained using trypan blue (TB) (e). Each perforation was visually divided into four sectors (S1–S4) and photographs of each sector were taken at 200x magnification (f)

### Assessment of cell survival in HAM

Each HAM sample on NCM, fresh and decontaminated, was rinsed with lukewarm phosphate buffered saline (PBS) and stained with 0.1% TB in PBS (Sigma-Aldrich, Prague, Czech Republic) for 70 s to stain dead cells (Fig. 1e) (Pegg 1989). The %DEC throughout the visible surface of HAM (spanning the NCM perforations) was examined under light microscope (Olympus BX51, Olympus Co., Tokyo, Japan) at 200× magnification. Each aperture was visually divided into four equal sectors (Fig. 1f) and one image of each sector recorded. The %DEC of sample was determined from collected images by computer assisted manual cell counting via Lucia computer analysis system (Laboratory Imaging, Prague, Czech Republic).

Additional staining of HAM epithelium with LIVE/DEAD® Viability/Cytotoxicity Kit for mammalian cells (Molecular Probes, Thermo Fisher, Prague, Czech Republic) was performed following the manufacturer's instructions and %DEC was determined from collected images (5–10 images per sample) by NIS Elements software (Laboratory Imaging for Nikon Co., Prague, Czech Republic). At least 1000 of EC in one micrograph were examined.

### Assessment of apoptotic cells in HAM

The cryopreserved pieces of HAM samples (fresh and decontaminated, all conditions) were thawed at RT, washed in PBS, cut into 3 × 5 mm pieces and adhered to a microscope glass slide by drying at RT for a few minutes—one piece epithelial side up and the other

epithelial side down. Cells were then stained for fragmented DNA, i.e. free 3'-OH ends, via terminal deoxynucleotidyl transferase (TdT) dUTP nick-end labelling (TUNEL) method (Gavrieli et al. 1992), with in situ Cell Death Detection kit, Fluorescein (Roche Diagnostics, Mannheim, Germany) according to the manufacturer's instructions. The positive control, pre-treated with deoxyribonuclease I (Sigma-Aldrich, Prague, Czech Republic), and negative control (TdT omitted) were included and labelled on an extra glass slide. Samples of fresh HAM (before cryopreservation) were also TUNEL labelled. Following TUNEL, specimens were covered with Vectashield—DAPI mounting medium (Vector Laboratories, Inc. Burlingame, USA) to counterstain cell nuclei. Images of labelled EC and MSC were recorded with Vosskühler VDS CCD-1300 camera (VDS Vosskühler GmbH, Osnabrueck, Germany) using fluorescent microscope Olympus BX51 at 200× magnification. The EC/MSc exhibiting apoptotic changes were counted in collected images (5–10 sectors per image) by NIS Elements software. At least 1000 of EC and 100 MSC in one micrograph (cell nuclei in the same focus plane) were examined.

#### Statistical analysis

All data were processed in MS Excel and expressed as the mean  $\pm$  SD from values counted from the individual micrographs. The Student's *t* test (unpaired, two-tailed) was performed to compare the results of the individual decontamination conditions with the control and only the data with *p*-value  $<0.05$  were considered statistically significant.

## Results

#### The EC viability in fresh HAM

Epithelial cells with TB positive staining of cell nucleus were considered non-viable and included in total %DEC assessment, Fig. 2. Table 1 summarises the %DEC for six individual placentas before decontamination (fresh HAM). The important dispersion of average values and high standard deviations values reflects the significant variability of %DEC both in individual placentas and among them. The mean %DEC ( $\pm$ SD) in fresh HAM from all placentas (All, Table 1) was  $12.9 \pm 18.1$ .

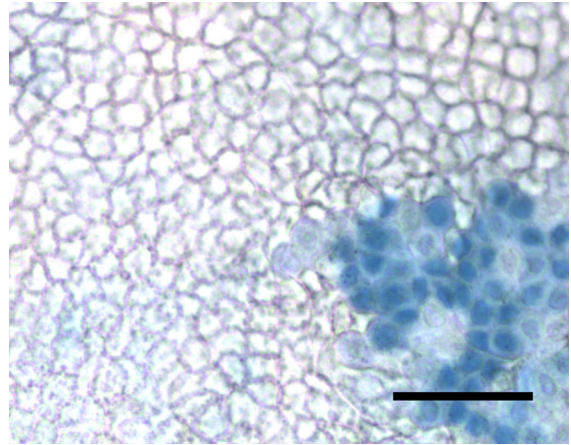


**Fig. 2** The epithelial surface of the HAM sheet after preparation and after trypan blue (TB) staining, showing the island of dead epithelial cells (blue) surrounded by mosaic of polygonal viable epithelial cells. Pieces of HAM on nitrocellulose scaffold were stained with 0.1% TB in phosphate buffered saline for 70 s and observed under the light microscope at 200x magnification. The scale bar represents 50  $\mu$ m

#### The EC viability in decontaminated HAM

The mean %DEC ( $\pm$ SD) values in decontaminated HAMs (incubated in BASE-128 or LDS) and control HAMs (Co; incubated in DMEM) from all six placentas (P1–P6) were determined, Table 2. The visually confirmed increase in %DEC was observed when longer decontamination periods (C2, C3) were used. Compared to Co, decontamination by both BASE-12 and LDS at all conditions increased the average %DEC, however, only in LDS at C3 this increase was statistically significant ( $p = 0.01$ ).

Due to the fact that relatively high variability in %DEC was present already in samples of fresh HAM, Table 1, we compared the mean %DEC of decontaminated HAM to the mean %DEC of the fresh HAM and expressed it as n-fold increase/decrease in %DEC for individual placentas and conditions (C1–C3; BASE-128, LDS, DMEM), Table 3. We also determined the statistical significance of these changes, relative to fresh HAM. As shown in Table 3, comparing the values of n-fold increase in %DEC ( $\uparrow$ %DEC) among LDS, BASE-128 and DMEM in each condition (C1–C3) individually, the increase was highest for LDS in 15 out of 18 cases, with the highest values in C3. The difference in n-fold increase in %DEC between BASE-128 and DMEM of each respective group was minimal. The slight decrease in %DEC

**Table 1** The mean percentage of the dead epithelial cells (%DEC  $\pm$  SD) in fresh HAM (before decontamination) from six placentas (P1–P6)

Placenta	P1	P2	P3	P4	P5	P6	All
%DEC $\pm$ SD	28.1 $\pm$ 30.3	4.8 $\pm$ 8.5	7.9 $\pm$ 8.1	10.3 $\pm$ 9.1	8.3 $\pm$ 12.7	19.4 $\pm$ 18.8	12.9 $\pm$ 18.1

Samples were stored in DMEM at room temperature and processed within 1 h after dissection

SD standard deviation

**Table 2** The mean percentage of the dead epithelial cells (%DEC  $\pm$  SD) in decontaminated HAM, from all six placentas

%DEC $\pm$ SD	C1: 6 h 37 °C	C2: 24 h RT	C3: 24 h 4 °C
BASE·128	18.3 $\pm$ 18.3	20.2 $\pm$ 12.6	30.2 $\pm$ 17.8
LDS	28.6 $\pm$ 23.4	31.6 $\pm$ 19.3	44.1 $\pm$ 19.0
DMEM (Co)	13.2 $\pm$ 13.0	12.2 $\pm$ 12.5	25.2 $\pm$ 20.5

The commercial decontamination solution BASE·128, laboratory-made decontamination solution (LDS) or Dulbecco's modified Eagle medium (DMEM) as a control solution (Co) were used. The HAM specimens were incubated for 6 h at 37 °C (C1), for 24 h at room temperature (RT) (C2), or for 24 h at 4 °C (C3). The statistically significant increase ( $p < 0.05$ ) in %DEC was observed in C3 using LDS

SD standard deviation

( $\downarrow$ %DEC), compared to the fresh HAM, was observed in some cases of cultivation of HAM in DMEM.

Treatment of HAM with BASE·128 at C1 resulted in significant %DEC worsening only for one placenta (P4) out of six, the same situation was observed for storage in DMEM (Table 3). Similarly, at C2, the %DEC change was statistically significant in two placentas (P1, P6) in case of HAM storage in BASE·128 ( $\uparrow$ %DEC) and in two placentas (P2:  $\uparrow$ %DEC, P6:  $\downarrow$ %DEC) in case of storage in DMEM. When using LDS, the %DEC increased almost for all placentas at all conditions with exception of P5 in C1 and P3 in C2. On the contrary, HAMs from most placentas were significantly affected ( $\uparrow$ %DEC) by storage at C3.

#### Assessment of apoptotic EC and MSC

The mean percentage of the apoptotic epithelial cells (%AEC) and the mean percentage of the apoptotic mesenchymal cells (%AMC) in HAM before/after decontamination with solutions (BASE·128, LDS) or incubation in Co are shown in Tables 4 and 5, respectively. In the fresh HAM samples (before/after

cryopreservation) from three placentas the mean %AEC was less than 1% and the mean %AMC was 42.0  $\pm$  18.5 (values from 16.1 to 59.7%). In all specimens after decontamination and in all conditions (before/after cryopreservation), the mean %AEC remained low, about 1–2% (Table 4) and mean %AMC increased significantly (except C3, BASE·128) up to 87.9% (C1, Co), compared to fresh HAM (Table 5). Changes in the mean %AEC among groups were not statistically significant.

Interestingly, during the microscopic evaluation of dead cells by TB staining, small intracellular and extracellular droplets of unknown origin, distributed throughout the HAM, were observed occasionally. Therefore we decided to stain HAM samples of all groups with histological dye Sudan III and Mayer's hematoxylin (performed at the Institute of Pathology, First Faculty of Medicine, Charles University; not included in "Materials and methods" section). It was determined that these droplets are of lipid origin and their presence is rather random (Fig. 3).

#### Discussion

Using perforated NCM as a carrier for HAM we have established a sampling scheme which can be used as a feasible model for the assessment of the quality of prepared HAM allowing the quick detection and visualisation of dead epithelial cells. The good adherence of the HAM tissue to the NCM during the whole procedure limited the HAM folding and thus minimized cell death as the consequence of mechanical stress.

We observed variations in the mean %DEC (4.8–28.1%) in the fresh HAM, despite the precautions we took. We suppose that this could be the result of the inherent tissue variability, the manipulation with placenta and stress applied on the cells exposed to

**Table 3** The n-fold increase/decrease in %DEC in decontaminated HAM, expressed for six individual placentas (P1–P6)

	C1: 6 h 37 °C			C2: 24 h RT			C3: 24 h 4 °C		
	BASE.128	LDS	DMEM	BASE.128	LDS	DMEM	BASE.128	LDS	DMEM
P1	1.2 (0.637)	2.2 (5.26E-07)***	0.8 (0.344)	1.9 (2.77E-04)***	2.7 (6.78E-13)***	0.7 (0.207)	1.9 (6.93E-04)***	2.6 (2.46E-10)***	0.8 (0.430)
P2	2.2 (0.062)	4.5 (2.475E-04)***	0.9 (0.725)	1.4 (0.178)	3.6 (8.29E-04)***	2.1 (0.044)*	1.6 (0.120)	4.3 (2.15E-05)***	1.8 (0.076)
P3	1.3 (0.162)	2.1 (0.003)***	1.2 (0.213)	0.8 (0.357)	1.3 (0.306)	1.5 (0.053)	1.9 (0.004)***	1.6 (0.042)*	2.4 (3.78E-04)***
P4	2.1 (1.581E-04)***	2.4 (3.792E-04)***	1.6 (0.011)*	1.0 (0.897)	2.9 (5.56E-06)***	1.4 (0.096)	1.1 (0.336)	5.3 (2.76E-20)***	2.4 (1.34E-06)***
P5	1.0 (0.994)	1.8 (0.052)	1.0 (0.937)	1.3 (0.226)	2.9 (4.26E-09)***	0.7 (0.267)	4.8 (7.18E-14)***	7.0 (1.57E-31)***	4.2 (1.67E-15)***
P6	1.4 (0.069)	1.7 (0.003)***	0.9 (0.613)	1.7 (0.002)***	1.8 (0.003)***	0.5 (0.013)*	2.8 (8.50E-14)***	2.4 (1.10E-12)***	2.1 (2.22E-04)***

Mean %DEC value for decontaminated HAM was compared with the mean %DEC value for the fresh HAM of respective placenta. Samples of fresh HAM were stored in DMEM at room temperature (RT) and processed within 1 h after dissection. For decontamination, HAM samples were stored in BASE.128 or laboratory decontamination solution (LDS) and were incubated for 6 h at 37 °C (C1), for 24 h at RT (C2), or for 24 h at 4 °C (C3). Control HAM for each condition was stored in DMEM. Statistical significance (Student's *t*-test, unpaired, two-tailed): \* *p* < 0.05; \*\* *p* < 0.01; \*\*\* *p* < 0.005 (*p*-value indicated in brackets)



**Table 4** The mean percentage of the apoptotic epithelial cells (%AEC  $\pm$  SD) after HAM decontamination, related to fresh HAM

%AEC $\pm$ SD	C1: 6 h 37 °C	C2: 24 h RT	C3: 24 h 4 °C
BASE-128	1.15 $\pm$ 0.68	0.72 $\pm$ 0.52	0.95 $\pm$ 0.17
LDS	1.17 $\pm$ 0.63	0.50 $\pm$ 0.07	1.63 $\pm$ 1.95
DMEM (Co)	1.73 $\pm$ 0.42	0.86 $\pm$ 0.26	1.28 $\pm$ 1.23

HAM was treated with BASE-128 or laboratory-made decontamination solution (LDS) or stored in Dulbecco's modified Eagle medium (DMEM) as a control solution (Co). The HAM specimens were incubated for 6 h at 37 °C (C1), for 24 h at room temperature (RT) (C2), or for 24 h at 4 °C (C3). Samples from three placentas were analysed. Changes in the mean %AEC were not statistically significant (*p*-values are thus not indicated)

SD standard deviation

the environment during the experimental procedure. We could observe the worsened quality of HAM in cases of less careful tissue handling; these HAMs were excluded from our experiments. Rather high values of SD for individual placentas are a consequence of the heterogeneity of %DEC throughout the sampled subareas. Nevertheless, in general our results are in accordance with other studies showing a good viability of EC in fresh HAM after processing (>80%) (Hennerbichler et al. 2006; Laurent et al. 2014).

The viability of EC was higher after decontamination of HAM with BASE-128 compared to LDS. The lowest %DEC was found after the treatment with BASE-128 for 6 h at 37 °C. Storage for 24 h was less beneficial to the quality of the tissue than storage for 6 h, independent of the type of decontamination solution (BASE-128, LDS). The worst survival rate

of the EC was observed after storage of HAM in AA solutions (and DMEM) at low temperature, 4 °C. This observation is in accordance with some other studies (Jackson et al. 2015), where the best preservation of the cell/tissue morphology was observed at temperatures between 12 and 24 °C. Further research on the effect of storage in various conditions on HAM quality is necessary.

The LDS showed higher toxicity on cells, despite having the composition and concentration of AA (diluted in physiological saline) similar to BASE-128. Although there is no information about the exact composition of BASE-128, specifically about the concentrations of AA, its composition was indicated in the publication of Gatto et al. (2013), describing BASE-128 as a mixture of AA and nutrients diluted in RPMI 1640 medium. It was shown that cells exposed to the stress, such as nutrient deprivation, accumulate reactive oxygen species and eventually die after a relatively short time (Altman and Rathmell 2012; Cabodevilla et al. 2013). Thus, LDS higher cytotoxicity, compared to BASE-128, can be explained by the lack of nutrients, rather than by the presence of AA. Focused mainly on AA, we used LDS of simplified composition in t decontamination is study. As we demonstrated, such solution has no dramatic impact on HAM epithelial cell viability and is simple to prepare at any time in the laboratory, when commercial solution is not available. Moreover, the basic formula of LDS can be optimised by enrichment with nutrient components to improve cell viability.

In our study we selected the TB staining as the fastest and simplest procedure for the detection of dead cells. Combined with the light microscopy we obtained information also about morphological

**Table 5** The mean percentage of the apoptotic mesenchymal cells (%AMC  $\pm$  SD) after HAM decontamination, related to fresh HAM

%AMCs $\pm$ SD ( <i>p</i> -value)	C1: 6 h 37 °C	C2: 24 h RT	C3: 24 h 4 °C
BASE-128	84.9 $\pm$ 14.0 (1.22E-04) ***	86.2 $\pm$ 10.2 (3.38E-05) ***	63.2 $\pm$ 31.5 (0.131)
LDS	82.2 $\pm$ 19.2 (7.853E-04) ***	77.7 $\pm$ 18.3 (0.002) ***	73.7 $\pm$ 17.6 (0.004) ***
DMEM (Co)	87.9 $\pm$ 12.3 (3.823E-05) ***	85.9 $\pm$ 8.2 (2.359E-05)***	75.3 $\pm$ 16.5 (0.002) ***

HAM was decontaminated with BASE-128 or laboratory-made decontamination solution (LDS) or stored in Dulbecco's modified Eagle medium (DMEM) as a control solution (Co). The HAM specimens were incubated for 6 h at 37 °C (C1), for 24 h at room temperature (RT) (C2), or for 24 h at 4 °C (C3). Samples from three placentas were analysed. Statistical significance (Student's *t*-test, unpaired, two-tailed): \* *p* < 0.05; \*\* *p* < 0.01; \*\*\* *p* < 0.005 (*p*-value indicated in brackets)

SD standard deviation

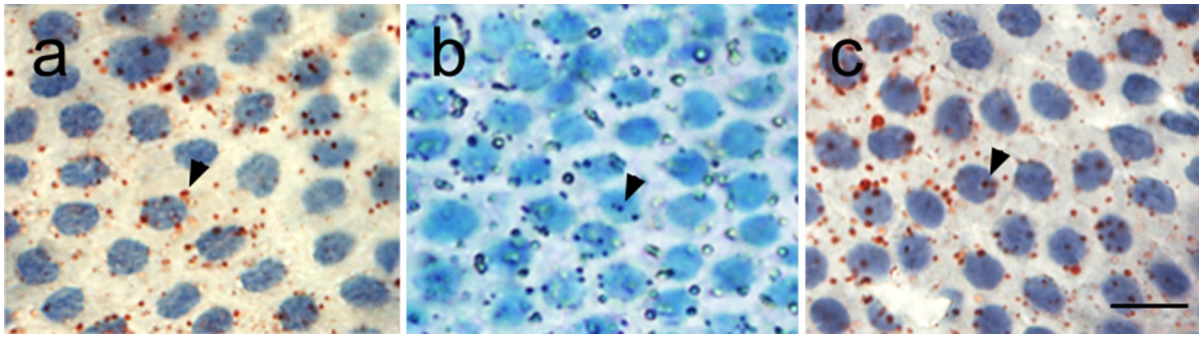


**Fig. 3** The light micrograph of the HAM epithelium, with lipid droplets (*arrowheads*) occurring over and inside the cells in fresh HAM (**a**) and in HAM after incubation in BASE-128 solution for 6 h at 37 °C (**b**, **c**). HAM epithelial cells were

stained with trypan blue (**b**) or Sudan III and Mayer's hematoxylin (**a**, **c**). Magnification 400x. Scale bar represents 20  $\mu$ m

changes in evaluated tissue. Fluorometric cell viability assay has been shown to have higher efficiency than TB staining (Mascotti et al. 2000), however, this technique is time demanding and does not routinely allow to assess multiple specimens in a short time, as we needed for our experiment. Nevertheless, in order to verify the efficiency and reliability of TB staining, we assessed %DEC also via LIVE/DEAD<sup>®</sup> Viability/Cytotoxicity test of the selected samples. The results were very similar to those obtained by TB staining (data not shown). The final values of %DEC were slightly lower using LIVE/DEAD, however the tendency of increase in %DEC with prolonged incubation time and lower temperature was maintained. On the other hand the fluorescent staining showed to be rather impractical, when high number of samples has to be processed in limited time (not mentioning the cost aspect) and therefore we decided to continue processing the samples by TB staining.

Using TUNEL method we found that MSC (exhibiting about 42% apoptotic cells before and 63–88% after decontamination, respectively) are more susceptible to external stress stimuli than EC. The apoptosis of EC did not exceed 2% at both conditions. Partially, this result could be explained by the fact, that AEC are released from the basement membrane (Kumagai et al. 2001) during the procedure, whilst dead MSC remain confined in the stroma. The other plausible explanation is that the cells die by other, rather fast, mechanism than apoptosis (necrosis) and therefore cannot be identified using TUNEL assay. The potential effect of AA on induction of apoptotic cell death was thus not confirmed.

During the microscopic assessment of %DEC tiny droplets through HAM layers have been observed, independent of solution, time and temperature used. They were also present in fresh HAM. Using standard Sudan III staining, we identified them as lipid particles. Their presence can reflect the cellular damage or they can be naturally present in HAM. Further investigation will be necessary in order to explain this phenomenon.

In conclusion, we have shown that there are only small differences in cell survival between the application of commercial and laboratory decontamination solution (BASE-128 and LDS) and we examined various decontamination protocols. These findings may help to better understand the impact of conditions used for the processing and preservation of HAM on the final quality of the potential tissue graft.

**Acknowledgements** The research leading to these results has received funding from the Norwegian Financial Mechanism 2009–2014 and the Ministry of Education, Youth and Sports under Project Contract No. MSMT-28477/2014, Project 7F14156. Institutional support was provided by the PRVOUK-P24/LF1/3 and SVV Project No. 260256/2016 programs of Charles University. Authors thank Brigita Vesela, Dana Sadilkova, Zuzana Rejnysova from Institute of Pathology, First Faculty of Medicine, Charles University and General University Hospital in Prague, Czech Republic, for their excellent technical assistance with the Sudan III staining.

#### Compliance with ethical standards

**Conflict of interest** Ingrida Smeringaiova, Peter Trosan, Miluse Berka Mrstinova, Jan Matecha, Jan Burkert, Jan Bednar and Katerina Jirsova declares that they have no conflict of interest.

## References

- Adds PJ, Hunt CJ, Dart JKG (2001) Amniotic membrane grafts, “fresh” or frozen? A clinical and in vitro comparison. *Br J Ophthalmol* 85(8):905–907
- Akle CA, Adinolfi M, Welsh KI, Leibowitz S, McColl I (1981) Immunogenicity of human amniotic epithelial cells after transplantation into volunteers. *Lancet* 2(8254):1003–1005
- Altman BJ, Rathmell JC (2012) Metabolic stress in autophagy and cell death pathways. *Cold Spring Harb Perspect Biol* 4(9):a008763
- Ashraf NN, Siyal NA, Sultan S, Adhi MI (2015) Comparison of efficacy of storage of amniotic membrane at  $-20$  and  $-80$  °C. *J Coll Physicians Surg Pak* 25(4):264–267
- Aykut V, Celik U, Celik B (2014) The destructive effects of antibiotics on the amniotic membrane ultrastructure. *Int Ophthalmol* 35(3):381–385
- Bourne GL (1960) The microscopic anatomy of the human amnion and chorion. *Am J Obstet Gynecol* 79:1070–1073
- Bourne GL (1962) The foetal membranes. A review of the anatomy of normal amnion and chorion and some aspects of their function. *Postgrad Med J* 38:193–201
- Cabodevilla AG, Sanchez-Caballero L, Nintou E et al (2013) Cell survival during complete nutrient deprivation depends on lipid droplet-fueled  $\alpha$ -oxidation of fatty acids. *J Biol Chem* 288(39):27777–27788
- Dua HS, Gomes JAP, King AJ, Maharajan VS (2004) The amniotic membrane in ophthalmology. *Surv Ophthalmol* 49(1):51–77
- Dua HS, Maharajan VS, Hopkinson A (2006) Controversies and limitations of amniotic membrane in ophthalmic surgery. In: Reinhard T, Larkin DFP (eds) *Cornea and external eye disease*. Springer, Berlin, pp 21–33
- Duan-Arnold Y, Gyurdieva A, Johnson A et al (2015) Soluble factors released by endogenous viable cells enhance the antioxidant and chemoattractive activities of cryopreserved amniotic membrane. *Adv Wound Care* 4(6):329–338
- Ganatra MA, Durrani KM (1996) Method of obtaining and preparation of fresh human amniotic membrane for clinical use. *J Pak Med Assoc* 46(6):126–128
- Gatto C, Giurgola L, D’Amato-Tothova J (2013) A suitable and efficient procedure for the removal of decontaminating antibiotics from tissue allografts. *Cell Tissue Bank* 14(1):107–115
- Gavrieli Y, Sherman Y, Ben-Sasson SA (1992) Identification of programmed cell death in situ via specific labeling of nuclear DNA fragmentation. *J Cell Biol* 119(3):493–501
- Gholipourmalekabadi M, Sameni M, Radenkovic D et al (2016) Decellularized human amniotic membrane: How viable is it as a delivery system for human adipose tissue-derived stromal cells? *Cell Prolif* 49(1):115–121
- Gruss JS, Jirsch DW (1978) Human amniotic membrane: a versatile wound dressing. *Can Med Assoc J* 118(10):1237–1246
- Hennerbichler S, Reichl B, Pleiner D, Gabriel C, Eibl J, Redl H (2006) The influence of various storage conditions on cell viability in amniotic membrane. *Cell Tissue Bank* 8(1):1–8
- Ishino Y, Sano Y, Nakamura T, Connon CJ et al (2004) Amniotic membrane as a carrier for cultivated human corneal endothelial cell transplantation. *Invest Ophthalmol Vis Sci* 45(3):800–806
- Jackson C, Eidet JR, Reppe S, Aass HCD, Tønseth KA, Roald B, Lyberg T, Utheim TP (2015) Effect of storage temperature on the phenotype of cultured epidermal cells stored in xenobiotic-free medium. *Curr Eye Res* 41(6):757–768
- Khokhar S, Sharma N, Kumar H, Soni A (2001) Infection after use of nonpreserved human amniotic membrane for the reconstruction of the ocular surface. *Cornea* 20(7):773–774
- Kim JC, Tseng SC (1995) Transplantation of preserved human amniotic membrane for surface reconstruction in severely damaged rabbit corneas. *Cornea* 14(5):473–484
- King AE, Paltoo A, Kelly RW, Sallenne JM, Bocking AD, Challis JRG (2007) Expression of natural antimicrobials by human placenta and fetal membranes. *Placenta* 28(2–3):161–169
- Kumagai K, Otsuki Y, Ito Y et al (2001) Apoptosis in the normal human amnion at term, independent of Bcl-2 regulation and onset of labour. *Mol Hum Reprod* 7(7):681–689
- Laurent R, Nallet A, Obert L et al (2014) Storage and qualification of viable intact human amniotic graft and technology transfer to a tissue bank. *Cell Tissue Bank* 15(2):267–275
- Lee SH, Tseng SC (1997) Amniotic membrane transplantation for persistent epithelial defects with ulceration. *Am J Ophthalmol* 123(3):303–312
- Lindenmair A, Hatlapatka T, Kollwig G et al (2012) Mesenchymal stem or stromal cells from amnion and umbilical cord tissue and their potential for clinical applications. *Cells* 1(4):1061–1088
- Malhotra C, Jain AK (2014) Human amniotic membrane transplantation: different modalities of its use in ophthalmology. *World J Transplant* 4(2):111–121
- Mamede AC, Carvalho MJ, Abrantes AM et al (2012) Amniotic membrane: from structure and functions to clinical applications. *Cell Tissue Res* 349(2):447–458
- Maral T, Borman H, Arslan H et al (1999) Effectiveness of human amnion preserved long-term in glycerol as a temporary biological dressing. *Burns* 25(7):625–635
- Mascotti K, McCullough J, Burger SR (2000) HPC viability measurement: trypan blue versus acridine orange and propidium iodide. *Transfusion* 40(6):693–696
- Mejía LF, Acosta C, Santamaria JP (2000) Use of nonpreserved human amniotic membrane for the reconstruction of the ocular surface. *Cornea* 19(3):288–291
- Mrázová H, Koller J, Kubišová K et al (2015) Comparison of structural changes in skin and amnion tissue grafts for transplantation induced by gamma and electron beam irradiation for sterilization. *Cell Tissue Bank* 17(2):255–260
- Paolin A, Cogliati E, Trojan D et al (2016) Amniotic membranes in ophthalmology: long term data on transplantation outcomes. *Cell Tissue Bank* 17(1):51–58
- Pegg DE (1989) Viability assays for preserved cells, tissues, and organs. *Cryobiology* 26(3):212–231
- Perepelkin NMJ, Hayward K, Mokoena T et al (2016) Cryopreserved amniotic membrane as transplant allograft: viability and post-transplant outcome. *Cell Tissue Bank* 17(1):39–50
- Rautmann G, Daas A, Buchheit KH (2010) Collaborative study for the establishment of the second international standard for amphotericin B. *Pharmeur Bio Sci Notes* 2010(1):1–13


- Riau AK, Beuerman RW, Lim LS, Mehta JS (2010) Preservation, sterilization and de-epithelialization of human amniotic membrane for use in ocular surface reconstruction. *Biomaterials* 31(2):216–225
- Singh R, Purohit S, Chacharkar MP et al (2007) Microbiological safety and clinical efficacy of radiation sterilized amniotic membranes for treatment of second-degree burns. *Burns* 33(4):505–510
- Tan EK, Cooke M, Mandrycky C et al (2014) Structural and biological comparison of cryopreserved and fresh amniotic membrane tissues. *J Biomater Tissue Eng* 4(5):379–388
- Thomasen H, Pauklin M, Steuhl KP, Meller D (2009) Comparison of cryopreserved and air-dried human amniotic membrane for ophthalmologic applications. *Graefe's Arch Clin Exp Ophthalmol* 247(12):1691–1700
- von Versen-Hoeynck F, Syring C, Bachmann S, Moller DE (2004) The influence of different preservation and sterilization steps on the histological properties of amnion allografts-light and scanning electron microscopic studies. *Cell Tissue Bank* 5(1):45–56
- von Versen-Hoeynck F, Steinfeld AP, Becker J et al (2008) Sterilization and preservation influence the biophysical properties of human amnion grafts. *Biologicals* 36(4):248–255
- Zidan SM, Eleowa SA, Nasef MA et al (2015) Maximizing the safety of glycerol preserved human amniotic membrane as a biological dressing. *Burns* 41(7):1498–1503

### *Appendix 3*

**Smeringaiova I**, Nyc O, Trosan P, Spatenka J, Burkert J, Bednar J, Jirsova K (2018). Antimicrobial efficiency and stability of two decontamination solutions. *Cell Tissue Bank*, 19(4), 581-589.



# Antimicrobial efficiency and stability of two decontamination solutions

Ingrida Smeringaiova  · Otakar Nyc · Peter Trosan · Jaroslav Spatenka · Jan Burkert · Jan Bednar · Katerina Jirsova

Received: 23 May 2018 / Accepted: 22 June 2018  
© Springer Nature B.V. 2018

**Abstract** Two decontamination solutions, commercially produced BASE•128 and laboratory decontamination solution (LDS), with analogous content of antibiotic and antimycotic agents, were compared in their antimicrobial efficiency and stability (pH and osmolarity). Both solutions were compared immediately after thawing aliquots frozen for 1, 3 or 6 months. Agar well diffusion method was used to test their antimicrobial efficiency against five human pathogens: *Staphylococcus aureus*, *Pseudomonas aeruginosa*, *Proteus mirabilis*, *Escherichia coli* and *Enterococcus faecalis*. The difference in the inhibition

of growth between the two decontamination solutions was mostly not statistically significant, with few exceptions. The most pronounced difference between the LDS and BASE•128 was observed in their decontamination efficacy against *E. coli* and *E. faecalis*, where the LDS showed to be more efficient than BASE•128. The osmolarity value of LDS decreased with cold-storage, the osmolarity values of the BASE•128 could not be measured as they were below the range of the osmometer. Slight changes were found in pH of the less stable LDS solution, whose pH increased from initial value  $7.36 \pm 0.07$  to  $7.72 \pm 0.19$  after 6 m-storage. We verified that BASE•128 and LDS are similarly efficient in elimination of possible placental bacterial contaminants and may be used for decontamination of various tissues.

---

I. Smeringaiova · P. Trosan · J. Bednar · K. Jirsova (✉)  
Laboratory of the Biology and Pathology of the Eye,  
Department of Paediatrics and Adolescent Medicine, First  
Faculty of Medicine, Charles University and General  
University Hospital, Prague, Czech Republic  
e-mail: katerina.jirsova@lf1.cuni.cz

I. Smeringaiova · P. Trosan · J. Bednar · K. Jirsova  
Laboratory of the Biology and Pathology of the Eye,  
Institute of Biology and Medical Genetics, First Faculty of  
Medicine, Charles University and General University  
Hospital, Prague, Czech Republic

O. Nyc  
Department of Clinical Microbiology, Second Faculty of  
Medicine, Charles University, Prague, Czech Republic

I. Smeringaiova · P. Trosan · J. Spatenka ·  
J. Burkert · K. Jirsova  
Department of Transplantation and Tissue Bank, Motol  
University Hospital, Prague, Czech Republic

**Keywords** Tissue decontamination · Amniotic membrane decontamination · Antimicrobial efficiency · Decontamination solution

## Introduction

The therapeutic potential of human amniotic membrane (HAM) is increasingly appreciated in a variety of clinical indications, particularly in ophthalmology and chronic wounds treatment due to its positive effect on wound healing—accelerated regeneration with minimal inflammation and scarring (Ilic et al.

2016; Herndon and Branski 2017; Jirsova and Jones 2017). Despite HAM wide-spread use, the general standardized protocol for handling HAM before transplantation surgery has not been adopted yet (Hopkinson et al. 2006; Rahman et al. 2009).

Prior grafting, the sterility of the tissue must be assured. It was demonstrated that the type of the tissue processing and preservation has an impact on final concentrations of endogenous soluble proteins and overall survival of HAM cells (Solomon et al. 2002; Hopkinson et al. 2006; Hennerbichler et al. 2007; Wolbank et al. 2009). It was found that the process of decontamination may be affected by several variables such as temperature, contact period, pH and concentration of the disinfectant, bioburden, organic soil and hardness of water used for dilution (Singh et al. 2012).

When processing HAM several important steps have to be implemented, such as the evaluation of the donor's medical and social history, serological screening of the maternal blood or microbiological screening of HAM before and after its aseptic preparation and processing (Lee and Tseng 1997). Placentas retrieved by vaginal delivery are not considered suitable source of HAM for grafting due to the higher bioburden of pathogens from the vagina compared to placenta obtained during the elective caesarean section delivery (Dua and Azuara-Blanco 1999; Adds et al. 2001). The Gram-positive *Staphylococcus* species are the most prevalent pathogens found on HAM obtained from placentas after both vaginal deliveries and caesarean sections (Gannaway et al. 1984; Aghayan et al. 2013; Binte Atique et al. 2013). Gram-positive bacteria have been also determined as the most frequent cause of microbial infections of HAM transplants in ocular surgery (Marangon et al. 2004). Interestingly, no fungi nor yeast have been detected on HAM samples retrieved either way of the delivery (Gannaway et al. 1984; Adds et al. 2001). In any case, HAM with any positive microbiology result after decontaminating step are unsuitable for grafting (Keitel 2017). Despite sterile processing and grafting of HAM, together with the pre-operative microbiological screening, post-operative contamination by Gram-positive isolates in rates of 1.6–8.0% have been reported (Khokhar et al. 2001; Messmer 2001; Marangon et al. 2004).

The decontamination is a crucial step especially when final sterilisation step is not performed during HAM processing. The tissue can be stored by cryopreservation, lyophilisation or air-drying, the last two

procedures being often followed by gamma irradiation as a final tissue sterilisation step (Burgos and Sergeant 1983; Singh et al. 2003, 2006; Rodriguez-Ares et al. 2009; Mrázová et al. 2016). HAM is typically cryopreserved in glycerol (Maral et al. 1999; Riau et al. 2010; Zidan et al. 2015), in a cultivation medium, e.g. Dulbecco's modified Eagle's medium (DMEM) or Minimum Essential Medium with added glycerol (Kim and Tseng 1995; Lee and Tseng 1997; Thomasen et al. 2009) or in a buffer with added dimethyl sulphoxide (DMSO) (Hanada et al. 2001; Paolin et al. 2016; Perepelkin et al. 2016). The HAM can be cryopreserved also in medium without glycerol (Hennerbichler et al. 2007). Before cryopreservation, HAM is decontaminated typically by treatment with sterile aqueous solutions containing antibiotics and antifungal drugs (Kim et al. 2000; Niknejad et al. 2011; Malhotra and Jain 2014; Keitel 2017). Various decontamination protocols have been published (Lee and Tseng 1997; Laurent et al. 2014; Ashraf et al. 2015; Duan-Arnold et al. 2015; Paolin et al. 2016), but none is generally accepted as a "gold standard". Several certified ready-to-use decontamination solutions are now available, e.g. BASE•128 or X-VIVO 10 media, but there is a lack of optimized decontamination protocols (Rama et al. 2001; Gatto et al. 2013; Perepelkin et al. 2016).

As only a limited number of certified tissue decontamination solutions is commercially available, we have recently proposed an alternative decontamination product with cytotoxicity (as assessed by viability of HAM epithelial cells) comparable with commercial solution BASE•128 (Smringaiova et al. 2017). The decontamination solution prepared in our laboratory (LDS—Laboratory Decontamination Solution) contains only components (physiological saline, antibiotics) approved as medical drugs and therefore it can be readily accepted by national authorities. The purpose of this fellow study was to compare the antimicrobial efficiency and stability (assessed as change of pH and osmolarity) of BASE•128 and LDS, after 1-, 3- and 6-month lasting storage of their respective aliquots.

## Materials and methods

### Decontamination solutions

The main components of the commercial solution BASE•128 (Alchimia, Ponte San Nicolò, Italy) are

Amphotericin B sodium deoxycholate 13,500–16,500 IU/l (14.3–17.5 mg/l; potency: 944 IU/mg) (Rautmann et al. 2010), cefotaxime, gentamicin, vancomycin 115.2–140.8 mg/l (same for the three). Vitamins, glucose, and balanced RPMI 1640 solution are also present in BASE•128 (Gatto et al. 2013). The normal pH of BASE•128 ranges between 7.20 to 7.40 and its osmolality values are 280–320 mOsm/kg (product accompanying information).

The LDS was prepared by mixing a physiological saline (Fresenius Kabi, Bad Homburg, Germany) with the concentrations of the antibiotics and antimycotic selected as the average values of concentration ranges published for BASE•128: Amphotericin B sodium deoxycholate 16 mg/l (Bristol-Myers Squibb, Farmar L'Aigle Usine, France), cefotaxime 130 mg/l, gentamicin 140 mg/l (Lek Pharmaceuticals, Ljubljana, Slovenia), vancomycin 130 mg/l (Mylan, S.A.S., France), as described previously (Smeringaiova et al. 2017).

Three lots of both solutions were used for experiments. Because the BASE•128 is supplied in frozen form, LDS was also frozen after its preparation. Before the experiments, both solutions were thawed (T0) and then frozen in a form of appropriate aliquots. Solutions were then tested after 1 (T1), 3 (T2) and 6 months (T3) of storage at  $-20^{\circ}\text{C}$ . Tested solutions were thawed at  $4^{\circ}\text{C}$  overnight, before the day of antimicrobial and stability testing.

### Bacterial strains

To verify antibacterial activity of the two tested decontamination solutions the multi-resistant isolates from clinical material (Motol University Hospital) or bacteria deposited by a non-profit organization The Czech Collection of Microorganisms (CCM), with defined antibiogram, were used—Table 1. The determined sensitivity to selected antibiotics was interpreted according to the recommendations of Clinical breakpoints—Bacteria, v 8.0 of The European Committee on Antimicrobial Susceptibility Testing (EUCAST) (EUCAST v 8.0 2018) and the Performance Standards for Antimicrobial Susceptibility Testing, 28th Edition of the Clinical and Laboratory Standards Institute (CLSI) (CLSI 28th edn. 2018).

### Antimicrobial activity

Antimicrobial activity test of the solutions was carried out by agar well diffusion method (AWDM). The AWDM is the second well-established method used for antimicrobial susceptibility testing, after the agar disk-diffusion method, used in many clinical microbiology laboratories. Both methods are equally valid for antimicrobial testing (Holder and Boyce 1994; Balouiri et al. 2016).

Three lots of both solutions were used for experiments. The Petri dishes with Mueller–Hinton agar (Oxoid Ltd., Hampshire, England) were inoculated with the bacterial pathogen, grown up to a density of an 0.5-McFarland Standard, then 1-cm wells were cut into the surface of the agar using a cork borer and 100  $\mu\text{l}$  of the decontamination solution, either BASE•128 or LDS, was added into each well. The agar plates were incubated at  $36^{\circ}\text{C}$  for 18 h (in an appropriate atmosphere) to allow the antimicrobial agents to diffuse in the agar medium and inhibit the growth of the microbial strain tested. The experiment was performed twice in triplicates. The diameter (mm) of clear zone around the wells, called the zone of inhibition or inhibitory zone (IZ) was measured by a digital caliper.

### Osmolarity and pH

The pH and osmolality values of both solutions were tested at T0–T3 directly after thawing of respective aliquot. The pH was determined by pH meter InoLAB pH 720 (WTW, Weilheim, Germany). The osmolality values were measured using TearLAB<sup>®</sup> Osmometer (TearLAB Corporation, San Diego, CA), following manufacturer's instructions. Both values, pH and osmolality, were measured at room temperature.

### Statistical analysis

The statistical analysis of collected data was performed using The Excel<sup>®</sup> (Microsoft). The data were expressed as mean  $\pm$  standard deviation (SD). The differences in IZ were evaluated using the Mann–Whitney test (BASE•128  $\times$  LDS at every time point T0–T3) and by Wilcoxon matched-pairs signed-ranks test (aliquot at T0  $\times$  T1  $\times$  T2  $\times$  T3) using the GraphPad Prism software (version 7.04, GraphPad Software, CA, USA). A probability of 5% or less was

**Table 1** Bacterial pathogens and their susceptibility to antibiotics (ATB), used in the present study

Bacterial strain (in-text abbreviation)	Source	Gram $\pm$	ATB susceptibility <sup>a</sup>	ATB resistance <sup>a</sup>
<i>Proteus mirabilis</i> ( <i>P. mirabilis</i> )	Clinical isolate	–	Cefotaxime	Gentamicin, fluoroquinolones
<i>Pseudomonas aeruginosa</i> ( <i>P. aeruginosa</i> )	ATCC <sup>b</sup> 27853	–	Gentamicin	Piperacilin, ceftazidime, carbapenems, fluoroquinolones
<i>Staphylococcus aureus</i> —methicillin resistant ( <i>S. aureus</i> ) isolate	Clinical isolate	+	Vancomycin	Beta-laktam agents, gentamicin, clindamycin, fluoroquinolones
<i>Escherichia coli</i> ( <i>E. coli</i> )	ATCC <sup>b</sup> 25922	–	Cefotaxime (cephalosporins), gentamicin (aminoglycosides)	Only natural resistance
<i>Enterococcus faecalis</i> ( <i>E. faecalis</i> )	ATCC <sup>b</sup> 29212	+	Vancomycin (glycopeptides and lipoglycopeptides)	Only natural resistance

<sup>a</sup>Based on the data from EUCAST and CLSI

<sup>b</sup>Source of bacterial strain: American Type Culture Collection (ATCC)

considered significant. The change of pH and osmolarity was expressed as mean  $\pm$  SD, but the statistical analysis was not performed due to lack of data (two measurements in each sample group).

## Results

### Antimicrobial activity

The antimicrobial activity of tested decontamination solutions, BASE•128 and LDS, was assessed by AWDm and expressed as the IZ value (mean  $\pm$  standard deviation), Table 2.

Both solutions were the most effective at elimination of *P. mirabilis*, whereas the activity of both solutions against *P. mirabilis* remained stable throughout the experiment, Table 2. Both solutions had the second highest antimicrobial activity against *P. aeruginosa*. There was not any statistical difference between the antimicrobial efficacy of both solutions at any time, Table 2.

The BASE•128 and LDS had the lowest antimicrobial activity against *S. aureus*. The only statistically significant difference was observed between the IZ (mm) of BASE•128 and LDS at T0, Table 2.

The BASE•128 showed slightly lower antimicrobial efficiency against *E. coli* and *E. faecalis*, compared to LDS. Both solutions were less efficient against *E. faecalis*, compared to their efficacy against *E. coli*. The differences between the two solutions were statistically significant in all cases, Table 2.

We further compared the IZ between the aliquots of BASE•128 and LDS, after various periods of cold-storage (T0–T3). In a case of *P. mirabilis* and *E. coli*, comparing values of IZ assessed for different periods of storage of solutions, i.e. T0  $\times$  T1  $\times$  T2  $\times$  T3, showed no statistically significant differences, Table 3.

The antimicrobial activity of both solutions against *S. aureus* slightly decreased with cold storage, being the lowest for both solutions at T2, Table 2. As shown in Table 3, when BASE•128 at T1/T2/T3 was compared to BASE•128 at T0, the decrease was statistically significant in all three cases. When LDS at T1/T2/T3 was compared to LDS at T0, the decrease was not statistically significant in any case, Table 3.

In case of *P. aeruginosa*, the antimicrobial efficacy of BASE•128 did not change significantly with prolonged storage (T1–T3), compared to solution at T0, Table 3. However, the antimicrobial efficacy of LDS against *P. aeruginosa* slightly decreased with prolonged storage, with lowest mean IZ (mm) value for LDS at T3, Table 2. This decrease was statistically significant, when compared to LDS at T1/T2/T3, Table 3.

Compared to BASE•128 at T0, the efficacy of BASE•128 against *E. faecalis* did not significantly change with prolonged storage. The highest efficacy against *E. faecalis* had the BASE•128 at T1 and this efficacy decreased with cold storage (T2, T3). This decrease was statistically significant only in two cases, Table 3. Antimicrobial efficacy of LDS against *E. faecalis* did not significantly change with prolonged storage, Table 3.

**Table 2** The effect of cold storage of BASE•128 and LDS, on their antimicrobial activity against five bacterial strains

Organism	IZ (mm), mean ± SD							
	BASE•128				LDS			
	T0	T1	T2	T3	T0	T1	T2	T3
<i>P. mirabilis</i>	49.8 ± 0.4	49.0 ± 0	49.0 ± 0	49.2 ± 0.8	49.8 ± 0.4	49.3 ± 0.5	50.0 ± 0 (0.001)***	49.0 ± 1.1
<i>P. aeruginosa</i>	39.6 ± 2.9	39.4 ± 3.1	39.7 ± 2.5	39.1 ± 3.8	40.3 ± 2.9	40.0 ± 2.5	39.5 ± 2.0	38.3 ± 3.3
<i>S. aureus</i>	30.5 ± 0.5 (0.015)*	29.0 ± 0	27.3 ± 0.5	28.2 ± 0.1	29.2 ± 0.8	28.7 ± 0.5	27.2 ± 0.4	27.3 ± 0.5
<i>E. coli</i>	35.3 ± 0.5	36.7 ± 0.5	36.0 ± 0	35.3 ± 0.5	37.8 ± 0.4 (0.003)**	37.8 ± 0.4 (0.007)*	37.3 ± 0.8 (0.009)*	36.5 ± 0.5 (0.013)*
<i>E. faecalis</i>	32.3 ± 0.5	32.7 ± 0.5	31.5 ± 0.5	31.0 ± 0.6	37.0 ± 0 (0.002)**	36.0 ± 0.6 (0.004)**	36.7 ± 0.5 (0.004)**	36.5 ± 0.5 (0.004)**

The effect is expressed as a mean ± standard deviation (SD) of a diameter (mm) of the inhibitory zone (IZ), assessed by agar-well diffusion method. Statistically significant difference between the IZ of the two solutions, cold-stored for a period of 0 (T0), 1 (T1), 3 (T2) or 6 months (T3), was counted—the *P* values: \**P* ≤ 0.05; \*\**P* ≤ 0.005; \*\*\**P* ≤ 0.001. The *P* values ≤ 0.05 are indicated in brackets, below the numerically higher mean IZ value out of a pair of means, relevant to compared solutions

**Table 3** Statistical significance of difference in inhibitory zones (IZ) between 0 (T0), 1 (T1), 3 (T2) or 6 months (T3)-stored solution (BASE•128, LDS). The antimicrobial efficiency was tested against five bacterial strains

Organism	Wilcoxon test – IZ ( <i>P</i> value)								
	BASE•128				LDS				
	T0	T1	T2	T3	T0	T1	T2	T3	
<i>P. mirabilis</i>	Difference not significant between any of the compared groups								
<i>P. aeruginosa</i>	ns				T0	–	ns	ns	0.001***
					T1	ns	–		0.001***
					T2	ns	ns	–	0.039*
					T3	0.001***	0.001***	0.039*	–
<i>S. aureus</i>	T0	T1	T2	T3	T0	T1	T2	T3	
	–	0.031*	0.031*	0.031*	T0	–	ns	ns	ns
	0.031*	–	0.031*	ns	T1	ns	–	0.031*	0.031*
	0.031*	0.031*	–	ns	T2	ns	0.031*	–	ns
	0.031*	ns	ns	–	T3	ns	0.031*	ns	–
<i>E. coli</i>	Difference not significant between any of the compared groups								
<i>E. faecalis</i>	T0	T1	T2	T3	T0	T1	T2	T3	
	–	ns	ns	ns	T0	ns			
	ns	–	0.031*	0.031*	T1				
	ns	0.031*	–	ns	T2				
	ns	0.031*	ns	–	T3				

Statistical significance (*P* value): \**P* ≤ 0.05; \*\**P* ≤ 0.005; \*\*\**P* ≤ 0.001, *ns* not significant

## Physical parameters

The LDS had higher pH values after storage, compared to BASE•128, Table 4. The most pronounced difference could be seen between the pH value of T3-LDS (pH  $7.72 \pm 0.19$ ) and T3-BASE•128 (pH  $7.58 \pm 0.07$ ), and between the T3-LDS and T0-LDS (pH  $7.36 \pm 0.07$ ). The osmolarity values of the BASE•128 were mostly below range of the osmolarity measurement instrument, used in the study. However, the osmolarity values of LDS could be measured and they dropped from 392.00 units (T0) to 277.50 units (T3), Table 4.

## Discussion

We evaluated and compared the antimicrobial efficacy and stability in time of two solutions, BASE•128 and LDS, which can be used for the decontamination of HAM prior to its surgical application. This study is a follow-up to our previous research (Smeringaiova et al. 2017), in which we compared the effect of the same solutions on viability of cells present in HAM.

We used both standard and clinical bacterial strains to investigate antibacterial property of the decontamination solutions by simple and quick method, the AWDM, which allows a comparison of inhibitory activity levels of the tested substances.

Both solutions were the most effective at elimination of *P. mirabilis*, the Gram-negative bacterium, which is susceptible to most antibiotics, except tetracyclines (EUCAST v 8.0 2018; CLSI 28th edn. 2018). *Proteus* species are part of normal human intestinal flora, but can also colonize both the skin and oral mucosa of patients and hospital personnel. *P.*

*mirabilis* causes 90% of *Proteus* infections (Gonzales 2017). According to the data from EUCAST and CLSI, the *P. mirabilis* is sensitive to cefotaxime, with the following susceptibility breakpoints: IZ  $\geq 20$  mm (EUCAST); IZ  $\geq 26$  or 23 mm (CLSI), assessed by the disk diffusion method. Our data shows that both solutions had sufficient antimicrobial efficacy against the *P. mirabilis*, with the IZ about 49 mm, and that they both retained antimicrobial efficacy against *P. mirabilis* after prolonged storage.

The decontamination efficacy of the two solutions against the remaining three common bacterial species was as follows: *P. aeruginosa* > *E. coli* > *E. faecalis*. The Gram-negative bacteria *P. aeruginosa* is a multi-drug resistant pathogen, susceptible to gentamicin. *P. aeruginosa* is one of the most frequent bacteria linked with ventilator-associated pneumonia (Friedrich 2017; Ramirez-Estrada et al. 2016). The *P. aeruginosa* was also detected in patients following HAM transplantation (Marangon et al. 2004). The susceptibility breakpoints of gentamicin for *P. aeruginosa* are: IZ  $\geq 15$  mm (EUCAST, CLSI). Despite small numerical differences, the efficacy of both solutions against *P. aeruginosa* was similar and the IZ reached values greater than the susceptibility breakpoints. The BASE•128 retained its antimicrobial efficacy after prolonged storage, thus being more stable than LDS.

The *E. coli*, present in normal human gastrointestinal tract, is responsible for common (extra-) intestinal bacterial infections, such as urinary tract infection, wound infections, neonatal sepsis, etc. It is a Gram-negative bacterium, most frequently found in the genital tract of women (Guiral et al. 2011), thus the *E. coli* is present on HAM after normal vaginal delivery (Gannaway et al. 1984; Adds et al. 2001). Standardly, these bacteria are sensitive to

**Table 4** Stability of the tested solutions (BASE•128, LDS), stored for different time-periods, i.e. 0 (T0), 1 (T1), 3 (T2) or 6 months (T3), expressed as changes in pH and osmolarity

Parameter	Mean $\pm$ SD									
	BASE•128				LDS					
	T0	T1	T2	T3	T0	T1	T2	T3	T3	
pH	7.46	$7.61 \pm 0.03$	$7.52 \pm 0.09$	$7.58 \pm 0.07$	$7.36 \pm 0.07$	$7.61 \pm 0.07$	$7.60 \pm 0.03$	$7.72 \pm 0.19$		
Osmol (mOsm/l)	BR	$288.50 \pm 19.90$	BR	BR	392.00	$285.00 \pm 4.24$	$285.00 \pm 8.49$	$277.50 \pm 2.12$		

BR below range of TearLAB® Osmometer



cephalosporins (cefotaxime) or aminoglycosides (gentamicin) (Madappa 2017). The EUCAST and CLSI susceptibility breakpoints of cefotaxime for *E. coli* are the same as for the *P. mirabilis*, the susceptibility breakpoints of gentamicin for *E. coli* are as follows: the  $IZ \geq 17$  mm (EUCAST) and  $IZ \geq 15$  mm (CLSI).

*Enterococci* are part of the normal human intestinal flora. These Gram-positive bacteria can cause life-threatening infections in humans. The *E. faecalis* can be found on HAM after both vaginal and caesarean section delivery (Addis et al. 2001). These bacteria are resistant to many commonly used antimicrobial agents; resistance to vancomycin is becoming more common (Faron et al. 2016). The susceptibility breakpoints of vancomycin for *E. faecalis* are as follows: the  $IZ \geq 12$  mm (EUCAST) and  $IZ \geq 17$  mm (CLSI). Both tested solutions were efficient against the *E. coli* and *E. faecalis*. However, the LDS was more efficient against the *E. coli* and *E. faecalis* than BASE•128, and this difference was statistically significant. The efficacy of BASE•128 against *E. coli* was better than that against *E. faecalis*.

The *S. aureus* is Gram-positive bacteria causing serious infections with growing incidence, accompanied by a rise in antibiotic-resistant strains, such as methicillin-resistant *S. aureus* and vancomycin-resistant strains (WHO 2018; Baorto 2017; de Kraker et al. 2011). The *S. aureus* is present on HAM after both vaginal and caesarean section delivery (Addis et al. 2001; Marangon et al. 2004; Aghayan et al. 2013). The susceptibility breakpoints of vancomycin are reported only in a form of minimum-inhibitory concentrations by EUCAST and CLSI. In our study, both tested solutions showed the lowest efficacy against *S. aureus*. At T0, the BASE•128 was slightly more efficient in elimination of *S. aureus* than LDS, and the efficacy of BASE•128 decreased after cold storage. Of note, the vancomycin is a glycopeptide with a large molecule (molar mass  $1449.3 \text{ g mol}^{-1}$ ) thus its diffusion rate in the Mueller–Hinton agar is slower than that of cefotaxime (molar mass  $455.5 \text{ g mol}^{-1}$ ) and gentamicin (molar mass  $477.6 \text{ g mol}^{-1}$ ). This may partially explain the lowest diameters of the IZ detected in case of *E. faecalis* and *S. aureus*, both susceptible to vancomycin. On the other hand, the bactericidal in vitro effect of vancomycin is enhanced, when used in combination with cefotaxime and gentamicin (Lam and Bayer 1984).

We observed the changes in pH and osmolarity of the two decontamination solutions, which are standardly cold-stored as batches before use. The reason of such storage is primarily the preservation of the substances, such as antibiotics or vitamins, in their active state. The starting pH of BASE•128 (T0) was 7.46, and slightly increased after cold storage (pH 7.58 after 6 months). The normal pH of fresh BASE•128 is pH 7.20–7.40. The BASE•128 was used as a reference solution to LDS, thus was frozen and thawed more than one time, as recommended by manufacturer. The pH change of LDS was more prominent, with an increase from pH 7.36 (T0) to pH 7.72 after 6 months (T3). Thus, the use of both solutions in fresh state is preferred, especially if the preservation of vital cells in HAM is important. Due to lack of data for BASE•128 it is difficult to compare the differences in osmolarity values between the two tested solutions. From a collected data, specifically the pH values, it seems that the BASE•128 is, with its current formula, a slightly more physiochemically stable solution than LDS, however, the improvement of formula of LDS is possible in the future.

There is a lack of solutions for decontamination of HAM before its use, which is essential to avoid transmission of pathogens from donors to patients. In our previous study (Smeringaiova et al. 2017) we offered the LDS, as an alternative solution to commercial BASE•128, with a sufficient preservation of viable epithelial cells in HAM. In this study we showed that the antimicrobial efficacy of LDS against common clinical pathogens is comparable to the one of BASE•128, and that the stability of LDS is good, but can be improved by proper changing of the current formula. In general, the differences between the two solutions are very weak and both solutions are suitable for successful HAM decontamination.

**Acknowledgements** This work was supported by European Regional Development Fund, Project BBMRI-CZ III: EF16\_013/0001674. Institutional support was provided by Progres-Q26/LF1 and by SVV, Project 260367/2017.

#### Compliance with ethical standards

**Conflict of interest** The authors declare that they have no conflicts of interest. The funding organizations had no role in the design or conduct of this research.

## References

- Adds PJ, Hunt C, Hartley S (2001) Bacterial contamination of amniotic membrane. *Br J Ophthalmol* 85(2):228–230
- Aghayan HR, Goodarzi P, Baradaran-Rafii A, Larijani B, Moradabadi L, Rahim F, Arjmand B (2013) Bacterial contamination of amniotic membrane in a tissue bank from Iran. *Cell Tissue Bank* 14(3):401–406
- Ashraf NN, Siyal NA, Sultan S, Adhi MI (2015) Comparison of efficacy of storage of amniotic membrane at 20 and 80 degrees centigrade. *J Coll Phys Surg Pak* 25(4):264–267
- Balouiri M, Sadiki M, Ibnsouda SK (2016) Methods for in vitro evaluating antimicrobial activity: a review. *J Pharm Anal* 6(2):71–79
- Baorto EP (2017) *Staphylococcus aureus* infection. Medscape. <https://emedicine.medscape.com/article/971358-overview>. Accessed 11 May 2018
- Binte Atique F, Ahmed KT, Asaduzzaman SM, Hasan KN (2013) Effects of gamma irradiation on bacterial microflora associated with human amniotic membrane. *Biomed Res Int* 2013:586561
- Burgos H, Sergeant RJ (1983) Lyophilized human amniotic membranes used in reconstruction of the ear. *J R Soc Med* 76(5):433
- Clinical and Laboratory Standards Institute (2018) M100—performance standards for antimicrobial susceptibility testing, 28th edn. Clinical and Laboratory Standards Institute, Wayne
- de Kraker ME, Wolkewitz M, Davey PG, Koller W, Berger J, Nagler J et al (2011) Clinical impact of antimicrobial resistance in European hospitals: excess mortality and length of hospital stay related to methicillin-resistant *Staphylococcus aureus* bloodstream infections. *Antimicrob Agents Chemother* 55(4):1598–1605
- Dua HS, Azuara-Blanco A (1999) Amniotic membrane transplantation. *Br J Ophthalmol* 83(6):748–752
- Duan-Arnold Y, Gyurdieva A, Johnson A, Jacobstein DA, Danilkovitch A (2015) Soluble factors released by endogenous viable cells enhance the antioxidant and chemoattractive activities of cryopreserved amniotic membrane. *Adv Wound Care* 4(6):329–338
- Faron ML, Ledeboer NA, Buchan BW (2016) resistance mechanisms, epidemiology, and approaches to screening for vancomycin-resistant enterococcus in the health care setting. *J Clin Microbiol* 54(10):2436–2447
- Friedrich M (2017) *Pseudomonas aeruginosa* infections. Medscape. <https://emedicine.medscape.com/article/226748-overview>. Accessed 10 May 2018
- Gannaway WL, Barry AL, Trelford JD (1984) Preparation of amniotic membranes for surgical use with antibiotic solutions. *Surgery* 95(5):580–585
- Gatto C, Giurgola L, D'Amato Tothova J (2013) A suitable and efficient procedure for the removal of decontaminating antibiotics from tissue allografts. *Cell Tissue Bank* 14(1):107–115
- Gonzales G (2017) *Proteus* infections. Medscape. <https://emedicine.medscape.com/article/226434-overview>. Accessed 10 May 2018
- Guiral E, Bosch J, Vila J, Soto SM (2011) Prevalence of *Escherichia coli* among samples collected from the genital tract in pregnant and nonpregnant women: relationship with virulence. *FEMS Microbiol Lett* 314(2):170–173
- Hanada K, Shimazaki J, Shimmura S, Tsubota K (2001) Multilayered amniotic membrane transplantation for severe ulceration of the cornea and sclera. *Am J Ophthalmol* 131(3):324–331
- Hennerbichler S, Reichl B, Pleiner D, Gabriel CH, Eibl J, Redl H (2007) The influence of various storage conditions on cell viability in amniotic membrane. *Cell Tissue Bank* 8(1):1–8
- Herndon DN, Branski LK (2017) Contemporary methods allowing for safe and convenient use of amniotic membrane as a biologic wound dressing for burns. *Ann Plast Surg* 78(2 Suppl 1):S9–S10
- Holder IA, Boyce ST (1994) Agar well diffusion assay testing of bacterial susceptibility to various antimicrobials in concentrations non-toxic for human cells in culture. *Burns* 20(5):426–429
- Hopkinson A, McIntosh RS, Tighe PJ, James DK, Dua HS (2006) Amniotic membrane for ocular surface reconstruction: donor variations and the effect of handling on TGF-beta content. *Investig Ophthalmol Vis Sci* 47(10):4316–4322
- Ilic D, Vicovac L, Nikolic M, Lazic Ilic E (2016) Human amniotic membrane grafts in therapy of chronic non-healing wounds. *Br Med Bull* 117(1):59–67
- Jirsova K, Jones GLA (2017) Amniotic membrane in ophthalmology: properties, preparation, storage and indications for grafting—a review. *Cell Tissue Bank* 18(2):193–204
- Keitel S (2017) Guide to the quality and safety of tissues and cells for human application, European Committee (Partial Agreement) on organ transplantation, European Directorate for the Quality of Medicines and HealthCare (EDQM), 3rd edn, Council of Europe, pp 197–201
- Khokhar S, Sharma N, Kumar H, Soni A (2001) Infection after use of nonpreserved human amniotic membrane for the reconstruction of the ocular surface. *Cornea* 20(7):773–774
- Kim JC, Tseng SC (1995) Transplantation of preserved human amniotic membrane for surface reconstruction in severely damaged rabbit corneas. *Cornea* 14(5):473–484
- Kim JS, Kim JC, Na BK, Jeong JM, Song CY (2000) Amniotic membrane patching promotes healing and inhibits proteinase activity on wound healing following acute corneal alkali burn. *Exp Eye Res* 70(3):329–337
- Lam K, Bayer AS (1984) In vitro bactericidal synergy of gentamicin combined with penicillin G, vancomycin, or cefotaxime against group G streptococci. *Antimicrob Agents Chemother* 26(2):260–262
- Laurent R, Nallet A, Obert L, Nicod L, Gindraux F (2014) Storage and qualification of viable intact human amniotic graft and technology transfer to a tissue bank. *Cell Tissue Bank* 15(2):267–275
- Lee SH, Tseng SC (1997) Amniotic membrane transplantation for persistent epithelial defects with ulceration. *Am J Ophthalmol* 123(3):303–312
- Madappa T (2017) *Escherichia coli* (*E. coli*) infections medication. medscape. <https://emedicine.medscape.com/article/217485-medication>. Accessed 10 Feb 2018
- Malhotra C, Jain AK (2014) Human amniotic membrane transplantation: different modalities of its use in ophthalmology. *World J Transplant* 4(2):111–121

- Maral T, Borman H, Arslan H, Demirhan B, Akinbingol G, Haberal M (1999) Effectiveness of human amnion preserved long-term in glycerol as a temporary biological dressing. *Burns* 25(7):625–635
- Marangon FB, Alfonso EC, Miller D, Remonda NM, Muallem MS, Tseng SC (2004) Incidence of microbial infection after amniotic membrane transplantation. *Cornea* 23(3):264–269
- Messmer EM (2001) Hypopyon after amniotic membrane transplantation. *Ophthalmology* 108(10):1714–1715
- Mrázová H, Koller J, Kubišová K, Fujeříková G, Klincová E, Babal P (2016) Comparison of structural changes in skin and amnion tissue grafts for transplantation induced by gamma and electron beam irradiation for sterilization. *Cell Tissue Bank* 17(2):255–260
- Niknejad H, Deihim T, Solati-Hashjin M, Peirovi H (2011) The effects of preservation procedures on amniotic membrane's ability to serve as a substrate for cultivation of endothelial cells. *Cryobiology* 63(3):145–151
- Paolin A, Cogliati E, Trojan D, Griffoni C, Grassetto A, Elbadawy HM, Ponzin D (2016) Amniotic membranes in ophthalmology: long term data on transplantation outcomes. *Cell Tissue Bank* 17(1):51–58
- Perepelkin NMJ, Hayward K, Mokoena T, Bentley MJ, Ross-Rodriguez LU, Marquez-Curtis L, McGann LE, Holovati JL, Elliott JA (2016) Cryopreserved amniotic membrane as transplant allograft: viability and post-transplant outcome. *Cell Tissue Bank* 17(1):39–50
- Rahman I, Said DG, Maharajan VS, Dua HS (2009) Amniotic membrane in ophthalmology: indications and limitations. *Eye (Lond)* 23(10):1954–1961
- Rama P, Giannini R, Bruni A, Gatto C, Tiso R, Ponzin D (2001) Further evaluation of amniotic membrane banking for transplantation in ocular surface diseases. *Cell Tissue Bank* 2(3):155–163
- Ramirez Estrada S, Borgatta B, Rello J (2016) *Pseudomonas aeruginosa* ventilator-associated pneumonia management. *Infect Drug Resist* 20(9):7–18
- Rautmann G, Daas A, Buchheit KH (2010) Collaborative study for the establishment of the second international standard for amphotericin B. *Pharmeuropa Bio Sci Notes* 1:1–13
- Riau AK, Beuerman RW, Lim LS, Mehta JS (2010) Preservation, sterilization and de-epithelialization of human amniotic membrane for use in ocular surface reconstruction. *Biomaterials* 31(2):216–225
- Rodriguez-Ares MT, López-Valladares MJ, Touriño R, Vieites B, Gude F, Silva MT, Couceiro J (2009) Effects of lyophilization on human amniotic membrane. *Acta Ophthalmol* 87(4):396–403
- Singh R, Gupta P, Kumar P, Kumar A, Chacharkar MP (2003) Properties of air dried radiation processed amniotic membranes under different storage conditions. *Cell Tissue Bank* 4(2–4):95–100
- Singh R, Gupta P, Purohit S, Kumar P, Vajjapurkar SG, Chacharkar MP (2006) Radiation resistance of the microflora associated with amniotic membranes. *World J Microbiol Biotechnol* 22(1):23–27
- Singh M, Sharma R, Gupta PK, Rana JK, Sharma M, Taneja N (2012) Comparative efficacy evaluation of disinfectants routinely used in hospital practice: India. *Indian J Crit Care Med* 16(3):123
- Smeringaiova I, Trosan P, Mrstinova MB, Matecha J, Burkert J, Bednar J, Jirsova K (2017) Comparison of impact of two decontamination solutions on the viability of the cells in human amnion. *Cell Tissue Bank* 18(3):413–423
- Solomon A, Meller D, Prabhasawat P, John T, Espana EM, Steuhl KP, Tseng SC (2002) Amniotic membrane grafts for nontraumatic corneal perforations, descemetocoeles, and deep ulcers. *Ophthalmology* 109(4):694–703
- The European Committee on Antimicrobial Susceptibility Testing (EUCAST) (2018) Breakpoint tables for interpretation of MICs and zone diameters. Version 8.0. <http://www.eucast.org>. Accessed 5 Feb 2018
- Thomassen H, Pauklin M, Steuhl KP, Meller D (2009) Comparison of cryopreserved and air-dried human amniotic membrane for ophthalmologic applications. *Graefes Arch Clin Exp Ophthalmol* 247(12):1691–1700
- Wolbank S, Hildner F, Redl H, van Griensven M, Gabriel C, Hennerbichler S (2009) Impact of human amniotic membrane preparation on release of angiogenic factors. *J Tissue Eng Regen Med* 3(8):651–654
- World Health Organization (2018) WHO publishes list of bacteria for which new antibiotics are urgently needed. <http://www.who.int/en/news-room/detail/27-02-2017-who-publishes-list-of-bacteria-for-which-new-antibiotics-are-urgently-needed>. Accessed 11 May 2018
- Zidan SM, Eleowa SA, Nasef MA, Abd-Almuktader MA, Elbatawy AM, Borhamy AG, Aboliela MA, Ali AM, Algamil MR (2015) Maximizing the safety of glycerol preserved human amniotic membrane as a biological dressing. *Burns* 41(7):1498–1503

#### *Appendix 4*

Trosan P, **Smeringaiova I**, Brejchova K, Bednar J, Benada O, Kofronova O, Jirsova K (2018). The enzymatic de-epithelialization technique determines denuded amniotic membrane integrity and viability of harvested epithelial cells. PloS one, 13(3), e0194820.

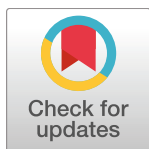
RESEARCH ARTICLE

# The enzymatic de-epithelialization technique determines denuded amniotic membrane integrity and viability of harvested epithelial cells

Peter Trosan<sup>1,2\*</sup>, Ingrida Smeringaiova<sup>1,2</sup>, Kristyna Brejchova<sup>1</sup>, Jan Bednar<sup>1,2</sup>, Oldrich Benada<sup>3</sup>, Olga Kofronova<sup>3</sup>, Katerina Jirsova<sup>1,2</sup>

**1** Laboratory of the Biology and Pathology of the Eye, Department of Paediatrics and Adolescent Medicine, First Faculty of Medicine, Charles University and General University Hospital, Prague, Czech Republic, **2** Laboratory of the Biology and Pathology of the Eye, Institute of Biology and Medical Genetics, First Faculty of Medicine, Charles University and General University Hospital, Prague, Czech Republic, **3** Institute of Microbiology of the Czech Academy of Sciences, Prague, Czech Republic

\* [peter.trosan@lf1.cuni.cz](mailto:peter.trosan@lf1.cuni.cz)



**OPEN ACCESS**

**Citation:** Trosan P, Smeringaiova I, Brejchova K, Bednar J, Benada O, Kofronova O, et al. (2018) The enzymatic de-epithelialization technique determines denuded amniotic membrane integrity and viability of harvested epithelial cells. PLoS ONE 13(3): e0194820. <https://doi.org/10.1371/journal.pone.0194820>

**Editor:** Alexander V. Ljubimov, Cedars-Sinai Medical Center, UNITED STATES

**Received:** October 6, 2017

**Accepted:** March 9, 2018

**Published:** March 27, 2018

**Copyright:** © 2018 Trosan et al. This is an open access article distributed under the terms of the [Creative Commons Attribution License](https://creativecommons.org/licenses/by/4.0/), which permits unrestricted use, distribution, and reproduction in any medium, provided the original author and source are credited.

**Data Availability Statement:** The authors confirm that all data underlying the findings are fully available without restriction. All relevant data are within the paper.

**Funding:** This work was supported by the Norwegian Financial Mechanism 2009-2014 and the Ministry of Education, Youth and Sports under Project Contract no. MSMT-28477/2014, project 7F14156 (<http://www.msmt.cz/vyzkum-a-vyvoj-2/financial-andreporting-issues-in-the-czech->

## Abstract

The human amniotic membrane (HAM) is widely used for its wound healing effect in clinical practice, as a feeder for the cell cultivation, or a source of cells to be used in cell therapy. The aim of this study was to find effective and safe enzymatic HAM de-epithelialization method leading to harvesting of both denuded undamaged HAM and viable human amniotic epithelial cells (hAECs). The efficiency of de-epithelialization using TrypLE Express, trypsin/ethylenediaminetetraacetic (EDTA), and thermolysin was monitored by hematoxylin and eosin staining and by the measurement of DNA concentration. The cell viability was determined by trypan blue staining. Scanning electron microscopy and immunodetection of collagen type IV and laminin  $\alpha 5$  chain were used to check the basement membrane integrity. De-epithelialized hAECs were cultured and their stemness properties and proliferation potential was assessed after each passage. The HAM was successfully de-epithelialized using all three types of reagents, but morphological changes in basement membrane and stroma were observed after the thermolysin application. About 60% of cells remained viable using trypsin/EDTA, approximately 6% using TrypLE Express, and all cells were lethally damaged after thermolysin application. The hAECs isolated using trypsin/EDTA were successfully cultured up to the 5<sup>th</sup> passage with increasing proliferation potential and decreased stem cell markers expression (*NANOG*, *SOX2*) in prolonged cell culture. Trypsin/EDTA technique was the most efficient for obtaining both undamaged denuded HAM and viable hAECs for consequent culture.

norwegian). This study was further supported by the Progres Q25/LF1 (<http://www.cuni.cz/UK-7368.html>), European Regional Development Fund, project EF16\_013/0001674 ([http://ec.europa.eu/regional\\_policy/en/funding/erdf/](http://ec.europa.eu/regional_policy/en/funding/erdf/)) and by BBMRI\_CZ LM2015089 (<http://biobanka.lf1.cuni.cz/cz/>) projects. PT was supported by SVV, project 260367/2017 (<http://www.cuni.cz/UK-3362.html>). The electron microscopy facility of IMIC was supported by the project LO1509 of the Ministry of Education, Youth and Sports of the Czech Republic (<http://www.msmt.cz/?lang=2>).

**Competing interests:** The authors have declared that no competing interests exist.

## Introduction

The human amniotic membrane (HAM) is the inner layer of the fetal membranes. It consists of a single layer of epithelial cells, basement membrane (BM), and an avascular stroma [1]. The two cell types of different embryological origin are located in the HAM: human amniotic epithelial cells (hAECs) derived from the embryonic ectoderm, and mesenchymal stromal cells (hAMSCs) derived from the embryonic mesoderm [1].

The wound healing effect of HAM mediated by numerous growth factors and cytokines and the presence of stem cells continuously increase interest in its potential in the medical treatment and tissue engineering [2–7]. The application of HAM is best established in ophthalmology, where it is used clinically for its wound-healing effect and as a substrate for limbal stem cells (LSCs) cultivation and consequent treatment in limbal stem cells deficiency (LSCD) [8].

Many published reports discussed whether intact or denuded HAM is more suitable for culture of LSCs. It has been shown that intact HAM mostly supports the growth of limbal explants [9–11], while denuded HAM is more suitable as a substrate for enzymatically dispersed LSCs [12–17]. Koizumi et al. found that denuded HAM supported the growth of well-stratified and differentiated LSCs, while on intact HAM a monolayer of less differentiated limbal cells was formed [18]. LSCs cultured on denuded HAM were better attached to the stroma [18].

The expression of stemness genes, e.g. octamer-4 (OCT-4), sex determining region Y-box 2 (SOX2), fibroblast growth factor 4, zinc finger protein 42 (REX-1), nanog homeobox (NANOG), ATP-binding cassette sub-family G member 2 (ABCG2) and bone marrow stromal cell antigen-1 (BST-1), was reported in hAECs [19]. The hAECs have highly multipotent differentiation ability and could be differentiated into all three germ layers [20]. Furthermore, these cells have immunoprivileged characteristics, expressing only very low levels of class IA and II human leukocyte antigens [21]. The ability to differentiate, low immunogenicity and anti-inflammatory effect indicate their potential to be used in the treatment of a various diseases and disorders, such as the treatment of Type I diabetes [22] or cardiovascular regeneration [23]. The hAECs can also be utilized for tissue engineering of skin [24] or as a feeder for expanding of various stem cells types, including human LSCs [22], or human and murine embryonic stem cells [25, 26]. Li et al. found that supernatant from hAECs inhibited the chemotactic activity of neutrophils and macrophages as well as reduced the proliferation of T and B cells after mitogenic stimulation [27].

Denuded HAM and hAECs can therefore be used separately for various purposes. Several approaches and methods exist to denude HAM. The most frequently used method is treatment with the trypsin/ethylenediaminetetraacetic acid (EDTA) [28, 29]. Besides that, sodium dodecyl sulphate (SDS) [30], Tris/EDTA followed by incubation with SDS [31], Tris/EDTA/aprotinin [32], EDTA [18], thermolysin [33], dispase [14] NaOH [34], or ammonium hydroxide [35], were successfully used.

The best established method for the isolation of viable hAECs is the trypsin/EDTA treatment [36–40], and its modified forms like several trypsin/EDTA incubation steps [41] or treatment with dispase [42, 43].

Each of the mentioned techniques has different effects on biological and physical properties of both HAM and hAECs. Many of these treatments take hours and may damage denuded HAM integrity, or viability of hAECs and hAMSCs or decrease the activity of growth factors. EDTA itself does not remove epithelium completely [14, 17], treatment with dispase can damage BM structure [13]. However, these studies were focused on either de-epithelialization or on obtaining of viable hAECs only.



In this study, TrypLE Express, trypsin/EDTA and thermolysin were applied to obtain both viable hAECs and undamaged denuded HAM at the same time. TrypLE Express is a recombinant fungal trypsin-like protease with similar dissociation kinetics to porcine trypsin, which has been successfully used for dissociation of human pluripotent stem cells [44]. Trypsin/EDTA application is generally used to detach seeding cells from the culture flask and for de-epithelialization of HAM [13, 36, 39]. Thermolysin is a zinc neutral, heat-stable metalloproteinase isolated from the *Bacillus stearothermophilus*, and it has been demonstrated that its use generated fully denuded HAM without any mechanical scrapping [33].

The aim of our study was to identify an enzymatic method which would result in two simultaneous advantages: 1) a complete HAM de-epithelialization safe for BM and stroma, and 2) harvesting viable hAECs usable for subsequent culture.

## Materials and methods

### Tissue

The study followed the standards of the Ethics Committee of Motol University Hospital, Prague and the General Teaching Hospital and 1<sup>st</sup> Medical Faculty of Charles University in Prague, and adhered to the tenets set out in the Declaration of Helsinki. Twelve term human placentas were obtained after the delivery by elective caesarean section (with donor informed consent) from the Motol University Hospital, Prague (study EK-503/16 approved on 04/14/2016). The donors were tested negative for hepatitis B, C, syphilis, HIV, and with CRP less than 10 mg/l. Each placenta was immediately placed in a sterile container filled with Hank's Balanced Salt Solution without calcium and magnesium (HBSS, Sigma-Aldrich, St. Louis, MO, USA). Special attention was paid to the gentle handling of each placenta during procurement, transport and subsequent manipulation. The preparation of HAM started at most within 2 h after the delivery. HAM was mechanically peeled off of the chorion and washed several times with HBSS to remove blood clots and debris. HAM was flattened onto a sterile nitrocellulose membrane (Bio-Rad, Hercules, CA, USA) with the epithelium surface facing up, cut into 2 x 2 cm (for consequent de-epithelialization) or 9 x 9 cm pieces (for the cell culture after de-epithelialization).

### HAM de-epithelialization and hAECs isolation

Three different protocols were used for HAM de-epithelialization: 1) incubation with TrypLE Express (Gibco, Grand Island, NY, USA) at 37°C for 10 min; 2) incubation with 0.1% w/v trypsin (Sigma-Aldrich)/0.25% w/v EDTA (Sigma-Aldrich) at 37°C for 30 min; 3) incubation with 125 µg/ml thermolysin (Sigma-Aldrich) at 37°C for 9 min. The incubations were stopped with the Dulbecco's modified Eagle medium (DMEM; Gibco) containing 10% fetal calf serum (FCS; Gibco), and antibiotics mixture (10 µl/ml of Antibiotic-Antimycotic (100X); Gibco), hereafter referred as the complete DMEM medium. After each de-epithelialization process, HAM pieces were gently scrapped with the cell scraper (Biologix, Shandong, P.R. China) to remove hAECs in sterile petri dish. The medium with cells was collected, centrifuged at 140g for 8 min and resuspended in complete DMEM medium. All experiments were done in duplicates from 8 placentas.

The viability of the hAECs was determined by exclusion of 0.1% w/v trypan blue dye (Gibco) and hAECs were counted with a hemocytometer. De-epithelialized and intact (used as a control) HAMs were frozen in Cryomount (Histolab AB, Askim, Sweden) and stored at -80°C. Tissues were cryosectioned at a thickness of 7 µm, and four slices were mounted per slide.

## Hematoxylin and eosin staining (H&E)

HAMs and HAM cryosections of the control and de-epithelialized HAMs were stained using H&E for the morphological assessment. The samples were examined by light microscopy with the use of Olympus BX51 (Olympus Co., Tokyo, Japan) at a magnification of 100 and 200x.

## DNA analysis

After each de-epithelialization processes, the tissues of size 1 x 1 cm were placed into Eppendorf tube and cut out with scissors. Intact HAM of the same size was used as a control. Tri Reagent (Molecular Research Center, Cincinnati, OH, USA) was added to the tissues, and total DNA was extracted according to the manufacturer's instructions. The concentration of the DNA was measured with NanoDrop (Thermo Scientific, Waltham, MA, USA).

## Immunostaining

Cryosections of the control and de-epithelialized HAMs from five independent experiments were fixed with iced acetone for 10 min. The samples were incubated with mouse anti-collagen type IV  $\alpha 2$  chain (MAB1910; 1:300, Chemicon International, Billerica, MA, USA) or mouse anti-laminin  $\alpha 5$  chain antibody (M0638; 1:25, DakoCytomation, Glostrup, Denmark) for one h at room temperature, washed three times with phosphate-buffered saline (PBS) and then incubated with a secondary donkey anti-mouse IgG antibody conjugated with fluorescein (FITC) (715-095-151; 1:200, Jackson ImmunoResearch Laboratories, West Grove, PA, USA). The samples were rinsed with PBS and mounted on slides and DNA counterstained using Vectashield—propidium iodide (Vector Laboratories, Inc. Burlingame, USA). Visualization was performed using Olympus BX51 fluorescence microscope (Olympus Co., Tokyo, Japan) at a magnification of 200x. Images were recorded using a Vosskühler VDS CCD-1300 camera, (VDS Vosskühler GmbH, Germany), and NIS Elements software (Laboratory Imaging, Czech Republic) was used for image analysis.

## Scanning electron microscopy (SEM)

Samples of intact and denuded HAM scaffolds (from two placentas) mounted in a CellCrown™ inserts (Scaffdex Oy, Tampere, Finland) were fixed in PBS buffered 3% glutaraldehyde, washed in PBS, postfixed with 1% OsO<sub>4</sub>, dehydrated in a graded ethanol series (25, 50, 75, 90, 96, and 100%) and critical point dried in a K850 Critical Point Dryer (Quorum Technologies Ltd, Ringmer, UK). The dried samples were sputter-coated with 3 nm of platinum in a Q150T Turbo-Pumped Sputter Coater (Quorum Technologies Ltd, Ringmer, UK). The final samples were examined in a FEI Nova NanoSEM scanning electron microscope (FEI, Brno, Czech Republic) at 5 kV using ETD, CBS and TLD detectors. Stereo-pair images were taken at tilts of -6°, 0° and +6° of compucentric goniometer stage. Final R-GB anaglyphs were constructed in a “Stereo module” of AnalySis3.2 software suite (EMSIS GmbH, Germany).

## Cell culture

The hAECs harvested from three placentas after trypsin/EDTA de-epithelialization from 9 x 9 cm HAM pieces were cultured in complete DMEM medium in 25-cm<sup>2</sup> tissue culture flasks (Techno Plastic Products, Trasadingen, Switzerland). Medium was changed every 3–4 days. When the cell culture confluence reached about 80–90%, the cells were passaged with 1 ml of TrypLE Express for 5 min in 37°C. The hAECs were collected, centrifuged at 140g for 8 min and counted with hemocytometer. After every passage, the cells ( $10 \times 10^3$  cells) were used for the WST-1 assay, approximately  $100 \times 10^3$  cells were transferred to the Eppendorf tubes with

Tri Reagent (Molecular Research Center, Cincinnati, OH) and one third of the cells were put back to the culture flask and cultured to the next confluence and passage. The cell images were taken before each passage, and similarly the metabolic activity and gene expression of the cells was determined.

### Determination of metabolic cell activity

The metabolic activity of living cells was determined by the WST-1 assay as we described before [45]. In brief, the hAECs ( $10 \times 10^3$  cells) were cultured in complete DMEM medium with or without epidermal growth factor (EGF) (Gibco) in 96-well tissue culture plate (VWR, Radnor, PA, USA) for 24 h at 37°C in an atmosphere of 5% CO<sub>2</sub>. WST-1 reagent (Roche, Mannheim, Germany) (10 µl/100 µl of the medium) was added to each well, and the plates were incubated for another 4 h to form formazan [46]. Formazan-containing medium (100 µl) was transferred from each well into the new 96-well tissue culture plate and the absorbance was measured using a Tecan Infinite M200 (Tecan, Männedorf, Switzerland) at a wave-length of 450 nm.

### Isolation of RNA and reverse transcription PCR (RT-PCR)

The cells were transferred into Eppendorf tubes containing 500 µl of TRI Reagent and total RNA was extracted according to the manufacturer's protocol as was described previously [47]. RNA quality was analyzed by  $\lambda 260/\lambda 280$  spectrophotometer analysis (Nanodrop). One µg of RNA was treated with deoxyribonuclease I (Promega, Madison, WI) and used for subsequent reverse transcription. The first-strand cDNA was synthesized using random hexamers (Promega) in a total reaction volume of 25 µl using M-MLV Reverse Transcriptase (Promega).

The first strand cDNA product (2µl) was amplified in a total volume of 20 µl PCR assay, containing 10 µl PPP Master Mix (Top Bio, Vestec, Czech republic), 1 µl of each primer and was filled up to a total volume with PCR water (Top Bio). The primers for  $\beta$ -ACTIN, SOX2, OCT-4, OCT-4A and NANOG were selected from previous works and specificity was examined with Primer-BLAST software (NCBI) [20, 39, 48]. Two pairs of primers for OCT-4 were used, because there are two possible spliced variants (OCT-4A and OCT-4B). Product sizes, annealing temperatures and primer sequences are listed in Table 1. The PCR cycles included denaturation at 94°C for 2 min followed by 35 to 40 cycles as follows: denaturation at 94°C for 30 s, annealing 57°C to 64°C for 30 s, elongation at 72°C for 1 min and 72°C extension for 10 min at the end of the program. RT-PCR products were visualized with Gel Red (Biotium, CA, USA) on a 1% agarose gel. Amplification of the housekeeping gene  $\beta$ -ACTIN transcripts was performed simultaneously in order to confirm RNA integrity. Induced pluripotent stem cells (iPS) were used as positive control and corneal fibroblasts as negative control for expression of stem cell markers. Both cell types were prepared as was described previously [49, 50]. Non template control (NTC) reactions were used without cDNA.

### Statistical analysis

The statistical significance of differences between individual groups was calculated using the Student's t-test.

## Results

### De-epithelialization of HAM and BM integrity

The integrity of HAM, the quality of de-epithelialization, and potential presence of hAECs were verified by H&E staining and SEM analysis. The surface of intact HAM consists of cuboidal epithelial cells, mesenchymal cells were observed scattered in the stroma (Fig 1).

**Table 1. Primer sequences used for real-time PCR.**

Primer	Sequence (5'-3')	Product size (bp)	Annealing temperature (°C)	Cycles	References
β-ACTIN	F: cgcaccactggcattgtcat R: ttctccttgatgtcacgcac	208	57	35	[20]
SOX2	F: gccgagtggaaacttttgtc R: gttcatgtgcgcgtaactgt	264	57	40	[20]
NANOG	F: ctgtgatttgtgggcctgaa R: tgtttgcctttgggactggt	153	57	35	[39]
OCT-4	F: gaggagtcccaggacatgaa R: gtggctctggctgaacacctt	151	57	40	[20]
OCT-4A	F: cttctcgcctccaggt R: aaatagaacccccagggtgagc	496	64	35	[48]

<https://doi.org/10.1371/journal.pone.0194820.t001>

All three enzymatic methods (TrypLE Express, trypsin/EDTA, and thermolysin) were comparable in term of efficiency of HAM de-epithelialization. Only few epithelial cells occasionally rested on denuded HAM with no difference of the used treatment. The hAMSCs from non-treated HAM exhibited spindle-shaped morphology, similarly as hAMSCs after TrypLE Express and trypsin/EDTA treatments. The thermolysin application led to loss of mesenchymal spindle-shaped cell morphology, showing rather round cell shape (Fig 1).

The DNA concentration in denuded HAM was significantly lower after the treatment with all de-epithelialization agents compared to control untreated samples (Fig 2). The small residual amount of DNA in treated specimens represents DNA of hAMSCs.

The mosaic layer of hAECs covered with dense microvilli was determined at the surface of intact HAM by SEM analysis (Fig 3A, 3B and 3C). BM is well preserved after trypsin/EDTA treatment, some residues of extracellular matrix (ECM) from epithelial cell layer are clearly detectable (Fig 3G, 3H and 3I). Partial damage of BM was observed after applying TrypLE Express treatment, but BM stayed still mostly intact (Fig 3D, 3E and 3F). When thermolysin was used for decellularization, the BM was damaged and numerous lesions were observed revealing the collagen network of compact layer under BM (Fig 3J, 3K and 3L), suggesting aggressive proteolysis.

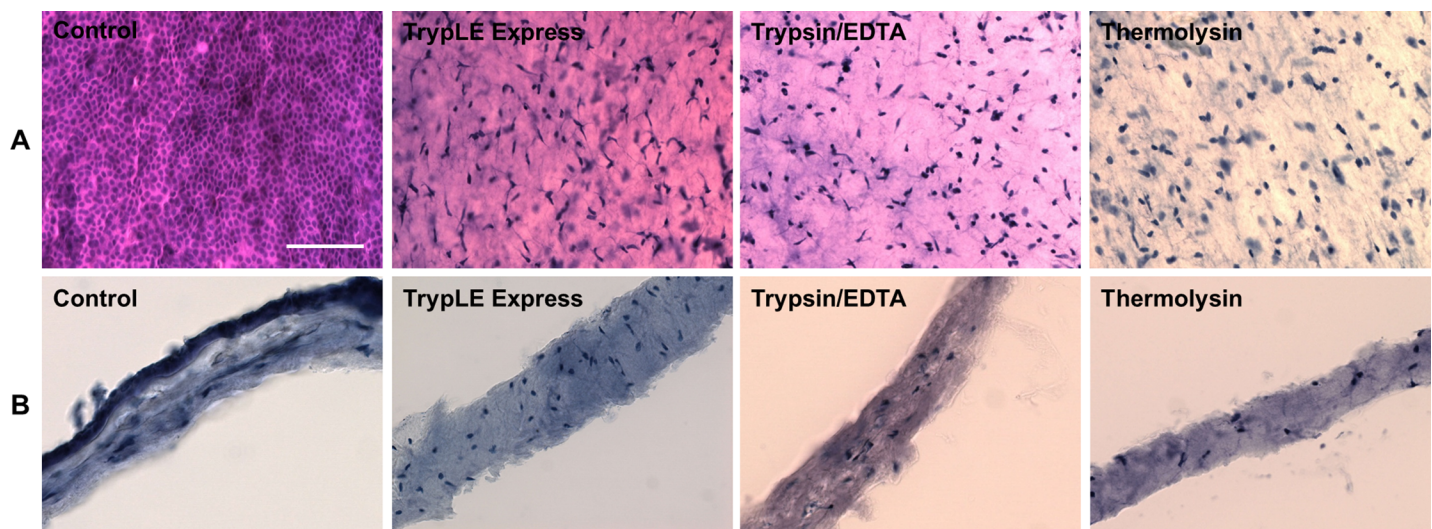


**Fig 1. Comparison of the intact and denuded HAMs and HAM cryosections.** Comparison of the intact (Control) and denuded HAMs (A) and HAM cryosections (B) after TrypLE Express, trypsin/EDTA and thermolysin treatment stained with H/E for light microscopy. Scale bar represents 100 μm.

<https://doi.org/10.1371/journal.pone.0194820.g001>

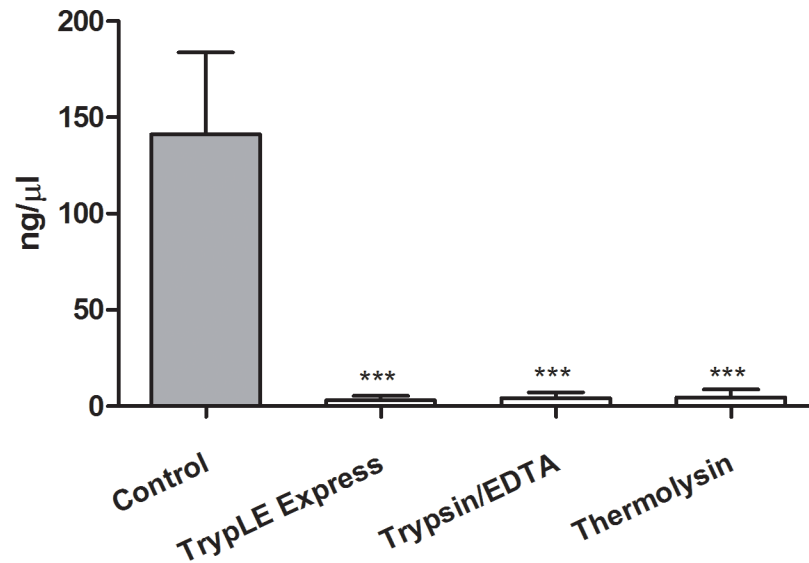


**Fig 2. Comparison of the DNA concentrations.** Comparison of the DNA concentration in the tissues from the intact (Control) and denuded HAMs with TrypLE Express (TrypLE), trypsin/EDTA and thermolysin treatment directly after de-epithelialization. Each bar represents mean  $\pm$  SD from 3 determinations (\*\*\*)  $P < 0.001$ .

<https://doi.org/10.1371/journal.pone.0194820.g002>

Collagen type IV and laminin  $\alpha 5$  chain showed clear positivity in BM of all control specimens and specimens after TrypLE Express and trypsin/EDTA treatment (Fig 4). After thermolysin application, two staining patterns were observed: in HAM specimens from three placentas, the staining for both proteins was properly localized just in BM without any visible integrity deterioration, on the other hand, the positive signal of collagen type IV and laminin  $\alpha 5$  was spread throughout the whole amniotic stroma in specimens from other two placentas. In these samples the positive line representing BM was not apparent (Fig 4A and 4B). Intact HAM was used as a negative control without using primary antibody.

### Viability, morphology, growth and expression pattern of hAECs

The viability of obtained hAECs immediately after de-epithelialization reached approximately 6% after TrypLE Express, and about 60% after trypsin/EDTA treatment (Fig 5). Only dead cells and cellular fragments were observed after de-epithelialization using thermolysin.

The hAECs harvested after trypsin/EDTA treatment were successfully cultured from all three HAMs. The morphology of hAECs changed from cuboidal shape at the beginning of the culture to more mesenchymal shape cells in the 4<sup>th</sup> and 5<sup>th</sup> passage (Fig 6). The higher proliferation activity was observed in later passages. When hAECs were co-cultured with EGF for 24 hours, the metabolic activity was slightly, but not significantly increased (Fig 7).

The expression of three stem cell markers in cultured hAECs was detected. SOX2 was present up to 2<sup>nd</sup> passage, NANOG up to 4<sup>th</sup> passage, and OCT-4 was present in all passages (Fig 8). No band was observed when primers for transcription variant specific for stem cells (OCT-4A) were used.

### Discussion

The three tested de-epithelialization approaches were efficient to remove epithelial cells from HAM surface. However, only the treatment with trypsin/EDTA was effective for simultaneous harvesting of viable hAECs. We have shown, that gentle mechanical scrapping necessary to



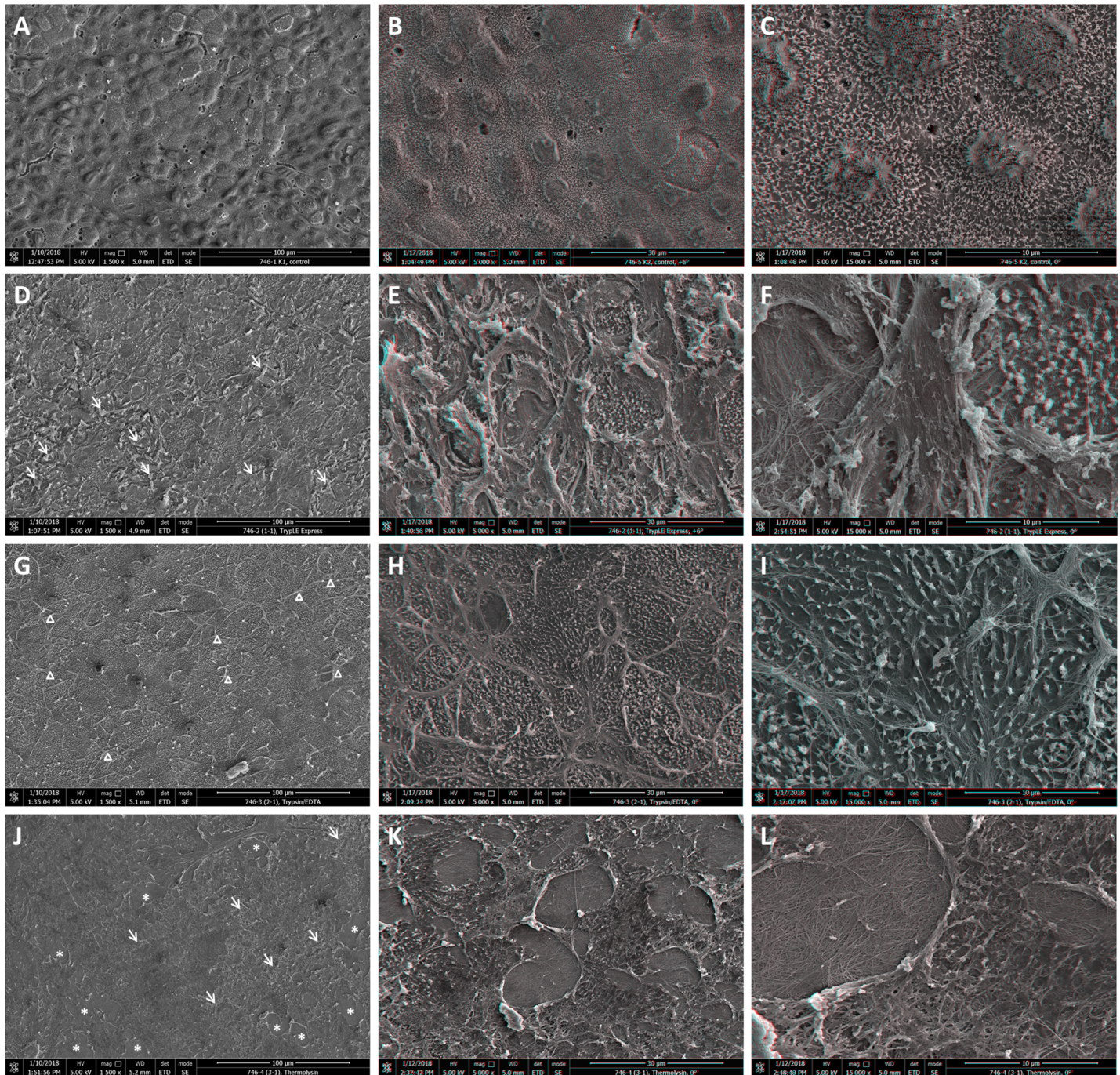


**Fig 3. Topography of intact and denuded HAM.** Scanning electron micrographs (A, D, G, J) and stereo anaglyphs (B, C, E, F, H, I, K, L) of the intact (A, B, C) and denuded HAM by TrypLE Express (D, E, F), trypsin/EDTA (G, H, I) and thermolysin (J, K, L). Areas of damaged BM are marked by arrows, ruptured gaps by \*, the residues of ECM by  $\Delta$ . Red-green or red-cyan glasses required for proper view of stereo anaglyphs.

<https://doi.org/10.1371/journal.pone.0194820.g003>

remove up to 100% of hAECs after each treatment does not affect the integrity of BM. The staining of HAM and DNA concentration measurement demonstrated the efficiency of all three de-epithelialization processes, with no significant difference between the methods.



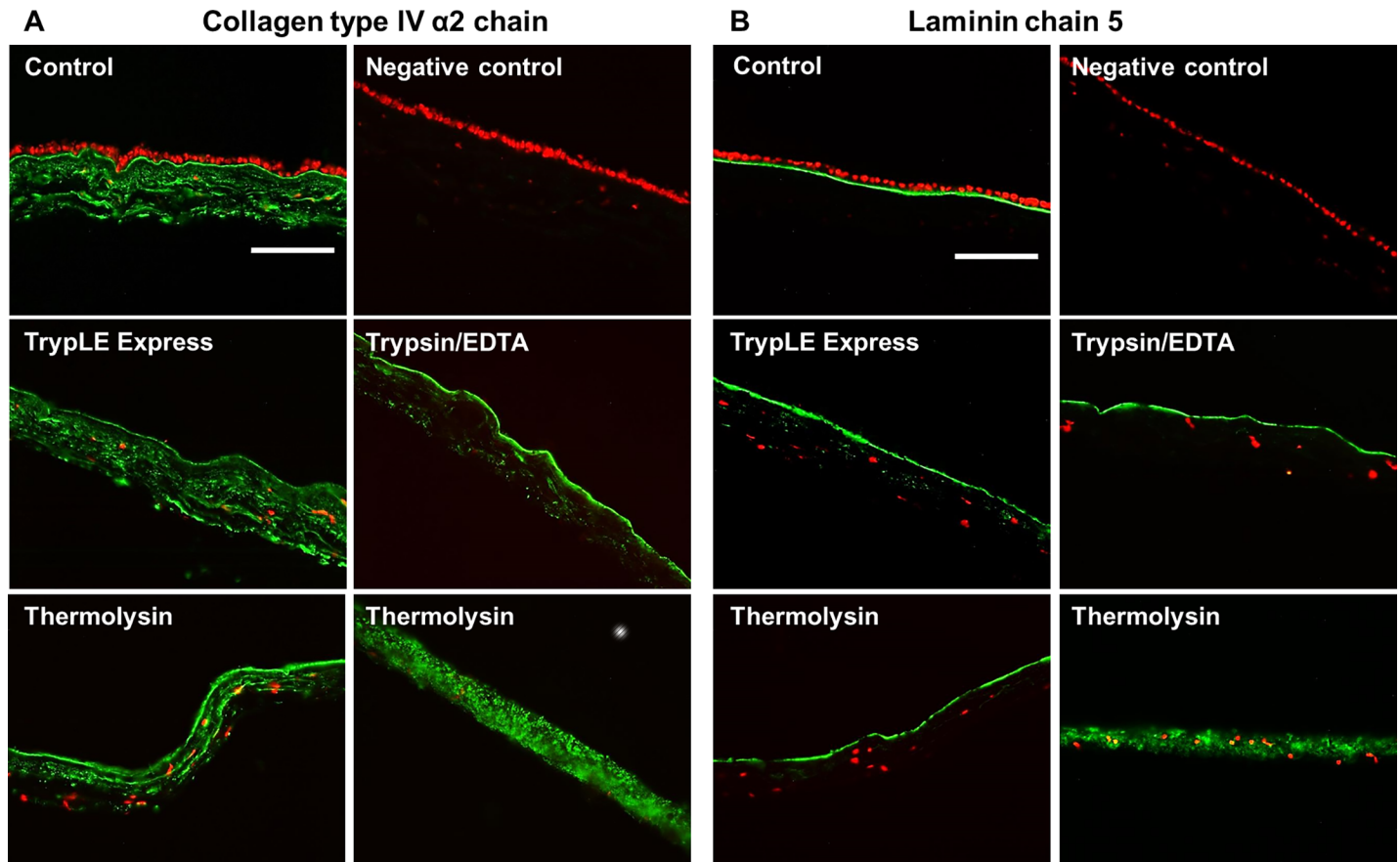


**Fig 4. Immunostaining of BM.** Distribution of BM collagen type IV  $\alpha 2$  chain (green; A) or laminin  $\alpha 5$  (green; B) in intact (Control) and denuded HAM: TrypLE Express, trypsin/EDTA, thermolysin treatment. Intact HAM (primary antibody omitted), was used as negative control. Cell nuclei were stained with the propidium iodide (red). Scale bar represents 100  $\mu\text{m}$ .

<https://doi.org/10.1371/journal.pone.0194820.g004>

On the other hand, the detections of collagen type IV and laminin  $\alpha 5$  as ubiquitous components of BM [51, 52] revealed some differences between used protocols. The regular staining of BM after TrypLE Express and trypsin/EDTA treatment indicates its integrity and is in agreement with previously published data [13]. We have shown that relatively low trypsin concentration (0.1% w/v) in trypsin/EDTA mixture does not affect BM integrity and cell vitality. BM degradation has been documented after treatment with higher (0.25% w/v) trypsin concentration [13]. The results from SEM analysis thoroughly confirm our original conclusions based on histology and immunohistochemistry data. Smooth surface and the presence of BM after trypsin/EDTA treatment were also already detected [13]. In our experiments only partial damage of BM has been noticed when TrypLE Express was used.

Different situation was observed after de-epithelialization using thermolysin, where almost 50% of specimens showed, beside integral BM staining, signal of collagen type IV and laminin  $\alpha 5$  dispersed in HAM stroma. Also loss of hAMSCs spindle shape morphology is consistent with damages induced by thermolysin. SEM analysis showed that BM was damaged and ruptured. The collagen fibres of the underlying compact layer were seen at locations where BM was missing. The similar image of collagen fibres was observed after de-epithelialization by disperse when entire BM was absent [13]. Thermolysin is a heat-stable metalloproteinase which acts specifically at hemidesmosome complex at the level of BM [53], most likely targeting

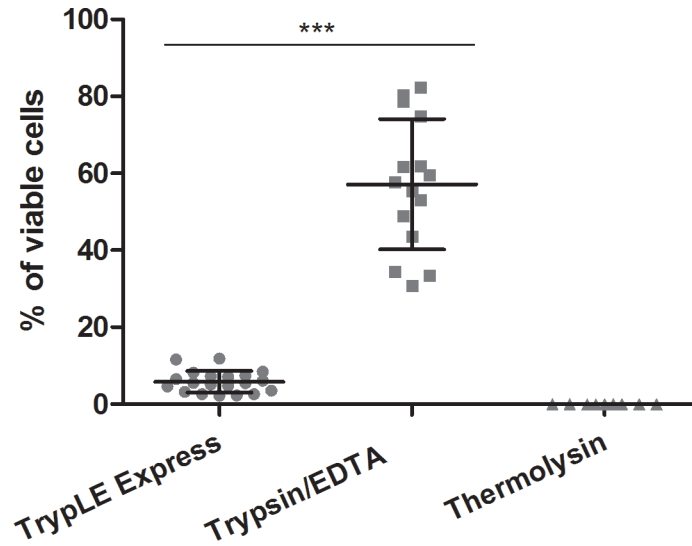


**Fig 5. The viability of hAECs.** Comparison of the hAECs viability after TrypLE Express, trypsin/EDTA and thermolysin treatment. Cells were stained with trypan blue and counted via hemocytometer. Each bar represents mean  $\pm$  SD from 15 determinations (\*\* $P < 0.001$ ).

<https://doi.org/10.1371/journal.pone.0194820.g005>

collagen IV but not laminin [53, 54]. Hopkinson et al. also noted certain damage of BM when thermolysin in combination with mechanical scrapping was used [33]. The improvement of BM integrity was achieved, when mechanical removal was replaced by simple washing [33].

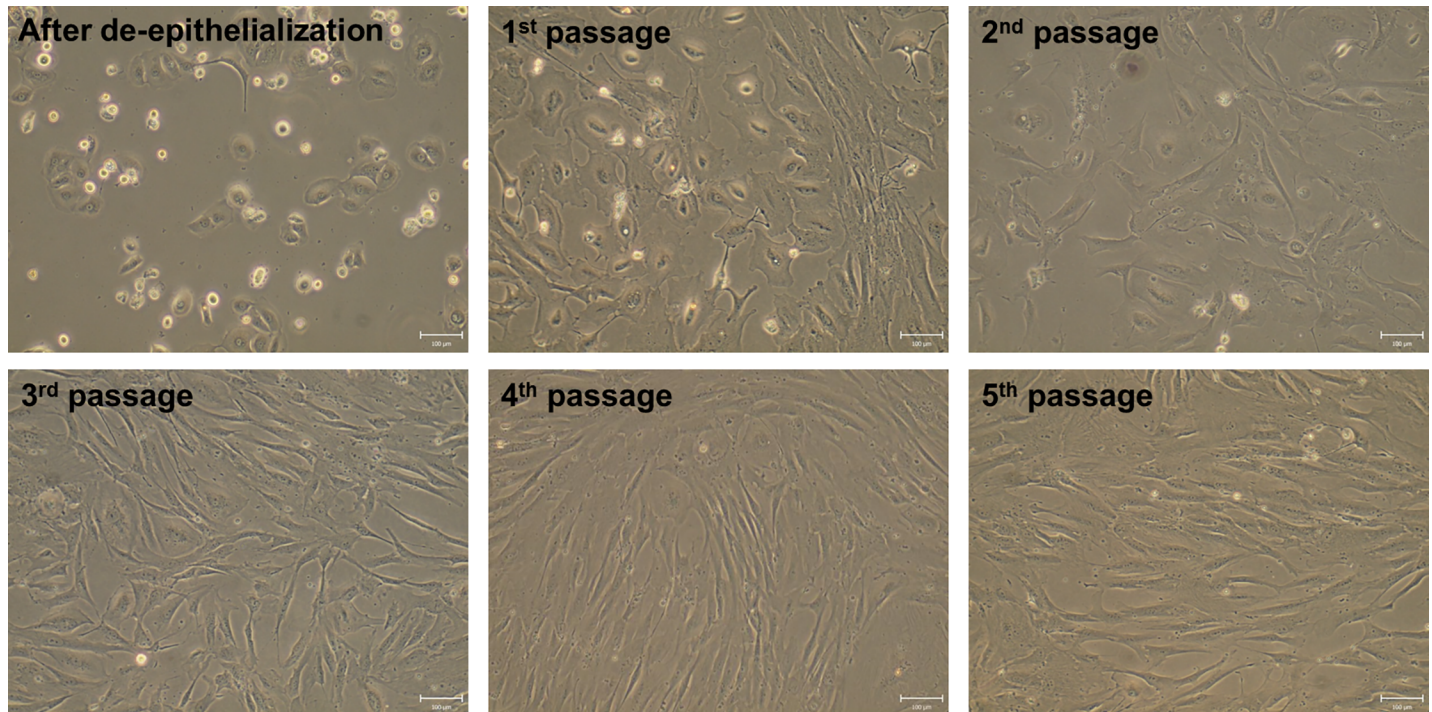


**Fig 6. The morphology of hAECs.** The comparison of morphology of cultured hAECs after trypsin/EDTA treatment in complete DMEM medium. The cells for the light microscopy were photographed before each passage (after de-epithelialization, before 1<sup>st</sup>, 2<sup>nd</sup>, 3<sup>rd</sup>, 4<sup>th</sup> and 5<sup>th</sup> passage). Results of one out of 3 identical experiment is shown. Scale bars represent 100  $\mu$ m.

<https://doi.org/10.1371/journal.pone.0194820.g006>

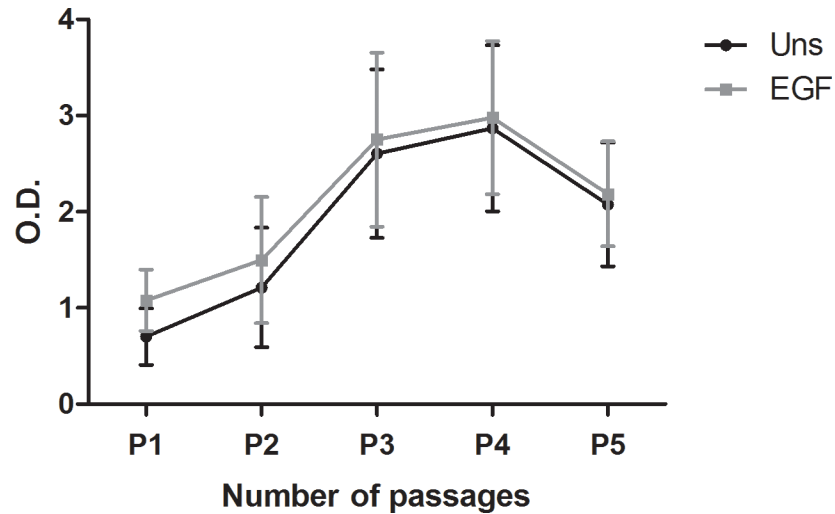


**Fig 7. The metabolic activity of hAECs.** Comparison of metabolic activity of the epithelial cells unstimulated (Uns) and stimulated with EGF (EGF) after each passage. WST-1 reagent was added to the cell cultures for 4 h to form formazan. The absorbance was measured at a wave-length of 450 nm. Each bar represents mean  $\pm$  SD from 3 determinations.

<https://doi.org/10.1371/journal.pone.0194820.g007>

Unfortunately, we were unable to denude the HAM completely with thermolysin only. The fragility and difficult handling of HAM after thermolysin treatment has been also reported in another study [34]. We consider that the damage of the BM is caused by the natural activity of this enzyme due to cleavage of collagen IV. Moreover the lesions are often of round or oval shape (see Fig 3K and 3L), but not cracks, as it would correspond to scraping damage.

De-epithelialization using thermolysin resulted in complete loss of hAECs viability. On the other hand thermolysin was successfully used for the isolation of epidermal or intestinal epithelial cells [53, 55], which are probably less sensitive to enzymatic treatment than the hAECs.

The highest viability of hAECs (about 60%) after trypsin/EDTA indicates that this method is gentle and safe. We have also tried to culture hAECs harvested after TrypLE Express method

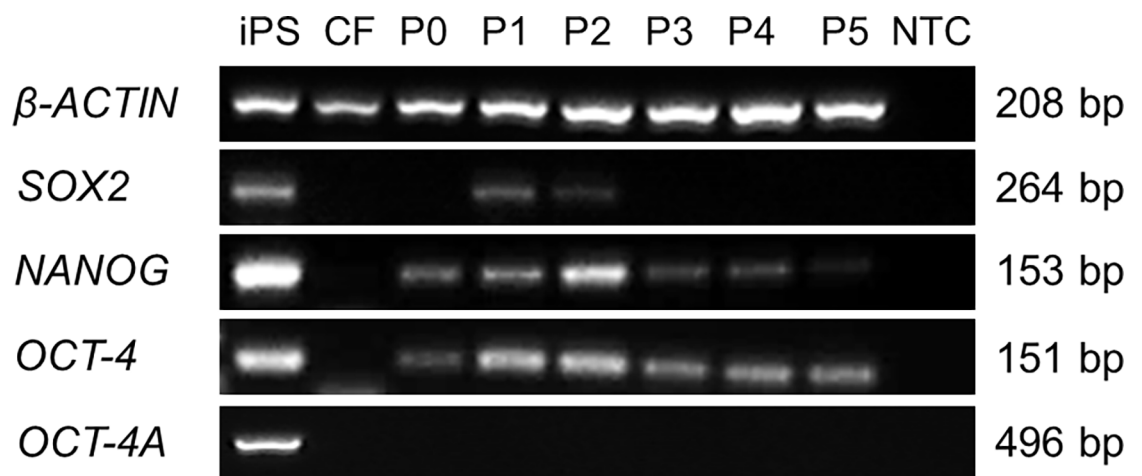


**Fig 8. The RT-PCR analysis of hAECs.** The RT-PCR analysis of hAECs after de-epithelialization and each passage (P0-P5). The iPS cells were used as a positive (iPS) and corneal fibroblasts as negative control (CF). Sample without cDNA (NTC) was used as non-template control. One representative experiment of 3 (with identical results) is shown.

<https://doi.org/10.1371/journal.pone.0194820.g008>

(6% viability), but these cells (probably due to low initial amount of cells) were growing very slowly and reached full confluence only after extended time periods. The viability of hAECs after TrypLE Express treatment did not change even if we used a prolonged time period (30 min). The hAECs obtained by trypsin/EDTA treatment were successfully cultured up to 5<sup>th</sup> passage and their proliferation activity increased after each passage up to the 4<sup>th</sup> one. It was reported that addition of EGF as mitogenesis promoter [56] significantly increases proliferative capacity of hAECs [41]. The addition of EGF for to 24-h culture period did not change proliferation activity significantly. The longer cultivation periods in our study was omitted as it has been found that 7-day cultivation of hAECs with EGF led to significantly increased proliferation, but lower expression of pluripotent genes *OCT-4*, *SOX2* and *NANOG* [57]. Our hAECs, isolated with trypsin/EDTA method, changed their morphology during culture and passaging from more cuboidal morphology at the beginning of culture to more mesenchymal shape from the 3<sup>rd</sup> passage. Similar observation was also described repeatedly [36]. Morphology and proliferation changes could be caused by epithelial to mesenchymal transition by autocrine production of transforming growth factor- $\beta$  during the culture of hAECs [58].

It has been shown that hAECs express molecular markers of pluripotent stem cells: *NANOG*, *SOX2* and *OCT-4* [20, 39]. We detected the expression of *NANOG* in cells after de-epithelialization and throughout cultivation; *SOX2* was present in two first passages only. The detection of *OCT-4* was more complex due to its nature. *OCT-4* plays a crucial role in regulating the self-renewal and maintaining pluripotency [59, 60] and encodes two main variants known as *OCT-4A* and *OCT-4B* [61]. While the expression of *OCT-4A* is restricted to embryonic stem cells and embryonal carcinoma cells, *OCT-4B* can be detected in various nonpluripotent cell types [48, 62, 63]. In recent studies some authors still used the primers fitted on both variants for PCR analysis [39, 57, 64]. Using primers suitable for both variants, we detected expression of *OCT-4* in each passage, but *OCT-4A* spliced variant (primers selected based on the work of Atlasi et al. [48]), was not detected in any passage of the cells. On the contrary, Izumi et al. confirmed *OCT-4A* expression in naive (but not cultured) hAECs by using a commercially available primer and probe set that matches *OCT-4A* specific exons by quantitative RT-PCR [65]. In summary, our data on detection of expression of pluripotent stem cell markers suggest that stemness of cultured hAECs decreases with each passage.

Out of three tested de-epithelialization protocols (TrypLE Express, trypsin/EDTA, thermolysin) trypsin/EDTA application showed to be the most efficient when both viable hAECs and intact BM are requested. We would like to stress here, that the term “intact” is used for visibly least damaged BM (judged by the SEM analysis) where no observable lesions were detected contrary to BM obtained by other two methods (see Fig 3). This does not necessarily mean, that some eventual minor structural modification do not occur during trypsin/EDTA treatment (e.g. collagen fiber structure modification), however, these have not an impact on the integrity of BM. The major goal of this study was to establish the conditions under which both undamaged BM and viable hAECs can be obtained and our results demonstrate, that the trypsin/EDTA treatment is the most efficient approach. It leads to successful de-epithelialization of HAM with undamaged BM with well-preserved integrity and at the same time to harvesting of viable epithelial cells which can be cultured up to 5<sup>th</sup> passage with gradually increasing proliferation capacity. The stemness properties of these cells, however, decrease with higher passages. The cell viability, on the other hand also correlates well with level of BM damage. The method which yields no viable cell (thermolysin) also provides BM with most profound lesions, while intact BM (Trypsin/EDTA, Fig 3G, 3H and 3I) correlates with the best viability of harvested cells (Fig 4). Therefore, we suggest that the trypsin/EDTA method is the method of choice when both intact HAM and viable hAECs are needed for subsequent use.



## Acknowledgments

We thank to Department of Obstetrics and Gynecology, Motol University Hospital and Department of Obstetrics and Gynecology, First Faculty of Medicine, Charles University and General University Hospital in Prague for providing of placentas. We thank to Robert Dobrovolny, Ph.D. for providing us with iPS cells.

## Author Contributions

**Conceptualization:** Peter Trosan, Katerina Jirsova.

**Data curation:** Peter Trosan.

**Funding acquisition:** Katerina Jirsova.

**Investigation:** Peter Trosan, Ingrida Smeringaiova, Kristyna Brejchova, Oldrich Benada, Olga Kofronova.

**Methodology:** Peter Trosan, Katerina Jirsova.

**Supervision:** Katerina Jirsova.

**Validation:** Peter Trosan, Jan Bednar, Katerina Jirsova.

**Writing – original draft:** Peter Trosan.

**Writing – review & editing:** Jan Bednar, Katerina Jirsova.

## References

1. van Herendael BJ, Oberti C, Brosens I. Microanatomy of the human amniotic membranes. A light microscopic, transmission, and scanning electron microscopic study. *American journal of obstetrics and gynecology*. 1978; 131(8):872–80. Epub 1978/08/15. PMID: [686087](#).
2. Koizumi N, Inatomi T, Quantock AJ, Fullwood NJ, Dota A, Kinoshita S. Amniotic membrane as a substrate for cultivating limbal corneal epithelial cells for autologous transplantation in rabbits. *Cornea*. 2000; 19(1):65–71. PMID: [10632011](#).
3. Shimazaki J, Yang HY, Tsubota K. Amniotic membrane transplantation for ocular surface reconstruction in patients with chemical and thermal burns. *Ophthalmology*. 1997; 104(12):2068–76. PMID: [9400767](#).
4. Tseng SC, Prabhasawat P, Lee SH. Amniotic membrane transplantation for conjunctival surface reconstruction. *American journal of ophthalmology*. 1997; 124(6):765–74. PMID: [9402822](#).
5. Mohan R, Bajaj A, Gundappa M. Human Amnion Membrane: Potential Applications in Oral and Periodontal Field. *J Int Soc Prev Commu*. 2017; 7(1):15–21. [https://doi.org/10.4103/jispcd.JISPCD\\_359\\_16](https://doi.org/10.4103/jispcd.JISPCD_359_16) PubMed PMID: WOS:000395980100003. PMID: [28316944](#)
6. Tenenhaus M. The Use of Dehydrated Human Amnion/Chorion Membranes in the Treatment of Burns and Complex Wounds Current and Future Applications. *Ann Plas Surg*. 2017; 78:S11–S3. <https://doi.org/10.1097/Sap.0000000000000983> PubMed PMID: WOS:000392860000004. PMID: [28079550](#)
7. Jirsova K, Jones GLA. Amniotic membrane in ophthalmology: properties, preparation, storage and indications for grafting—a review. *Cell Tissue Bank*. 2017; 18(2):193–204. <https://doi.org/10.1007/s10561-017-9618-5> PubMed PMID: WOS:000401422700006. PMID: [28255771](#)
8. Tsai RJ, Li LM, Chen JK. Reconstruction of damaged corneas by transplantation of autologous limbal epithelial cells. *N Engl J Med*. 2000; 343(2):86–93. <https://doi.org/10.1056/NEJM200007133430202> PMID: [10891515](#).
9. Kolli S, Lako M, Figueiredo F, Mudhar H, Ahmad S. Loss of corneal epithelial stem cell properties in outgrowths from human limbal explants cultured on intact amniotic membrane. *Regenerative medicine*. 2008; 3(3):329–42. <https://doi.org/10.2217/17460751.3.3.329> PMID: [18462056](#).
10. Li W, Hayashida Y, He H, Kuo CL, Tseng SC. The fate of limbal epithelial progenitor cells during explant culture on intact amniotic membrane. *Investigative ophthalmology & visual science*. 2007; 48(2):605–13. <https://doi.org/10.1167/iov.06-0514> PMID: [17251456](#); PubMed Central PMCID: PMC3197022.



11. Sudha B, Sitalakshmi G, Iyer GK, Krishnakumar S. Putative stem cell markers in limbal epithelial cells cultured on intact & denuded human amniotic membrane. *The Indian journal of medical research*. 2008; 128(2):149–56. PMID: [19001678](#).
12. Riau AK, Beuerman RW, Lim LS, Mehta JS. Preservation, sterilization and de-epithelialization of human amniotic membrane for use in ocular surface reconstruction. *Biomaterials*. 2010; 31(2):216–25. <https://doi.org/10.1016/j.biomaterials.2009.09.034> PMID: [19781769](#).
13. Zhang T, Yam GH, Riau AK, Poh R, Allen JC, Peh GS, et al. The effect of amniotic membrane de-epithelialization method on its biological properties and ability to promote limbal epithelial cell culture. *Investigative ophthalmology & visual science*. 2013; 54(4):3072–81. <https://doi.org/10.1167/iov.12-10805> PMID: [23580491](#).
14. de Melo GB, Gomes JA, da Gloria MA, Martins MC, Haapalainen EF. [Morphological assessment of different amniotic membrane epithelial denuding techniques]. *Arquivos brasileiros de oftalmologia*. 2007; 70(3):407–11. PMID: [17768545](#).
15. Higa K, Shimmura S, Kato N, Kawakita T, Miyashita H, Itabashi Y, et al. Proliferation and differentiation of transplantable rabbit epithelial sheets engineered with or without an amniotic membrane carrier. *Investigative ophthalmology & visual science*. 2007; 48(2):597–604. <https://doi.org/10.1167/iov.06-0664> PMID: [17251455](#).
16. Shortt AJ, Secker GA, Lomas RJ, Wilshaw SP, Kearney JN, Tuft SJ, et al. The effect of amniotic membrane preparation method on its ability to serve as a substrate for the ex-vivo expansion of limbal epithelial cells. *Biomaterials*. 2009; 30(6):1056–65. <https://doi.org/10.1016/j.biomaterials.2008.10.048> PMID: [19019426](#).
17. Shortt AJ, Secker GA, Rajan MS, Meligonis G, Dart JK, Tuft SJ, et al. Ex vivo expansion and transplantation of limbal epithelial stem cells. *Ophthalmology*. 2008; 115(11):1989–97. <https://doi.org/10.1016/j.optha.2008.04.039> PMID: [18554721](#).
18. Koizumi N, Rigby H, Fullwood NJ, Kawasaki S, Tanioka H, Koizumi K, et al. Comparison of intact and denuded amniotic membrane as a substrate for cell-suspension culture of human limbal epithelial cells. *Graefes's archive for clinical and experimental ophthalmology = Albrecht von Graefes Archiv fur klinische und experimentelle Ophthalmologie*. 2007; 245(1):123–34. <https://doi.org/10.1007/s00417-005-0095-3> PMID: [16612639](#).
19. Simat SF, Chua KH, Abdul Rahman H, Tan AE, Tan GC. The stemness gene expression of cultured human amniotic epithelial cells in serial passages. *The Medical journal of Malaysia*. 2008; 63 Suppl A:53–4. PMID: [19024980](#).
20. Miki T, Lehmann T, Cai H, Stolz DB, Strom SC. Stem cell characteristics of amniotic epithelial cells. *Stem cells*. 2005; 23(10):1549–59. <https://doi.org/10.1634/stemcells.2004-0357> PMID: [16081662](#).
21. Ilancheran S, Michalska A, Peh G, Wallace EM, Pera M, Manuelpillai U. Stem cells derived from human fetal membranes display multilineage differentiation potential. *Biol Reprod*. 2007; 77(3):577–88. <https://doi.org/10.1095/biolreprod.106.055244> PMID: [17494917](#).
22. Chen YT, Li W, Hayashida Y, He H, Chen SY, Tseng DY, et al. Human amniotic epithelial cells as novel feeder layers for promoting ex vivo expansion of limbal epithelial progenitor cells. *Stem cells*. 2007; 25(8):1995–2005. <https://doi.org/10.1634/stemcells.2006-0677> PubMed PMID: WOS:000248411000015. PMID: [17495107](#)
23. Fang CH, Jin J, Joe JH, Song YS, So BI, Lim SM, et al. In vivo differentiation of human amniotic epithelial cells into cardiomyocyte-like cells and cell transplantation effect on myocardial infarction in rats: comparison with cord blood and adipose tissue-derived mesenchymal stem cells. *Cell transplantation*. 2012; 21(8):1687–96. <https://doi.org/10.3727/096368912X653039> PMID: [22776022](#).
24. Ito A, Takizawa Y, Shinkai M, Honda H, Hata K, Ueda M, et al. Proliferation and stratification of keratinocyte on cultured amniotic epithelial cells for tissue engineering. *J Biosci Bioeng*. 2003; 95(6):589–93. <https://doi.org/10.1263/Jbb.95.589> PubMed PMID: WOS:000184813200007. PMID: [16233462](#)
25. Avila-Gonzalez D, Vega-Hernandez E, Regalado-Hernandez JC, De la Jara-Diaz JF, Garcia-Castro IL, Molina-Hernandez A, et al. Human amniotic epithelial cells as feeder layer to derive and maintain human embryonic stem cells from poor-quality embryos. *Stem Cell Res*. 2015; 15(2):322–4. <https://doi.org/10.1016/j.scr.2015.07.006> PMID: [26246271](#).
26. Lai DM, Cheng WW, Liu TJ, Jiang LZ, Huang Q, Liu T. Use of Human Amnion Epithelial Cells as a Feeder Layer to Support Undifferentiated Growth of Mouse Embryonic Stem Cells. *Cloning Stem Cells*. 2009; 11(2):331–40. <https://doi.org/10.1089/clo.2008.0047> PubMed PMID: WOS:000267016400014. PMID: [19508128](#)
27. Li HC, Niederkorn JY, Neelam S, Mayhew E, Word RA, McCulley JP, et al. Immunosuppressive factors secreted by human amniotic epithelial cells. *Investigative ophthalmology & visual science*. 2005; 46(3):900–7. <https://doi.org/10.1167/iov.04-0495> PubMed PMID: WOS:000227216900018. PMID: [15728546](#)

28. Madhira SL, Vemuganti G, Bhaduri A, Gaddipati S, Sangwan VS, Ghanekar Y. Culture and characterization of oral mucosal epithelial cells on human amniotic membrane for ocular surface reconstruction. *Mol Vis*. 2008; 14(24–25):189–96. PubMed PMID: WOS:000256595500001.
29. Sangwan VS, Vemuganti GK, Singh S, Balasubramanian D. Successful reconstruction of damaged ocular outer surface in humans using limbal and conjunctival stem cell culture methods. *Biosci Rep*. 2003; 23(4):169–74. PMID: [14748537](https://pubmed.ncbi.nlm.nih.gov/14748537/).
30. Wilshaw SP, Kearney JN, Fisher J, Ingham E. Production of an acellular amniotic membrane matrix for use in tissue engineering. *Tissue engineering*. 2006; 12(8):2117–29. <https://doi.org/10.1089/ten.2006.12.2117> PMID: [16968153](https://pubmed.ncbi.nlm.nih.gov/16968153/).
31. Roy R, Haase T, Ma N, Bader A, Becker M, Seifert M, et al. Decellularized amniotic membrane attenuates postinfarct left ventricular remodeling. *The Journal of surgical research*. 2016; 200(2):409–19. <https://doi.org/10.1016/j.jss.2015.08.022> PMID: [26421709](https://pubmed.ncbi.nlm.nih.gov/26421709/).
32. Wilshaw SP, Kearney J, Fisher J, Ingham E. Biocompatibility and potential of acellular human amniotic membrane to support the attachment and proliferation of allogeneic cells. *Tissue engineering Part A*. 2008; 14(4):463–72. <https://doi.org/10.1089/tea.2007.0145> PMID: [18370928](https://pubmed.ncbi.nlm.nih.gov/18370928/).
33. Hopkinson A, Shanmuganathan VA, Gray T, Yeung AM, Lowe J, James DK, et al. Optimization of amniotic membrane (AM) denuding for tissue engineering. *Tissue engineering Part C, Methods*. 2008; 14(4):371–81. <https://doi.org/10.1089/ten.tec.2008.0315> PMID: [18821842](https://pubmed.ncbi.nlm.nih.gov/18821842/).
34. Saghizadeh M, Winkler MA, Kramerov AA, Hemmati DM, Ghiam CA, Dimitrijevic SD, et al. A simple alkaline method for decellularizing human amniotic membrane for cell culture. *PloS one*. 2013; 8(11):e79632. <https://doi.org/10.1371/journal.pone.0079632> PMID: [24236148](https://pubmed.ncbi.nlm.nih.gov/24236148/); PubMed Central PMCID: [PMC3827346](https://pubmed.ncbi.nlm.nih.gov/PMC3827346/).
35. Noguchi Y, Uchida Y, Endo T, Ninomiya H, Nomura A, Sakamoto T, et al. The induction of cell differentiation and polarity of tracheal epithelium cultured on the amniotic membrane. *Biochemical and biophysical research communications*. 1995; 210(2):302–9. PMID: [7755604](https://pubmed.ncbi.nlm.nih.gov/7755604/).
36. Fatimah SS, Ng SL, Chua KH, Hayati AR, Tan AE, Tan GC. Value of human amniotic epithelial cells in tissue engineering for cornea. *Human cell*. 2010; 23(4):141–51. <https://doi.org/10.1111/j.1749-0774.2010.00096.x> PMID: [21166885](https://pubmed.ncbi.nlm.nih.gov/21166885/).
37. Miki T, Marongiu F, Ellis E, S CS. Isolation of amniotic epithelial stem cells. *Current protocols in stem cell biology*. 2007; Chapter 1: Unit 1E 3. <https://doi.org/10.1002/9780470151808.sc01e03s3> PMID: [18785168](https://pubmed.ncbi.nlm.nih.gov/18785168/).
38. Pratama G, Vaghjiani V, Tee JY, Liu YH, Chan J, Tan C, et al. Changes in culture expanded human amniotic epithelial cells: implications for potential therapeutic applications. *PloS one*. 2011; 6(11):e26136. <https://doi.org/10.1371/journal.pone.0026136> PMID: [22073147](https://pubmed.ncbi.nlm.nih.gov/22073147/); PubMed Central PMCID: [PMC3206797](https://pubmed.ncbi.nlm.nih.gov/PMC3206797/).
39. Evron A, Goldman S, Shalev E. Human amniotic epithelial cells cultured in substitute serum medium maintain their stem cell characteristics for up to four passages. *International journal of stem cells*. 2011; 4(2):123–32. PMID: [24298345](https://pubmed.ncbi.nlm.nih.gov/24298345/); PubMed Central PMCID: [PMC3840962](https://pubmed.ncbi.nlm.nih.gov/PMC3840962/).
40. Mahmood R, Choudhery MS, Mehmood A, Khan SN, Riazuddin S. In Vitro Differentiation Potential of Human Placenta Derived Cells into Skin Cells. *Stem Cells Int*. 2015. doi: Artn 841062 <https://doi.org/10.1155/2015/841062> PubMed PMID: WOS:000357813100001. PMID: [26229539](https://pubmed.ncbi.nlm.nih.gov/26229539/)
41. Tabatabaei M, Mosaffa N, Nikoo S, Bozorgmehr M, Ghods R, Kazemnejad S, et al. Isolation and partial characterization of human amniotic epithelial cells: the effect of trypsin. *Avicenna journal of medical biotechnology*. 2014; 6(1):10–20. PMID: [24523953](https://pubmed.ncbi.nlm.nih.gov/24523953/); PubMed Central PMCID: [PMC3895574](https://pubmed.ncbi.nlm.nih.gov/PMC3895574/).
42. Diaz-Prado S, Muinos-Lopez E, Hermida-Gomez T, Rendal-Vazquez ME, Fuentes-Boquete I, de Toro FJ, et al. Multilineage differentiation potential of cells isolated from the human amniotic membrane. *J Cell Biochem*. 2010; 111(4):846–57. <https://doi.org/10.1002/jcb.22769> PMID: [20665539](https://pubmed.ncbi.nlm.nih.gov/20665539/).
43. Rutigliano L, Corradetti B, Valentini L, Bizzaro D, Meucci A, Cremonesi F, et al. Molecular characterization and in vitro differentiation of feline progenitor-like amniotic epithelial cells. *Stem Cell Res Ther*. 2013; 4(5):133. <https://doi.org/10.1186/scrt344> PMID: [24405576](https://pubmed.ncbi.nlm.nih.gov/24405576/); PubMed Central PMCID: [PMCPMC3854755](https://pubmed.ncbi.nlm.nih.gov/PMCPMC3854755/).
44. Nishishita N, Muramatsu M, Kawamata S. An effective freezing/thawing method for human pluripotent stem cells cultured in chemically-defined and feeder-free conditions. *American journal of stem cells*. 2015; 4(1):38–49. PMID: [25973330](https://pubmed.ncbi.nlm.nih.gov/25973330/); PubMed Central PMCID: [PMC4396159](https://pubmed.ncbi.nlm.nih.gov/PMC4396159/).
45. Trosan P, Javorkova E, Zajicova A, Hajkova M, Hermankova B, Kossl J, et al. The Supportive Role of Insulin-Like Growth Factor-I in the Differentiation of Murine Mesenchymal Stem Cells into Corneal-Like Cells. *Stem Cells Dev*. 2016; 25(11):874–81. <https://doi.org/10.1089/scd.2016.0030> PMID: [27050039](https://pubmed.ncbi.nlm.nih.gov/27050039/).
46. Zajicova A, Pokorna K, Lencova A, Krulova M, Svobodova E, Kubinova S, et al. Treatment of ocular surface injuries by limbal and mesenchymal stem cells growing on nanofiber scaffolds. *Cell transplantation*. 2010; 19(10):1281–90. <https://doi.org/10.3727/096368910X509040> PMID: [20573307](https://pubmed.ncbi.nlm.nih.gov/20573307/).

47. Trosan P, Svobodova E, Chudickova M, Krulova M, Zajicova A, Holan V. The key role of insulin-like growth factor I in limbal stem cell differentiation and the corneal wound-healing process. *Stem Cells Dev.* 2012; 21(18):3341–50. <https://doi.org/10.1089/scd.2012.0180> PMID: 22873171; PubMed Central PMCID: PMC3516427.
48. Atlasi Y, Mowla SJ, Ziaee SA, Gokhale PJ, Andrews PW. OCT4 spliced variants are differentially expressed in human pluripotent and nonpluripotent cells. *Stem cells.* 2008; 26(12):3068–74. <https://doi.org/10.1634/stemcells.2008-0530> PMID: 18787205.
49. Dudakova L, Liskova P, Trojek T, Palos M, Kalasova S, Jirsova K. Changes in lysyl oxidase (LOX) distribution and its decreased activity in keratoconus corneas. *Exp Eye Res.* 2012; 104:74–81. <https://doi.org/10.1016/j.exer.2012.09.005> PMID: 23041260.
50. Reboun M, Rybova J, Dobrovolny R, Vcelak J, Veselkova T, Storkanova G, et al. X-Chromosome Inactivation Analysis in Different Cell Types and Induced Pluripotent Stem Cells Elucidates the Disease Mechanism in a Rare Case of Mucopolysaccharidosis Type II in a Female. *Folia Biol-Prague.* 2016; 62(2):82–9. PubMed PMID: WOS:000377711700004.
51. Aplin JD, Campbell S, Allen TD. The extracellular matrix of human amniotic epithelium: ultrastructure, composition and deposition. *Journal of cell science.* 1985; 79:119–36. PMID: 3914477.
52. Modesti A, Scarpa S, D'Orazi G, Simonelli L, Caramia FG. Localization of type IV and V collagens in the stroma of human amnion. *Progress in clinical and biological research.* 1989; 296:459–63. PMID: 2740400.
53. Germain L, Guignard R, Rouabhia M, Auger FA. Early basement membrane formation following the grafting of cultured epidermal sheets detached with thermolysin or Dispase. *Burns: journal of the International Society for Burn Injuries.* 1995; 21(3):175–80. PMID: 7794497.
54. Miyoshi S, Nakazawa H, Kawata K, Tomochika K, Tobe K, Shinoda S. Characterization of the hemorrhagic reaction caused by *Vibrio vulnificus* metalloprotease, a member of the thermolysin family. *Infection and immunity.* 1998; 66(10):4851–5. PMID: 9746589; PubMed Central PMCID: PMC108600.
55. Perreault N, Beaulieu JF. Use of the dissociating enzyme thermolysin to generate viable human normal intestinal epithelial cell cultures. *Exp Cell Res.* 1996; 224(2):354–64. <https://doi.org/10.1006/excr.1996.0145> PubMed PMID: WOS:A1996UJ21000015. PMID: 8612712
56. Carpenter G, Cohen S. Epidermal growth factor. *Annual review of biochemistry.* 1979; 48:193–216. <https://doi.org/10.1146/annurev.bi.48.070179.001205> PMID: 382984.
57. Fatimah SS, Tan GC, Chua KH, Tan AE, Hayati AR. Effects of epidermal growth factor on the proliferation and cell cycle regulation of cultured human amnion epithelial cells. *J Biosci Bioeng.* 2012; 114(2):220–7. <https://doi.org/10.1016/j.jbiosc.2012.03.021> PMID: 22578596.
58. Alcaraz A, Mrowiec A, Insausti CL, Garcia-Vizcaino EM, Ruiz-Canada C, Lopez-Martinez MC, et al. Autocrine TGF-beta induces epithelial to mesenchymal transition in human amniotic epithelial cells. *Cell transplantation.* 2013; 22(8):1351–67. <https://doi.org/10.3727/096368912X657387> PMID: 23031712.
59. Scholer HR, Ruppert S, Suzuki N, Chowdhury K, Gruss P. New type of POU domain in germ line-specific protein Oct-4. *Nature.* 1990; 344(6265):435–9. <https://doi.org/10.1038/344435a0> PMID: 1690859.
60. Niwa H, Miyazaki J, Smith AG. Quantitative expression of Oct-3/4 defines differentiation, dedifferentiation or self-renewal of ES cells. *Nat Genet.* 2000; 24(4):372–6. <https://doi.org/10.1038/74199> PMID: 10742100.
61. Takeda J, Seino S, Bell GI. Human Oct3 gene family: cDNA sequences, alternative splicing, gene organization, chromosomal location, and expression at low levels in adult tissues. *Nucleic Acids Res.* 1992; 20(17):4613–20. PMID: 1408763; PubMed Central PMCID: PMC334192.
62. Cauffman G, Liebaers I, Van Steirteghem A, Van de Velde H. POU5F1 isoforms show different expression patterns in human embryonic stem cells and preimplantation embryos. *Stem cells.* 2006; 24(12):2685–91. <https://doi.org/10.1634/stemcells.2005-0611> PMID: 16916925.
63. Lee J, Kim HK, Rho JY, Han YM, Kim J. The human OCT-4 isoforms differ in their ability to confer self-renewal. *J Biol Chem.* 2006; 281(44):33554–65. <https://doi.org/10.1074/jbc.M603937200> PMID: 16951404.
64. Garcia-Castro IL, Garcia-Lopez G, Avila-Gonzalez D, Flores-Herrera H, Molina-Hernandez A, Portillo W, et al. Markers of Pluripotency in Human Amniotic Epithelial Cells and Their Differentiation to Progenitor of Cortical Neurons. *PloS one.* 2015; 10(12):e0146082. <https://doi.org/10.1371/journal.pone.0146082> PMID: 26720151; PubMed Central PMCID: PMC4697857.
65. Izumi M, Pazin BJ, Minervini CF, Gerlach J, Ross MA, Stolz DB, et al. Quantitative comparison of stem cell marker-positive cells in fetal and term human amnion. *J Reprod Immunol.* 2009; 81(1):39–43. <https://doi.org/10.1016/j.jri.2009.02.007> PMID: 19501410.

### *Appendix 5*

Azqueta A, Rundén-Pran E, Elje E, Nicolaissen B, Berg KH, **Smeringaiova I**, Jirsova K, Collins AR (2018). The comet assay applied to cells of the eye. *Mutagenesis*, 33(1), 21-24.

## Review

# The comet assay applied to cells of the eye

Amaya Azqueta<sup>1,2</sup>, Elisa Rundén-Pran<sup>3</sup>, Elisabeth Elje<sup>3</sup>,  
Bjørn Nicolaisen<sup>4</sup>, Kristiane Haug Berg<sup>4</sup>, Ingrida Smeringaiova<sup>5</sup>,  
Katerina Jirsova<sup>5</sup> and Andrew R. Collins<sup>6,\*</sup>

<sup>1</sup>Department of Nutrition, Food Science and Toxicology, Schools of Pharmacy and Sciences, University of Navarra, Irunlarrea 1, 31009 Pamplona, Spain, <sup>2</sup>IdiSNA, Navarra Institute for Health Research, <sup>3</sup>NILU (Norwegian Institute for Air Research), Instituttveien 18, 2007 Kjeller, Norway, <sup>4</sup>Centre for Eye Research, Department of Ophthalmology, Oslo University Hospital, Ullevål and University of Oslo, Kirkeveien 166, 0450 Oslo, Norway, <sup>5</sup>Laboratory of the Biology and Pathology of the Eye, Institute of Inherited Metabolic Disorders, First Faculty of Medicine, Charles University and General University Hospital, Ke Karlovu 455/2, 128 08 Prague 2, Czech Republic and <sup>6</sup>Department of Nutrition, Institute for Basic Medical Sciences, University of Oslo, Sognsvannsveien 9, 0372 Oslo, Norway

\*To whom correspondence should be addressed. Tel: +47 22851360; Email: [a.r.collins@medisin.uio.no](mailto:a.r.collins@medisin.uio.no)

Received 9 June 2017; Editorial decision 24 August 2017; Accepted 26 August 2017.

## Abstract

The human eye is relatively unexplored as a source of cells for investigating DNA damage. There have been some clinical studies, using cells from surgically removed tissues, and altered DNA bases as well as strand breaks have been measured using the comet assay. Tissues examined include corneal epithelium and endothelium, lens capsule, iris and retinal pigment epithelium. For the purpose of biomonitoring for exposure to potential mutagens in the environment, the eye—relatively unprotected as it is compared with the skin—would be a valuable object for study; non-invasive techniques exist to collect lachrymal duct cells from tears, or cells from the ocular surface by impression cytology, and these methods should be further developed and validated.

## Introduction

Damage to the DNA molecule, in the form of breaks, base alterations or adducts and cross-links, is the immediate consequence of exposure of cells to genotoxins, and so its measurement in individuals can be used as a marker of exposure and (arguably) as a possible indicator of cancer risk, though this link has not been established except in a few specific cases, such as the association between bulky aromatic DNA adducts and lung cancer (1). The comet assay (single cell gel electrophoresis) is widely and increasingly used in human biomonitoring and clinical studies to measure DNA damage (2). Whether run under alkaline or (less commonly) neutral conditions, it detects both single and double strand breaks (SBs) in DNA. With the incorporation of a suitable lesion-specific enzyme, such as formamidopyrimidine DNA glycosylase (Fpg) or endonuclease III (EndoIII or Nth), it also detects altered bases (oxidised purines and pyrimidines respectively in the case of Fpg and EndoIII); the enzyme T4EndoV is used to detect cyclobutane pyrimidine dimers induced by UV light (3). DNA repair capacity

is sometimes also studied as a biomarker, using a modification of this assay (4).

For the purpose of human biomonitoring, the comet assay is generally applied to white blood cells, for various reasons: blood can be obtained by a relatively non-invasive method; standard procedures exist for isolating peripheral blood mononuclear (PBMC) cells (or whole blood can be used) and the cells behave well in the assay. In addition, as they are circulating cells, they apparently reflect whole-body exposure—while also being sensitive to the internal environment, whether healthy or diseased, in a state of homeostatic balance or of stress. However, there are advantages in using cells from other sources; for instance, from specific tissues that represent a target in terms of disease incidence, or alternatively from tissues that are subject to specific exposure. The common routes of exposure to environmental mutagens are by ingestion, by breathing or by contact with the external surface of the body.

Buccal epithelial cells can be used to detect effects of ingested toxins (5); they are easy to obtain, but are not as 'clean' as PBMC cells, as debris, dead cells and contaminating lymphocytes can be



present; also, the comet assay needs to be modified with a protease digestion to allow comet tails to form. Nasal epithelial cells (6) are appropriate for measuring effects of atmospheric pollutants.

Occasionally other cell types are available—e.g., cells from tumours and from surrounding tissue removed during surgery. Studies of such material from colorectal cancer patients (7) showed a good correlation between tumour tissue and healthy tissue, and between healthy tissue and PBMN cells, when measuring either nucleotide or base excision repair with the comet assay.

Our theme here is the exploitation of a relatively uncommon source of cells for biomonitoring, namely the human eye. Most experiments so far have made use of corneal epithelial cells from transplant material, or lens epithelial cells obtained during surgery. More relevant to molecular epidemiology is the possibility of removing cells from the ocular surface, i.e. from the corneal and conjunctival epithelium, which is exposed to any particulate matter, reactive gases and volatile organic chemicals in the atmosphere. If such cells can be removed in a non-invasive way, in a state suitable for various investigatory procedures, including the comet assay, this would make way for a valuable addition to our battery of human biomarker assays.

We include here a review of published studies, some recent experiments, and promising ideas for future work. Our emphasis is on the use of primary cells derived from various tissues of the human eye; we do not discuss experiments with non-human material, or (in general) experiments with established cell lines. We cover clinical studies, as well as the (so far limited) use of cells from tears or from the ocular surface in molecular epidemiology. We do not intend to give detailed practical information; the reader is referred to the excellent methodological review of the comet assay applied to various human epithelial cell types (including cells from the eye) (8).

## Corneal Epithelial and Endothelial Cells

Epithelial cells are able to proliferate when cornea is cultured in the laboratory, by regeneration from the limbus, a narrow band of tissue surrounding the periphery of the cornea. Corneal endothelial cells, in contrast, do not proliferate after birth; in organ culture, lesions in the endothelium are repaired by enlargement of neighbouring cells and by cell migration from the periphery, where the endothelial cells are present at higher density. In cell (not organ) culture, endothelial cells may proliferate and lose their endothelial phenotype.(9)

In an examination of the effects of different storage conditions on corneas destined for transplantation,(10) segments of tissue from corneas (from 10 patients) initially stored under hypothermic conditions in Optisol GS (Bausch & Lomb, USA) were transferred to organ culture medium at 32°C for 1 week. Before and after the transfer and culture, the epithelium was scraped from the surface and gently pipetted to create a single cell suspension for comet assay analysis incorporating Fpg, EndoIII, or T4EndoV. Generally Fpg-sites were higher than EndoIII-sites, which were higher than T4EndoV-sites. Organ culture of the corneas led to an overall increase in SBs, but the individual samples varied widely in their response to culture, some showing a modest or no increase while others evidently accumulated substantial damage (Figure 1).

Figure 2 shows results of (unpublished) experiments with epithelium from corneal segments—with and without incubation. Levels of SBs after culture were again very variable; in some cases the % tail DNA was so high that it was not possible to estimate net enzyme-sensitive sites accurately by subtraction. EndoIII-sites were lower

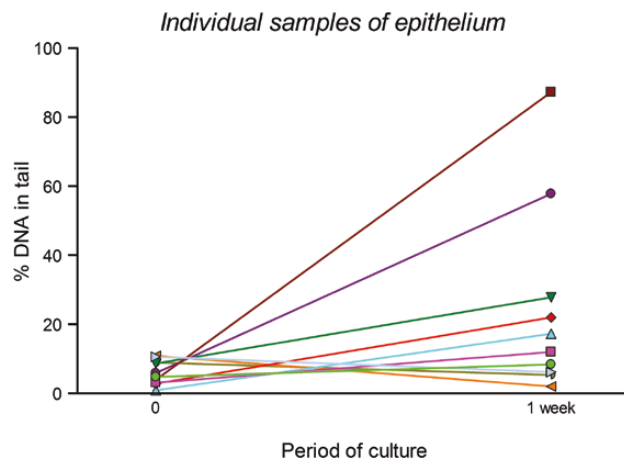


**Figure 1.** Levels of DNA SBs in individual samples of corneal epithelium, before and after organ culture. Data are from experiments in ref. (10).

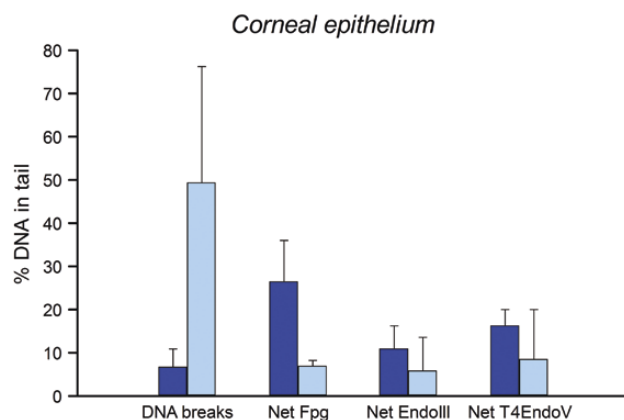


**Figure 2.** DNA damage in corneal epithelial cells, before (dark bars) or after one week of organ culture (light bars): DNA SBs (after lysis alone), oxidised purines detected with Fpg, oxidised pyrimidines with EndoIII and pyrimidine dimers with T4EndoV. Mean values from 7 samples (before culture) and 5 samples (after culture), with SD. (In the case of epithelium after culture, enzyme-sensitive sites could only be calculated for those samples with non-saturating levels of SBs.) (A. Azqueta, unpublished data; methods as in ref. (10)).

than Fpg-sites, and Fpg-sites showed a distinct decrease on incubation in organ culture medium for a week. Endothelial cells tended to have lower levels of SBs—data not shown—consistent with the fact that, while endothelial cells do not proliferate, dying cells, presumably those with elevated levels of DNA damage, are released from the endothelial surface.

## Cells From the Lens Capsule

A similar approach to that employed in the study of corneal cells was used in experiments with epithelial cells from the lens capsule, obtained from patients undergoing cataract surgery (11) (Figure 3). SBs were at an extremely low level, before and after 1 week of culture; Fpg-sites were very high compared with the other enzyme-sensitive sites, and increased on incubation—indicating that some oxidation was occurring during culture, in contrast to the corneal cells in which oxidation damage decreased. Whether this difference is due to intrinsic differences in the cell types, or their response to the culture environment, is not known (and should be followed up).

Age-related cataracts (ARC) were used as a source of epithelial cells also by Zhang et al. (12). Usefully, they had control samples of cells obtained from patients undergoing surgery for retinal detachment but who had clear lenses. The levels of SBs were higher in ARC patients' cells than in those of controls. Zhang et al. also measured DNA damage in lymphocytes of these patients, and found a significant positive correlation ( $r = 0.4$ ) between the two cell types.

Significantly higher levels of SBs were reported in lens epithelial cells from ARC patients, compared with controls—i.e. cells from lenses obtained during surgical removal of epiretinal membrane.(13) There were also higher levels of SBs in lens epithelial cells from cataracts of senile patients, compared with lens epithelium from healthy (non-cataract) elderly patients.(14)

### Other Eye Tissues

Li et al.(15) applied the comet assay to human trabecular meshwork cells, which are located close to the corneal endothelium and in which stem cells for the endothelium may be present. They claim that over-expression of miR-183 (a microRNA cluster whose expression during development is linked to maturation of sensory organs) increased the level of damage induced by UVC ( $10 \text{ Jm}^{-2}$ ). However, UV-induced DNA damage (cyclobutane pyrimidine dimers) does not break DNA directly, and the observed SBs might rather have been transient DNA repair intermediates.

Szaflik et al.(16) collected iris tissue biopsies during cataract surgery on patients with glaucoma, with diabetes type 2, with both glaucoma and diabetes, or with neither. SBs, EndoIII- and Fpg-sites were measured, and significantly more oxidised bases (both pyrimidines and purines) were seen in those with disease, especially with both glaucoma and diabetes.

Retinal pigment epithelial (RPE) cells from donor eyes, and an immortalised cell line established from lens epithelium (HLE B-3), were used by Chignell et al.(17) not (obviously) for biomonitoring, but to test the possible toxicity of alkaloids palmatine and berberine, present in plant preparations used in traditional medicine for the treatment of trachoma. They exposed cells to the alkaloids plus light; on HLE B-3 cells, the IC<sub>50</sub> for berberine + UV(A) was

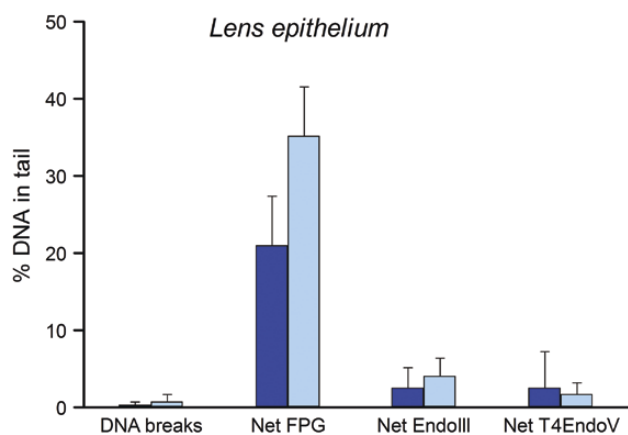


**Figure 3.** DNA damage in lens epithelial cells, freshly isolated (dark bars) or after culture of capsulotomy samples for 1 week (light bars): DNA breaks (after lysis alone), oxidised purines detected with Fpg, oxidised pyrimidines with EndoIII and pyrimidine dimers with T4EndoV. Mean values from 11 samples, with SD. Redrawn from data in Osnes-Ringen et al. (11) with permission from John Wiley and Sons Inc.

between 5 and 10  $\mu\text{M}$ , while palmatine was less toxic. Both caused mild DNA breakage at 10  $\mu\text{M}$  with UV(A). Light of <400 nm wavelength does not penetrate the anterior part of the eye, and so RPE cells were only tested with visible light: palmatine was not toxic, while berberine caused DNA breaks but only at much higher concentrations than with the lens cells. Chignell et al. suggest that caution should be exercised in using plant extracts containing these alkaloids medicinally, as the concentrations of the alkaloids are relatively very high.

### Non-invasive Methods; Applications in Human Biomonitoring

Application of the comet assay to cells from tears was described almost 20 years ago,(18) though at that time only DNA SBs were measured. Nasal brushing was used to stimulate release of tear duct cells; tears were collected into 20  $\mu\text{l}$  capillary tubes, and mixed with agarose for the comet assay. Subjects came from parts of Mexico city with differing kinds of pollution; the south of the city is more polluted with ozone, while in the north particulate matter and hydrocarbons are prevalent. Subjects from the south showed the higher levels of DNA SBs in tear duct cells

'Impression cytology' is a promising approach, in which cells from the ocular surface, particularly from the conjunctiva, are gently adsorbed onto a membrane (such as a nitrocellulose filter) and then detached into buffer for agarose embedding. This method has been used successfully to obtain cells for histological/cytological examination, and for analysis of the frequency of micronuclei (19) and is currently being tried as a source of cells for the comet assay. Figure 4 shows typical images from preliminary experiments; cells were removed from the membrane by trypsinisation, and it is not known whether the damage clearly present in some of the cells results from this isolation procedure, or from *in vivo* exposure to damaging agents in the air. Further assay development is required, but if successful, this approach will provide us with a powerful

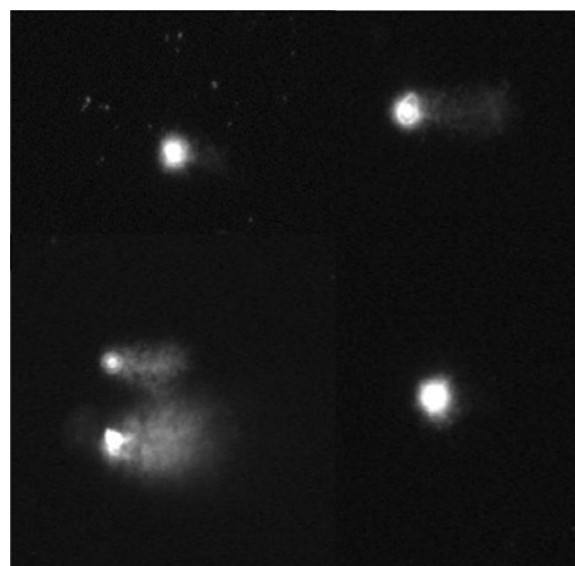


**Figure 4.** Comet images from cells obtained by impression cytology (E. Rundén-Pran, E. Elje, unpublished data). As in comet assay experiments in general, the extent of migration of DNA under electrophoresis, i.e. the % of DNA in the comet tail, reflects the frequency of DNA breaks.

(non-invasive) biomarker assay for the genotoxic effects of atmospheric pollutants, and a possible diagnostic tool for neoplasms on the ocular surface (K. Jirsova, manuscript in preparation).

## Conclusions

Up until now, most of the studies conducted on cells from the human eye with the comet assay have used transplant tissue or cells removed during surgical procedures. There is a limit to the information that can be obtained from such work: in the case of diseases of the eye, it is rarely possible to obtain healthy tissue to act as a control; and as the procedures are invasive, standard epidemiological trials such as prospective or intervention studies or studies of the effects of occupational or environmental exposure to genotoxic agents are not feasible. However, these experiments have at least demonstrated that cells from the various tissues examined are amenable to measurement of DNA damage, both SBs and altered bases.

Non-invasive techniques are restricted to cells of the surface of the eye, but these are potentially excellent material for examining effects of air-borne pollutants. They are at present a virtually untapped resource, and further development of the comet assay, whether applied to tears or to cells taken from the ocular surface, should provide us with a valuable new approach to biomonitoring.

## Funding

The research leading to these results was supported with funding from the Norwegian Financial Mechanism 2009–2014 under Project Contract no. MSMT-28477/2014, project 7F14156, EYEFORTX. K.J. was supported by projects Progres Q26/LF1 and LM2015089.

## Acknowledgements

A.A. thanks the Ministerio de Economía y Competitividad ('Ramón y Cajal' programme, RYC-2013-14370) of the Spanish Government for personal support. The authors are grateful to the COST Action CA15132, 'hCOMET', for support.

Conflict of interest statement: None declared.

## References

- Veglia, F., Loft, S., Matullo, G., et al.; Genair-EPIC Investigators. (2008) DNA adducts and cancer risk in prospective studies: a pooled analysis and a meta-analysis. *Carcinogenesis*, 29, 932–936.
- Dusinska, M. and Collins, A. R. (2008) The comet assay in human biomonitoring: gene-environment interactions. *Mutagenesis*, 23, 191–205.
- Collins, A. R. (2014) Measuring oxidative damage to DNA and its repair with the comet assay. *Biochim. Biophys. Acta*, 1840, 794–800.
- Collins, A. R. and Azqueta, A. (2012) DNA repair as a biomarker in human biomonitoring studies; further applications of the comet assay. *Mutat. Res.*, 736, 122–129.
- Sánchez-Alarcón, J., Milić, M., Gómez-Arroyo, S., Montiel-González, J. M. R. and Valencia-Quintana, R. (2016) Assessment of DNA damage by comet assay in buccal epithelial cells: problems, achievement, perspectives. In Larramendy, M. L. and Soloneski, S. (eds.), *Environmental Health Risk - Hazardous Factors to Living Species*, INTECH.
- Calderón-Garcidueñas, L., Wen-Wang, L., Zhang, Y. J., Rodríguez-Alcaraz, A., Osnaya, N., Villarreal-Calderón, A. and Santella, R. M. (1999) 8-hydroxy-2'-deoxyguanosine, a major mutagenic oxidative DNA lesion, and DNA strand breaks in nasal respiratory epithelium of children exposed to urban pollution. *Environ. Health Perspect.*, 107, 469–474.
- Slyskova, J., Korenkova, V., Collins, A. R., et al. (2012) Functional, genetic, and epigenetic aspects of base and nucleotide excision repair in colorectal carcinomas. *Clin. Cancer Res.*, 18, 5878–5887.
- Rojas, E., Lorenzo, Y., Haug, K., Nicolais, B. and Valverde, M. (2014) Epithelial cells as alternative human biomatrices for comet assay. *Front. Genet.*, 5, 386.
- Roy, O., Leclerc, V. B., Bourget, J. M., Thériault, M. and Proulx, S. (2015) Understanding the process of corneal endothelial morphological change in vitro. *Invest. Ophthalmol. Vis. Sci.*, 56, 1228–1237.
- Haug, K., Azqueta, A., Johnsen-Soriano, S., et al. (2013) Donor cornea transfer from Optisol GS to organ culture storage: a two-step procedure to increase donor tissue lifespan. *Acta Ophthalmol.*, 91, 219–225.
- Øsnes-Ringen, O., Azqueta, A. O., Moe, M. C., Zetterström, C., Røger, M., Nicolais, B. and Collins, A. R. (2013) DNA damage in lens epithelium of cataract patients in vivo and ex vivo. *Acta Ophthalmol.*, 91, 652–656.
- Zhang, J., Wu, J., Yang, L., Zhu, R., Yang, M., Qin, B., Shi, H. and Guan, H. (2014) DNA damage in lens epithelial cells and peripheral lymphocytes from age-related cataract patients. *Ophthalmic Res.*, 51, 124–128.
- Wang, Y., Zhang, J., Wu, J. and Guan, H. (2017) Expression of DNA repair genes in lens cortex of age-related cortical cataract. *Exp. Mol. Pathol.*, 102, 219–223.
- Sorte, K., Sune, P., Bhake, A., Shivkumar, V. B., Gangane, N. and Basak, A. (2011) Quantitative assessment of DNA damage directly in lens epithelial cells from senile cataract patients. *Mol. Vis.*, 17, 1–6.
- Li, G., Luna, C. and Gonzalez, P. (2016) miR-183 inhibits UV-induced DNA damage repair in human trabecular meshwork cells by targeting of KIAA0101. *Invest. Ophthalmol. Vis. Sci.*, 57, 2178–2186.
- Szaflik, J. P., Rusin, P., Zaleska-Zmijewska, A., Kowalski, M., Majsterek, I. and Szaflik, J. (2010) Reactive oxygen species promote localized DNA damage in glaucoma-iris tissues of elderly patients vulnerable to diabetic injury. *Mutat. Res.*, 697, 19–23.
- Chignell, C. F., Sik, R. H., Watson, M. A. and Wielgus, A. R. (2007) Photochemistry and photocytotoxicity of alkaloids from Goldenseal (*Hydrastis canadensis* L.) 3: effect on human lens and retinal pigment epithelial cells. *Photochem. Photobiol.*, 83, 938–943.
- Rojas, E., Valverde, M., Lopez, M. C., Naufal, I., Sanchez, I., Bizarro, P., Lopez, I., Fortoul, T. I. and Ostrosky-Wegman, P. (2000) Evaluation of DNA damage in exfoliated tear duct epithelial cells from individuals exposed to air pollution assessed by single cell gel electrophoresis assay. *Mutat. Res.*, 468, 11–17.
- Jirsova, K., Juklova, K., Alfakih, A. and Filipec, M. (2007) Presence of snake-like chromatin in epithelial cells of keratoconjunctivitis sicca followed by a large number of micronuclei. *Acta Cytol.*, 51, 541–546.